SELECTIVE ALKYLATION OF BENZENE WITH ETHANOL USING MODIFIED HZSM-5 TO PRODUCE ETHYLBENZENE

Ph.D. THESIS

by

ABDI NEMERA EMANA

DEPARTMENT OF CHEMICAL ENGINEERING

INDIAN INSTITUTE OF TECHNOLOGY ROORKEE

ROORKEE – 247667 (INDIA)

APRIL, 2016

SELECTIVE ALKYLATION OF BENZENE WITH ETHANOL USING MODIFIED HZSM-5 TO PRODUCE ETHYLBENZENE

A THESIS

Submitted in partial fulfilment of the requirements for the award of the degree of

DOCTOR OF PHILOSOPHY

in

CHEMICAL ENGINEERING

by

ABDI NEMERA EMANA

DEPARTMENT OF CHEMICAL ENGINEERING
INDIAN INSTITUTE OF TECHNOLOGY ROORKEE
ROORKEE-247667 (INDIA)
APRIL, 2016

INDIAN INSTITUTE OF TECHNOLOGY ROORKEE
ROORKEE

CANDIDATE'S DECLARATION

I hereby certify that the work which is being presented in the thesis entitled ''**SELECTIVE ALKYLATION OF BENZENE WITH ETHANOL USING MODIFIED HZSM-5 TO PRODUCE ETHYLBENZENE**'' in partial fulfillment of the requirements for the award of the Degree of Doctor of Philosophy and submitted in the Department of Chemical Engineering of the Indian Institute of Technology Roorkee, Roorkee is an authentic record of my own work carried out during a period from July, 2012 to April, 2016 under the supervision of Dr. Shri Chand, Professor, Department of Chemical Engineering, Indian Institute of Technology Roorkee, Roorkee.

The matter presented in this thesis has not been submitted by me for the award of any other degree of this or any other Institute.

(ABDI NEMERA EMANA)

This is to certify that the above statement made by the candidate is correct to the best of my knowledge.

(Shri Chand)
Supervisor

Date…….

The Ph.D. Viva-Voce Examination of **Mr. ABDI NEMERA EMANA,** Research Scholar, has been held on …….

Chairman, SRC

Signature of External Examiner

This is to certify that the student has made all the corrections in the thesis.

Signature of Supervisor

Head of the Department

ABSTRACT

Alkylation of benzene to produce ethylbenzene is a considerable importance due to the increasing demand of ethylbenzene and diethylbenzene in chemical industries. The demand of ethylbenzene is found to be higher due to its use in the manufacture of plastics and many petrochemicals. The commercial process for ethylbenzene from benzene and either ethylene or ethanol involves the vapor phase or liquid phase alkylation of benzene with ethylating agents over a variety of acidic zeolites.

Several researchers have proposed the alternative catalytic reaction pathways for the production of ethylbenzene. The catalytic reaction which uses ethanol for benzene alkylation, instead of ethylene, would eliminate the ethylene production step and, therefore, leading to the commercial and environmental benefits in the ethylbenzene manufacturing. In addition to the intrinsic scientific interest, the direct use of ethanol (instead of ethylene) in the manufacture of ethylbenzene also has economic significance in those countries like Brazil and India, where biomass-derived alcohol is an additional feedstock for the manufacture of chemicals.

Alkylation of benzene with ethanol yields ethylbenzene, polyalkylates, especially diethylbenzene (DEB), toluene and mixtures of xylenes as major products inside zeolite pores. The products subsequently diffuse out of the zeolite pores. Owing to its smaller size and very high diffusivity, ethylbenzene diffuses out of the pores at a very high rate in comparison to diethylbenzene. Several researchers have shown enhanced ethylbenzene selectivity of zeolites by the use of modifier agents such as rare earth metals. These modifier agents have been reported to partially block the pores and block the unselective active sites and inactivate the external active sites for secondary isomerization.

Based on the fact that modification of a HZSM-5 zeolite may lead to (i) selectivity of the reactions based on the nature of the cation (ii) blockage of the zeolite pore mouth in proportion to the size of the exchanged ion, leading to shape selectivity for the desired product (ethylbenzene in the present case) and also (iii) greater stability of the exchanged zeolite than the unmodified form, the present work has been under taken.

Alkylation reactions are known to be depending on the activity and selectivity of catalysts. Further developments of catalysts which can provide higher benzene conversion and ethylbenzene selectivity are necessary to ensure successful development of the industrial process for alkylation of benzene with ethanol. It is important to design highly stable, active and selective catalysts to perform the reaction at atmospheric pressure and 300-500^{o}C temperature.

Significant numbers of studies have been reported on the alkylation of benzene with ethanol using rare earth metals as modifying agent for HZSM-5. However, at the time of the start of work in this thesis (year 2012), no studies were reported on various possible application of boron, magnesium monometallic and bimetallic as modifying elements for HZSM-5 in the alkylation of benzene with ethanol for the formation of ethylbenzene. Therefore, in the present study boron, magnesium monometallic and boron-magnesium bimetallic catalyst having acidic sites for alkylation of benzene with ethanol were tested.

The present work deals with the preparation, characterization and activity tests of the magnesium, boron monometallic and boron-magnesium bimetallic modified HZSM-5 for the alkylation of benzene with ethanol. The effect of support composition as well as metal loading on the catalyst was studied. To investigate the physico-chemical properties of fresh and used catalysts, various characterization techniques including BET surface area, X-ray diffraction (XRD), temperature programmed desorption (TPD), Scanning electron microscopy (SEM-EDAX), transmission electron microscopy (TEM), thermogravimetric analysis (TGA) and Fourier transmission infrared spectroscopy (FTIR) were used. The effect of reaction temperature, benzene to ethanol ratio, amount of metal loading and different silicon to aluminium ratio HZSM-5 were studied to maximize ethylbenzene selectivity in the temperature range of 300-500^{o}C.

From the experimental results we observed that for HZSM-5 silicon to aluminium ratio 31 (SAR=31) with benzene to ethanol ratio 2:1 by volume ethylbenzene was the primary product while diethylbenzene, triethylbenzene, toluene and xylene mixtures also exist in the product. Highest selectivity of ethylbenzene (72.79%) and higher conversion of benzene (75.17%) was obtained by bimetallic catalyst (Mg(5%)-B(4%)-HZSM-5) at 500^{o}C and 400^{o}C respectively. Boron modified showed lower benzene conversion (62.2%) while magnesium modified showed approximately the same benzene conversion (71.7%) when compared to unmodified HZSM-5 (71.3%). The existence of abundant ethanol may facilitate the alkylation of benzene to produce ethylbenzene and then further alkylation to diethylbenzene and tri ethylbenzene.

Our investigation demonstrates again that ethylbenzene was the primary product while diethylbenzene, triethylbenzene, toluene and xylene mixtures also exist in the product for magnesium monometallic modified HZSM-5 (SAR=90). The highest selectivity of ethylbenzene (71.14%) was obtained by 15%Mg-HZSM-5 while the lowest ethylbenzene selectivity (49.74%) was obtained by 10%Mg-HZSM-5 for 2:1 benzene to ethanol ratio by

volume. For benzene to ethanol ratio 4:1 also the highest selectivity for ethylbenzene (67.59%) was observed by 15%Mg-HZSM-5 while the lowest selectivity of ethylbenzene (63.35%) was obtained by 5%Mg-HZSM-5. In terms of ethylbenzene yield all HZSM-5 catalysts modified by magnesium resulted approximately in the range of 34-42%. The highest conversion of benzene (71.82%) was obtained by 15%Mg-HZSM-5.

Similar to magnesium monometallic HZSM-5 modified, boron modified HZSM-5 showed that ethylbenzene was the primary product while diethylbenzene, triethylbenzene, toluene and xylene mixtures also exist in the product. The highest selectivity of ethylbenzene (57.48%) was obtained by 15%B-HZSM-5 while the lowest ethylbenzene selectivity (42.00%) was obtained by10%B-HZSM-5 and 5%B-HZSM-5 for 4:1 benzene to ethanol ratio by volume. However, for benzene to ethanol ratio 2:1 all the catalysts showed approximately the same selectivity for ethylbenzene (48%). Except 15%B-HZSM-5, in terms of ethylbenzene yield both HZSM-5 catalysts modified by boron resulted on approximately 40.00%. The highest yield of ethylbenzene demonstrated by 15%B-HZSM-5 was 44.18% at 450^{o}C for benzene to ethanol ratio 4:1 by volume. The highest conversion of benzene approximately (83%) was obtained by both 5%B-HZSM-5 and 10%Mg-HZSM-5. The existence of abundant ethanol may facilitate the alkylation of benzene to produce ethylbenzene and then further alkylation to diethylbenzene and tri ethylbenzene. Therefore, it would be essential to use lower ethylating agents.

According to results obtained from experiments, ethylbenzene was the primary product while diethylbenzene, triethylbenzene, toluene and xylene mixtures also exist in the product. The highest selectivity of ethylbenzene (76.22%) was obtained by (Mg + B)-15%-HZSM-5 and the lowest ethylbenzene selectivity (49.15%) was obtained by (Mg + B)-5%-HZSM-5 using 2:1 benzene to ethanol ratio by volume. However, for benzene to ethanol ratio 4:1 (Mg+B)-5%-HZSM-5 and (Mg+B)-15%-HZSM-5 catalysts were showed approximately the same selectivity for ethylbenzene (67.01%). The highest yield of ethylbenzene demonstrated by (Mg+B)-5%-HZSM-5 was 43.63% at 450^{o}C for benzene to ethanol ratio 4:1 by volume. The highest conversion of benzene approximately (77.01%) was obtained by (Mg + B)-5%-HZSM-5 for 4:1 benzene to ethanol ratio by volume.

ACKNOWLEDGMENT

All gratitude is due to “God” who guides to bring forth to light this thesis.

The author always believes that no work could be completed without the proper guidance. I wish to express my heartiest thanks to Dr. Shri Chand, Professor, Department of Chemical Engineering, and Indian Institute of Technology Roorkee, for his constant inspiration, encouragement and guidance at each level of this research work.

The author is thankful to Ethiopian Ministry of Higher Education especially to Haramaya University for encouraging me to go for higher studies. I thank also Ethiopian Embassy in New Delhi and Indian Institute of Technology Roorkee for providing me the opportunity to pursue this at this renowned Indian Institute of Technology Roorkee.

I wish to thank my research colleagues Mr. Mukesh Bhat, Mr. Abrham Bayeh, Mr. Lovjeet Singh and Mr. Muse Degefa for all kind of help and encouragement during the course of this work.

I acknowledge the help provided by the laboratory staff of the Department of Chemical Engineering (Mr. Arvind Kumar and Mr. S. Pal) and Institute Instrumentation centre of IIT Roorke.

I deeply indebted to Ms. Addisalem Enjigu, Dr. Gelan Nemera, Mr. Getu Assefa, Ms. Bizunesh Adugna and my parents.

ABDI NEMERA EMANA

TABLE OF CONTENT

LIST OF FIGURES

LIST OF SCHEMES

LIST OF TABLES

NOMENCLATURE

λ: X-ray wavelength

θ: Bragg's angle of diffraction

D: Crystal size

L: The peak width at half height

H_s: Peak height for the sample

H_r: Peak height for the reference

B: Benzene

E: Ethanol

T: Toluene

(P, m, o,)-Xylene: (Para, Meta, Ortho)-Xylene respectively

DEB: Diethylbenzene

TEB: Triethylbenzene

SAR: Silicon to Aluminium Ratio

WHSV: Weight Hour Space Velocity

X_B: Benzene conversion

S_{EB}: Selectivity of Ethylbenzene

Y_{EB}: Yield of Ethylbenzene

TEM: Transmission Electron Microscope

TGA: Thermo-gravimetric Analysis

SEM: Scanning Electron Microscope

XRD: X-ray Diffraction

W = Mass of catalyst

A = Bed cross sectional area

Z = Bed length

F_{BO} = Benzene feed flow rate

C_T = Total concentration of active sites

C_S = Concentration of vacant sites

C = Concentration

K = Equilibrium constant

k = Reaction rate constant

r_{obs} = Experimental observed rate of reaction

$\Delta G^o_{ads,i}$ = Gibbs free energy for adsorption of species i at standard conditions

$\Delta H^o_{ads,i}$ = Change of enthalpy for adsorption of species i at standard conditions

$\Delta S^o_{ads,i}$ = Change of entropy for adsorption of species i at standard conditions

y_i = Experimental conversion

y_i' = Predicted conversion

LIST OF PUBLICATIONS

1. 'Alkylation of benzene with ethanol over modified HZSM-5 zeolite catalysts' by Abdi Nemera Emana and Shri Chand., **Journal of Applied Petrochemical Research, 5 (2015) 121-134**.
2. 'Alkylation of benzene with ethanol over HZSM-5 zeolite catalyst' by Abdi Nemera Emana and Shri Chand, **Intl. J. of Innovative Research in Science, Engineering and Technology, 4(8) (2015) 7587-7598.**
3. 'Alkylation of benzene with ethanol using different silicon to aluminum ratio HZSM-5 zeolite catalysts' by Abdi Nemera Emana and Shri Chand, **3rd International Conference on Advanced Science and Technology (ICAST-2015), Bahir Dar Institute of Technology, Bahir Dar University, Ethiopia. Proceedings, Vol. III, P. 47-55.**
4. 'Direct Synthesis of Diethylbenzene from Alkylation of Benzene with Ethanol over Boron Modified HZSM-5' by Abdi Nemera Emana and Shri Chand. (Communicated)
5. 'Kinetic study of alkylation of benzene with ethanol over bimetallic modified HZSM-5 zeolite catalyst and effects of percentage metal loading' by Abdi Nemera Emana and Shri Chand, **Journal of Catalysis, Structure and Reactivity, 2 (2016) 13-24.**

CHAPTER ONE
GENERAL INTRODUCTION

Aromatics have an extensive variety of applications in the chemical and petrochemical industries. They are an important raw material for many intermediates of commodity petrochemicals and valuable fine chemicals, such as monomers for engineering plastics, polyesters and intermediates for detergents, agricultural products, pharmaceuticals and explosives. Among them, toluene, benzene and xylenes are the three basic materials for most intermediates of aromatic derivatives (Figure 1.1) [1]. Benzene is produced from either pyrolysis gasoline or pure alkyl aromatic hydrocarbons, mostly toluene, thermally or catalytically [2].

In the chemical industry, the alkylation reaction of hydrocarbons such as aromatics with olefins is widely utilized. World benzene demand in 1999 was 29.3 million tonnes. However, approximately 70% of it was expected to be spent for the production of cumene and ethylbenzene with propylene (17%) and ethylene (53%) by acid catalysed alkylation reaction, respectively [3].

Several authors have proposed alternative catalytic reaction pathways for the production of ethylbenzene. Using ethanol in the catalytic reaction for benzene alkylation, instead of ethylene, would eliminate the ethylene production step and, therefore, leading to the commercial and environmental benefits in the ethylbenzene manufacturing [4]. The direct use of ethanol (instead of ethylene) in the manufacture of ethylbenzene also has economic significance in those countries like India and Brazil, where biomass-derived alcohol is an additional feedstock for the manufacture of chemicals in addition to the intrinsic scientific interest.

Almost all ethylbenzene demand in the world is determined primarily by styrene production. Polystyrene, acrylonitrile-butadiene-styrene and styrene-acrylonitrile resins, styrene-butadiene elastomers and latexes, and unsaturated polyester resins are produced by using styrene as an intermediate. The major styrene industry markets include packaging, electrical/electronic/appliances, construction, and consumer products. Consumption of ethylbenzene for other purposes than the production of styrene is estimated as lower than 1%. These applications include use as solvents and on occasion in the manufacture of diethylbenzene, acetophenone and ethylanthraquinone. With no styrene producers in India, there is no demand for ethylbenzene. However, styrene is consumed for polystyrene

production. During 2014, about 59% of imported styrene was consumed for general-purpose polystyrene, 12% for EPS, and 9% for ABS (acrylonitrile butadiene styrene) resin. Demand for styrene is driven by India (88%) and Pakistan (12%). Ethylbenzene consumption for the production of styrene in China is expected to grow at just over 9% per year from 2014 through 2019. This rate of growth is slower than that of the last five years (at about 13% during 2009-14), but higher than the last two years. Slower growth in 2014 was a consequence of the stagnating Chinese economy, following tighter financial controls and a slowdown in the construction sector, which especially affected the expanded polystyrene market, a major downstream demand driver for ethylbenzene/styrene. World ethylbenzene consumption will increase at an average annual rate of 2.1% for the next five years to 2019. The fastest consumption growth is expected in China [5].

Ethylene is a hydrocarbon which has the formula C_2H_4 or $H_2C=CH_2$. It is a colourless flammable gas with a faint "sweet and musky" odour when pure. Major industrial reactions of ethylene include in order of scale: 1) polymerization, 2) oxidation, 3) halogenation and hydrohalogenation, 4) alkylation, 5) hydration, 6) oligomerization, and 7) hydroformylation. In the United States and Europe, approximately 90% of ethylene is used to produce ethylene oxide, ethylene dichloride, ethylbenzene and polyethylene. Ethylene is produced in the petrochemical industry by steam cracking. In this process, gaseous or light liquid hydrocarbons are heated to 750-950 °C, inducing numerous free radical reactions followed by immediate quench to stop these reactions. Ethylene is separated from the resulting complex mixture by repeated compression and distillation [6].

Ethanol (ethyl alcohol) used in alcoholic beverages has also been used as fuel. It is most often used as a motor fuel, mainly as a biofuel additive for gasoline. It is commonly made from biomass such as corn or sugar. The basic steps for large-scale production of ethanol are: microbial (yeast) fermentation of sugars, distillation, dehydration (requirements vary), and denaturing (optional). Prior to fermentation, some crops require saccharification or hydrolysis of carbohydrates such as cellulose and starch into sugars. Saccharification of cellulose is called cellulolysis. Enzymes are used to convert starch into sugar [7].

1.1 ETHYLBENZENE

Ethylbenzene ($C_6H_5CH_2CH_3$) is one of among organic chemical compound which is categorized under an aromatic hydrocarbon. It is a highly flammable, colorless liquid with an

odor like that of gasoline. Its main use is in the petrochemical industry as an intermediate material for the production of styrene, which is in turn used for the production of polystyrene, a plastic material commonly used [8]. Although ethylbenzene which is largely produced by the combination of the petrochemicals benzene and ethylene in acid catalysed chemical reaction is often exist in small quantities in crude oil [8, 9]. Catalytic dehydrogenation of ethylbenzene gives hydrogen gas and styrene. This product is also important for the formation of vinyl benzene [10]. In 2012, more than 99% of ethylbenzene was used in the production of styrene. Ethylbenzene is also used for production of other chemicals, in fuel and as a solvent in inks, rubber adhesives, varnishes and paints [11].

1.2 BACKGROUND OF ETHYLBENZENE

The alkylation reaction of hydrocarbons with olefins over $AlCl_3$ catalyst was first reported by Balsohn 1879 but Charles Friedel and James M. Crafts initiated plentiful of the early research on alkylation reaction and $AlCl_3$ catalyst. About a century later, the alkylation reaction which employs classical Friedel-Crafts reaction process remained as a major source of ethylbenzene production. Ethylbenzene was initially manufactured on a commercial scale in the 1930s by Dow Chemical in the US and by BASF in the Federal Republic of Germany [3]. Until 1980s almost all ethylbenzene was produced with an aluminum chloride catalyst using a Friedel-Crafts reaction mechanism. A couple of ethylbenzene production units using another Friedel-Crafts catalyst called boron trifluoride. Ethylbenzene in small quantity as byproducts recovered from mixed xylenes streams with intensive distillation process [3]. In 1980s, the first commercial plant has allowed a zeolite-based process and the lack of maintenance and environmental problems associated with the Friedel-Crafts catalyst completely displace to zeolite catalyst in every modern production facilities. The first zeolite process was based on vapour phase reaction at temperature of over 400^oC. However, reactions such as isomerisation, cracking, disproportionation and hydrogen transfer can produce a number of by products that contaminate the ethylbenzene product in this temperature range. Efforts have been made to reduce byproduct formation by changing reaction condition, but it did not until the advent of liquid phase processes operating at temperatures lower than 270^oC.

In 1990s, the first high purity zeolite based on technology by UOP and ABB Lummus Global developed and launched [3, 12]. Ethylbenzene - styrene industry remained relatively unimportant until the Second World War. The enormous demand for synthetic butadiene rubber in World War I prompted accelerated technological improvements and huge capacity

expansion. This enormous war effort led to the construction of several large-scale factories, turning styrene production fast becoming a huge industry. In 1965, the super fraction of mixed xylene by catalytic reforming of naphtha streams generated 10 % of ethylbenzene production. In 1986, the world's annual production capacity was 14 * 10^6t [13]. Ethylbenzene is a key raw material in the synthesis of styrene which is the most important industrial monomer. The ethylbenzene production in 2010 was approximately estimated to be about 34 *10^6 metric tons. The competing technologies intended for ethylbenzene production based on zeolite catalysts mainly include Mobil-Badger, Mobil-Badger EBMax, Lummus-UOP and CDtech processes in the petrochemical industry [14].

1.3 PROPERTIES OF ETHYLBENZENE

1.3.1 Physical Properties

Under ordinary conditions, ethylbenzene is a clear liquid with a characteristic aromatic odour. Ethylbenzene is an irritant to the skin and eyes and is ordinarily toxic by ingestion and skin adsorption. The properties are as follows:

Table 1-1: Physical properties of Ethylbenzene [11]

IUPAC Name	Ethylbenzene
Other names	Ethylbenzol, EB, Phenylethane
CAS Number	[100-41-4]
RTECS Number	DA0700000
Molecular Formula	C_8H_{10}
Molar Mass	106.167 g/mol
Appearance	Colourless liquid
Density (at 25^{o}C)	0.86262 g/cc
M.P.	-94.949 ^{o}C
B.P. (at 101.3 K Pa)	136.86 ^{o}C
Refractive index (at 25^{o}C)	1.49320
Critical pressure	3609 K Pa (36.09 bar)
Critical temperature	344.02 ^{o}C

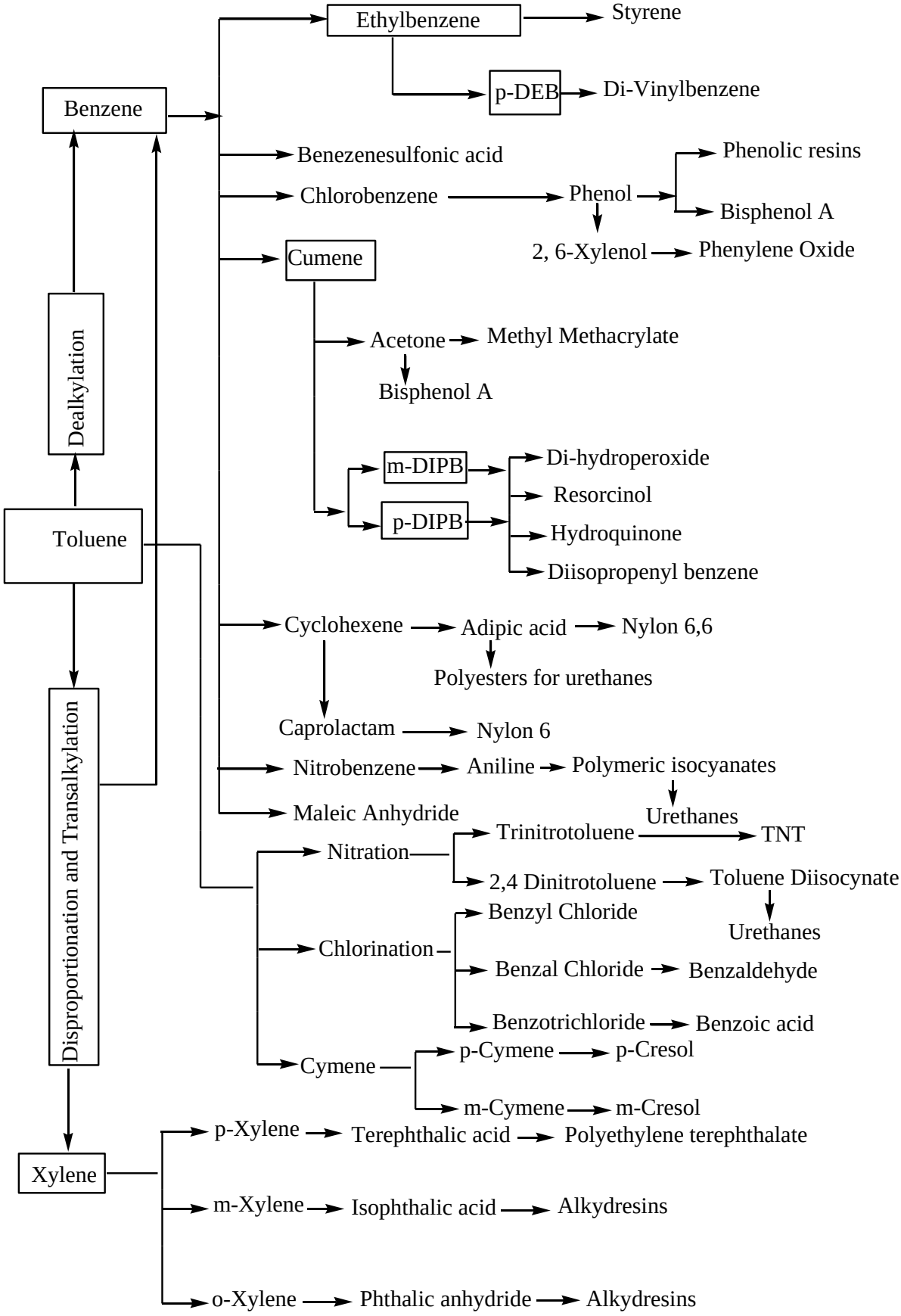

Figure 1-1: Derivatives of benzene, toluene and xylene [1]

1.3.2 Chemical Properties of Ethylbenzene:

Dehydrogenation to styrene is the most important chemical reactions of ethylbenzene. The reaction is carried out at:

- High temperature (600 - 670 ^{o}C)
- Over an iron oxide catalyst
- As diluent steam is used

Commercially, selectivities to styrene range from 89-96% with per pass conversion 65-70%. Additional commercial importance is the reaction of ethylbenzene with air to form hydroperoxides C_6H_5CH (OOH) CH_3. The reaction takes place in the liquid phase, with no catalyst required. Ethylbenzene can be converted to xylenes with a suitable catalyst. Commercial processes for isomerising xylenes usually involve the catalytic isomerization or dealkylation of ethylbenzene. Ethylbenzene may be dealkylated catalytically or thermally to benzene. Styrene is an industrially important chemical that is used for production of plastics and rubbers. It is industrially produced by two subsequent reactions: the alkylation of benzene with ethylene to produce ethylbenzene and its dehydrogenation to styrene [15].

1.4 ZEOLITE

Catalysts have a very important role in various industrial processes and also in the survival and effective operation of all biological systems. Remarkable progresses have been made in recent decades towards understanding the basic processes in catalysis at atomic level. Zeolites have been extensively used as heterogeneous catalysts for shape selective reactions in various practices in the refining and oil industry. Nanochemistry, supramolecular catalysis and photochemistry are other sensational area where nowadays the practice of zeolites has been prolonged. Uses of zeolites as shape selective in industrial catalysts and knowing the properties of these materials has stimulated and directed vast amount of synthetic work in formulating new microporous materials with various pore sizes and structures, which is capable of catalysing new processes.

Almost two and half centuries have passed since zeolite was discovered and named by Cronstedt in 1756. The first zeolite mineral found by this Swedish mineralogist was Stilbite. The mineral was shown to have swelling property when heated in a blowpipe flame. The term zeolite is derived from two Greek words, zeo and lithos, meaning "to boil" and "stone", respectively [16].

Zeolites are crystalline microporous materials with tetrahedrally coordinated framework structures incorporating well defined channel systems and cavities [17]. The well-defined porous structure of zeolites makes them true shape-selective molecular sieves with wide ranging applications in catalysis, ion exchange and adsorption processes. Besides the different pore size and shape, the hydrophilic/hydrophobic nature of zeolites renders them as useful selective sorbents and hosts for guest molecules (organic or inorganic) that are stable in gas and liquid phase [18]. Because of their outstanding solid-acid and adsorption–desorption properties for small molecules, zeolites have been widely used as catalysts and adsorbents in industry [17].

According to the International Zeolite Association (2014) until now, there are 218 type codes zeolite framework that have been discovered. World consumption of zeolites (natural and synthetic) is estimated at about 5 million tons per year. In 2008, the annual market for synthetic zeolites and molecular sieves developed vastly to 1,800,000 tonnes in the world [19].

1.4.1 Molecular Sieves and Zeolites

Porous solids with pore size of molecular dimensions, 0.3-2.0 nm in diameter are called molecular sieves such as zeolites, glasses, carbons and oxides. Some are crystalline with a uniform pore size and described in more detail due to their crystal structure like zeolites [20].

Zeolite catalysts are so special when compared to other crystalline inorganic oxide materials due to a combination of the following advantages. Such as to provide the microporous character with uniform pore size so that certain hydrocarbon molecules can enter while others rejected based on molecular size, Ion-exchange properties that can be all kinds to accomplish ion exchange reactions, the capacity to advance internal acidity that makes the zeolites interesting materials for the catalysis of organic reactions and the high thermal stability of zeolites [21].

Zeolites are microporous crystalline aluminosilicates, composed of TO_4 tetrahedra (T = Si, Al) with O atoms connecting neighbouring tetrahedra. For a completely siliceous structure, combination of TO_4 (T = Si) units in this fashion leads to silica (SiO_2), which is an uncharged solid. Upon incorporation of Al into the silica framework, the +3 charge on the Al makes the framework negatively charged, and requires the presence of extra framework cations (inorganic and organic cations can satisfy this requirement) within the structure to keep the overall framework neutral. The cations and adsorbed water molecules are located in the channels or cages [22]. Generally, zeolites are crystalline aluminosilicates of group IA and group IIA

elements, such as sodium, potassium, magnesium and calcium. Chemically, they are represented by the empirical formula:

$$M_{x/n}[(AlO_2)_x(SiO_2)_y] \cdot wH_2O$$

where M is an alkali or alkaline earth cation, n is the valence of the cation, w is the number of water molecules per unit cell, x and y are the total number of tetrahedra per unit cell, and the ratio y/x usually has values of 1 to 5, though for the silica zeolite, y/x can be ranging from 10 to 100 [21].

1.4.2 Structural Overview

1.4.2.1 Structural Building Units of Zeolites

In zeolite frameworks, there are several types of building units present. The individual tetrahedral TO_4 unit which is the primary building unit of zeolite structure (Fig.1.2). Framework T atoms commonly refer to Si, Al, or P atoms. In some cases, other atoms such as B, Ga, Be, and Ge, etc., are also involved. The basic structural building units of a zeolite framework are these [SiO_4], [AlO_4], or [PO_4] tetrahedra. Lowenstein was formulated that, when two tetrahedra are linked through an oxygen bridge, the center of only one of them can be occupied by Al; the other center should be occupied by Si or other small ions of electrovalency four or more. In short, the structures of aluminosilicate zeolites obey the Lowenstein's rule with an avoidance of Al-O-Al linkages [23].

Primary building units (PBU) elements when assembled they form the molecular complexes which are called secondary building units (SBU). In most zeolite structures the primary structural units AlO_4 or SiO_4 tetrahedra are assembled into secondary building units such as hexagonal prisms, cubes or cubo-octahedra. There are nine such building units, which might be accustomed to describe all famous zeolite catalysts. The topologies of these units are presented (see Figure 1-3). Assemblages of the secondary building units form the final framework structure [24].

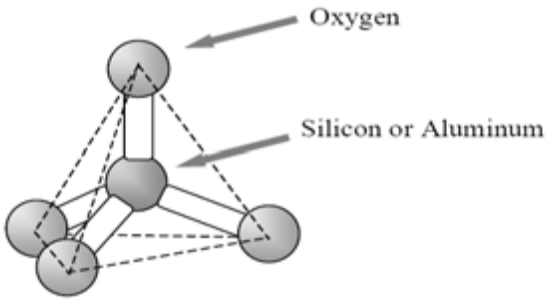

Figure 1-2: Primary building unit of zeolite structure [24]

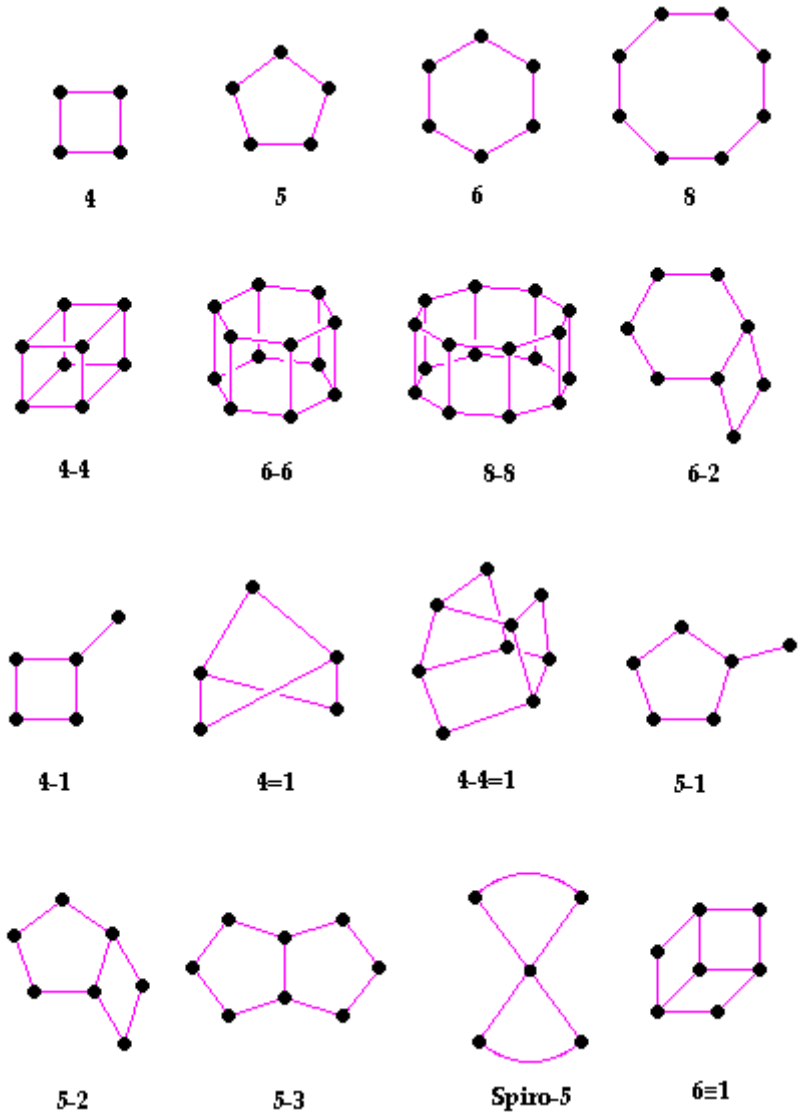

Figure 1-3: Secondary building units (SBU's) in zeolites. [Note that the corner of the polyhedra represents tetrahedral atoms [25]].

Table 1-2: Classification of zeolite structures [24]

Number of linked tetrahedra	SBU created	Shorthand Description
4	4 oxygen ring	S4R
5	5 oxygen ring	S5R
6	6 oxygen ring	S6R
8	8 oxygen ring	S8R
8	4-4 oxygen ring	D4R
12	6-6 oxygen ring	D6R
16	8-8 oxygen ring	D8R

(S = single, D = double, R = ring)

1.4.3 Zeolites Classification

Zeolites classification has been made on the basis of various aspects such as their morphological characteristics, chemical composition, crystal structure, effective pore diameter and natural occurrence.

Table 1-3: Classification of zeolites according to chemical composition

No.	**Class**	**Si/Al ratio**	**Examples**
1	Low silica zeolites	1-1.5	A, X
2	Intermediate silica zeolites	2-5.0	(a) Natural zeolites: Erionite, Chabazite, Clinoptilolite, mordenite (b) Synthetic zeolites: L, Y, omega, large pore mordenite
3	High silica zeolites	10-several thousands	(a) By direct synthesis: ZSM-5, ZSM-11, EU-1, EU-2, Beta (b) By thermochemical framework modification: Mordenite, Erionite, highly silicious variant of Y

Bragg classified zeolites based on their morphology. According to Bragg classification, zeolites are classified as fibrous, lamellar and those having framework structures. Meier and Barrer further modified Bragg's classification according to the secondary building units present in them.

Classification of a zeolite depending on their chemical composition has been made on the basis of their silica to alumina ratio (Table 1.3). The thermal stability increases with increasing silica content. For example, it increases from about 700^{o}C in the low silica zeolites to 1300^{o}C in the high silica molecular sieves.

Zeolites can be also classified depending on their pore openings into small, medium and large pore zeolites which contain 8, 10 and 12 membered ring pore openings, respectively. According to their pore opening, some of the common zeolites which take account of both natural and synthetic zeolites are listed in Table 1-4. Small pore zeolites are zeolites with pores that are consist of eight T-atoms and eight oxygen atoms. They have free diameters of 3.0 - 4.5 Å. Medium pore zeolites are zeolites with pores that are consist of ten T-atoms and ten oxygen atoms and with 4.5 - 6.0 Å free diameter. Large pore zeolites are zeolites with twelve or more T-atoms in rings that make up the pores and they have free diameter of 8.0 Å or more.

Table 1-4: Classification of zeolites according to the pore openings

Eight-Membered Ring (Small pore)	Ten-Membered Ring (Medium pore)	Twelve-Membered Ring (Large pore)
Linde A	Dachiardite	Cancrinite
Bikitaite	Epistilbite	Linde X, Y, L, EMT
Brewsterite	Ferrierite	Gmelinite
Chabazite	Heulandite	Mazzite
TMA-E	Laumonitite	Mordenite
Edingtonite	ZSM-5	ZSM-12
Erionite	ZSM-11	Omega
Gismondine	EU-l	Beta
ZK-5	EU-2	
Levynite	Stilbite	

A. Natural Zeolite

Zeolites can either occur naturally or produced industrially on a large scale. Over 40 naturally occurring zeolite frameworks are known and 206 unique zeolite frameworks have been identified as of October 2012 [26].

When volcanic rocks and ash layers exposed to alkaline groundwater, natural zeolite will be formed. Over periods extending from thousands to millions of years in shallow marine basins in post-depositional environments zeolites can also formed. Various degrees of other minerals, metals, quartz, or other zeolites might contaminate naturally occurring zeolites. Therefore, naturally occurring zeolites are not often pure. For this reason, naturally occurring zeolites are absent from many important commercial applications where uniformity and purity are required.

Table 1-5: The most common natural zeolites [27]

Zeolite type	Crystallographic formula
Analcime	$Na\,[AlSi_2O_6] \cdot H_2O$
Chabazite	$(Ca_{0.5}, Na, K)_4\,[Al_4Si_4O_{24}] \cdot 12H_2O$
Clinoptilolite[1]	$(Me^{I}, Me^{II}_{0.5})_6\,[Al_6Si_{30}O_{72}] \cdot\sim 20H_2O$
Erionite	$K_2\,(Na, Ca_{0.5})_8\,[Al_{10}Si_{26}O_{72}] \cdot\sim 30H_2O$
Faujasite[2]	$(Na, Ca_{0.5}, Mg_{0.5}, K)_x\,[Al_xSi_{12-x}O_{24}] \cdot 16H_2O$
Ferrierite	$(K, Na, Mg_{0.5}, Ca_{0.5})_6\,[Al_6Si_{30}O_{72}] \cdot 18H_2O$
Heulandite[1]	$(Me^{II}_{0.5}, Me^{I})_9\,[Al_9Si_{27}O_{72}] \cdot \sim 24H_2O$
Laumonitite	$Ca_4\,[Al_8Si_{16}O_{48}] \cdot 18H_2O$
Mordenite	$(Na_2, Ca, K_2)_4\,[Al_8Si_{40}O_{96}] \cdot 28H_2O$
Phillipsite[3]	$(K, Na, Ca_{0.5}, Ba_{0.5})_x\,[Al_xSi_{16-x}O_{32}] \cdot 12H_2O$

[1]Isostructural species, code [HEU]; Me^{I} = (Na, K); Me^{II} = (Ca, Sr, Ba, Mg)

[2]x =3.2–4.4

[3]$x \approx 4–7$

B. Synthetic Zeolites

The first attempts to prepare synthetic zeolites were made more than a century ago. St. Claire Deville in 1862 succeeded to synthesize a zeolite named Levynite [28]. Nowadays more than 170 zeolite structure types are known, most of them have no natural analogues [29]. However, the organized research efforts on synthetic zeolites were started by Richard M. Barrer in the late 1930's. He initiated the first classification of zeolites depending on size in relation to molecular sieve properties (Barrer, 1945). Researchers at Union Carbide developed synthesis techniques for preparation of the earliest synthetic zeolites such as zeolites A, X, and Y that would find industrial applications following Richard M. Barrer ground breaking work. There has been continuous and vigorous industrial interest and involvement in zeolite research since then.

1.4.4 Nomenclature of Zeolites

Zeolites are designated by three capital letters, following IUPAC rules. These codes are not dependent upon atomic composition, cell dimensions or geometry. They are derived from the names of the types of the materials.

Due to various ways in which the secondary building units can be linked to form different polyhedra, a number of possible zeolite structures can be formed. For example, cubo-octahedron also referred to as a sodalite unit or β-cage results only if 24 tetrahedra are linked as shown in Figure 1-4. It is an important secondary building unit from which various zeolite structures drives. Networks of regular channels and cavities are created by these polyhedra. Each sodalite cage consists of 24 linked tetrahedral which are further connected to form different zeolites with distinct framework topologies as showed in Figure 1-5. The last one presents the general framework topologies of zeolites A/ZK-4 and zeolites X/Y, and that of sodalite, $Na_3Al_3Si_3O_{12}$. The small face sharing β-cages characteristic of sodalite are linked through double four ring and six ring units in zeolites A/ZK-4 and zeolites X/Y, respectively, to produce larger cages. Each type of zeolite has specific uniform pore size such as 3.5-4.5 Å for zeolite LTA, 4.5-6.0 Å for ZSM-5 and 6.0-8.0 Å for zeolite X, Y type [21].

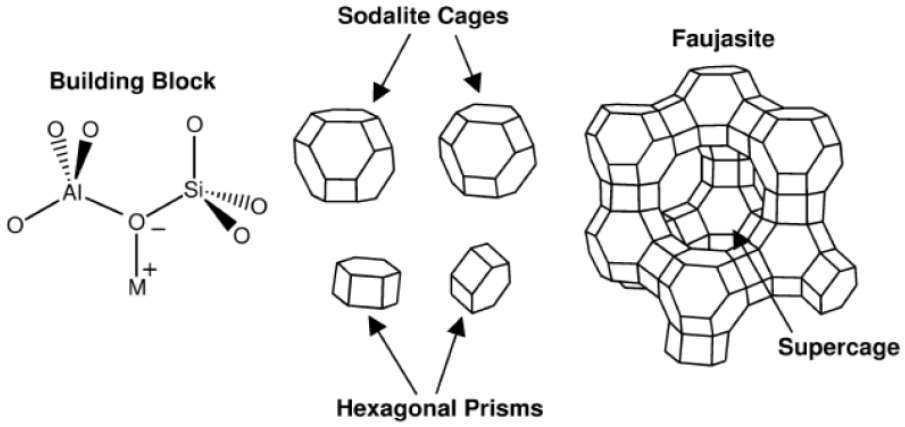

Figure 1-4: Schematic diagram of a faujasite-type zeolite, M^+ is a charge-balancing cation [30].

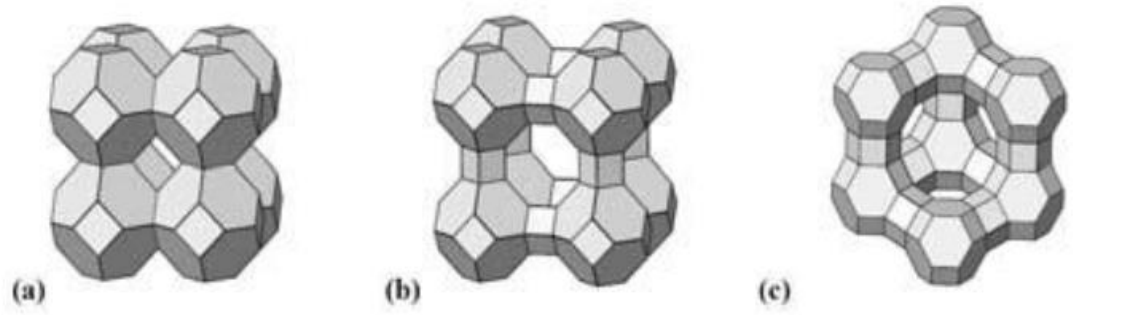

Figure 1-5: Framework topologies of: (a) Sodalite; (b) Zeolite A/ZK-4; (c) Zeolites X/Y

Three-dimensional frameworks are given by a unique three-letter code. On the basis of crystallographic reports the Structure Commission of the International Zeolite Association (IZA) determines and assigns a three letter code to zeolite "topology" [31]. A convenient but arbitrary subdivision of phases in this range is given by Barrer. The International Zeolite Association database shows that the number of structural types of unique microporous frameworks has been growing rapidly, from 27 in 1970 to 133 in 2001, whereas currently this has reached 180 [31, 32]. Zeolites framework types have been presented (See Table 1-6).

Table 1-6: Zeolites Framework Types [33]

ABW	ACO	AEI	AEL	AEN	AET	AFG	AFI	AFN	AFO	AFR	AFS
AFT	AFX	AFY	AHT	ANA	APC	APD	AST	ASV	ATN	ATO	ATS
ATT	ATV	AWO	AWW	BCT	*BEA	BEC	BIK	BOF	BOG	BPH	BRE
BSV	CAN	CAS	CDO	CFI	CGF	CGS	CHA	-CHI	-CLO	CON	CZP
DAC	DDR	DFO	DFT	DOH	DON	EAB	EDI	EMT	EON	EPI	ERI
ESV	ETR	EUO	EZT	FAR	FAU	FER	FRA	GIS	GIU	GME	GON
GOO	HEU	IFR	IHW	IMF	IRR	ISV	ITE	ITH	ITR	-ITV	ITW
IWR	IWS	IWV	IWW	JBW	JRY	JST	KFI	LAU	LEV	LIO	-LIT
LOS	LOV	LTA	LTF	LTJ	LTL	LTN	MAR	MAZ	MEI	MEL	MEP
MER	MFI	MFS	MON	MOR	MOZ	*MRE	MSE	MSO	MTF	MTN	MTT
MTW	MVY	MWW	NAB	NAT	NES	NON	NPO	NPT	NSI	OBW	OFF
OSI	OSO	OWE	-PAR	PAU	PHI	PON	PUN	RHO	-RON	RRO	RSN
RTE	RTH	RUT	RWR	RWY	SAF	SAO	SAS	SAT	SAV	SBE	SBN
SBS	SBT	SFE	SFF	SFG	SFH	SFN	SFO	SFS	*SFV	SGT	SIV
SOD	SOF	SOS	SSF	SSY	STF	STI	*STO	STT	STW	-SVR	SZR
TER	THO	TOL	TON	TSC	TUN	UEI	UFI	UOS	UOZ	USI	UTL
UWY	VET	VFI	VNI	VSV	WEI	-WEN	YUG	ZON			

1.4.5 Active Sites in Zeolite

The charge imbalance of the silicon and aluminium ions in the zeolite framework structure is responsible for the creation of acidic sites. These acid sites impart the activity to the catalysts. Thus, each aluminium atom present within the framework constitutes an active site.

The Bronsted and Lewis acid models classify active sites in zeolites. Bronsted acidity arises when the cation balancing the anionic framework charge is a proton (H^+), where as a trigonally coordinated aluminium atom, which acts as an electron acceptor, behaves as a Lewis acid site (See Figure 1-6). High temperature (>500 ^oC) may cause the transformation of the Bronsted acid sites to Lewis acid sites by dehydroxylation [34].

Hydrothermal treatment of the zeolite may result in the dealumination of zeolite producing a varity of cationic and neutral aluminium containing species which function as Lewis acid sites [35]. These extra framework cationic species can also enhance the activity of nearby Bronsted acid sites.

Measurement of acidity is an important step in estimating the activity of the catalyst. The activity and acid strength distribution in zeolites can be quantitatively determined by a variety of techniques like adsorption of bases, thermomertic titration, differential scanning calorimetry (DSC), temperature programmed desorption (TPD), IR specroscopy, MAS NMR, etc may be used to determine the activity and acid strength distribution in the zeolites.

Temperature programmed desorption is useful, simple and versatile method to determine the acidity but is strongly affected by heat and mass transfer as well as by multiple adsorption / desorption phenomena. Some researchers have also used gravimetric alkali titration to determine the acidity of zeolites [36].

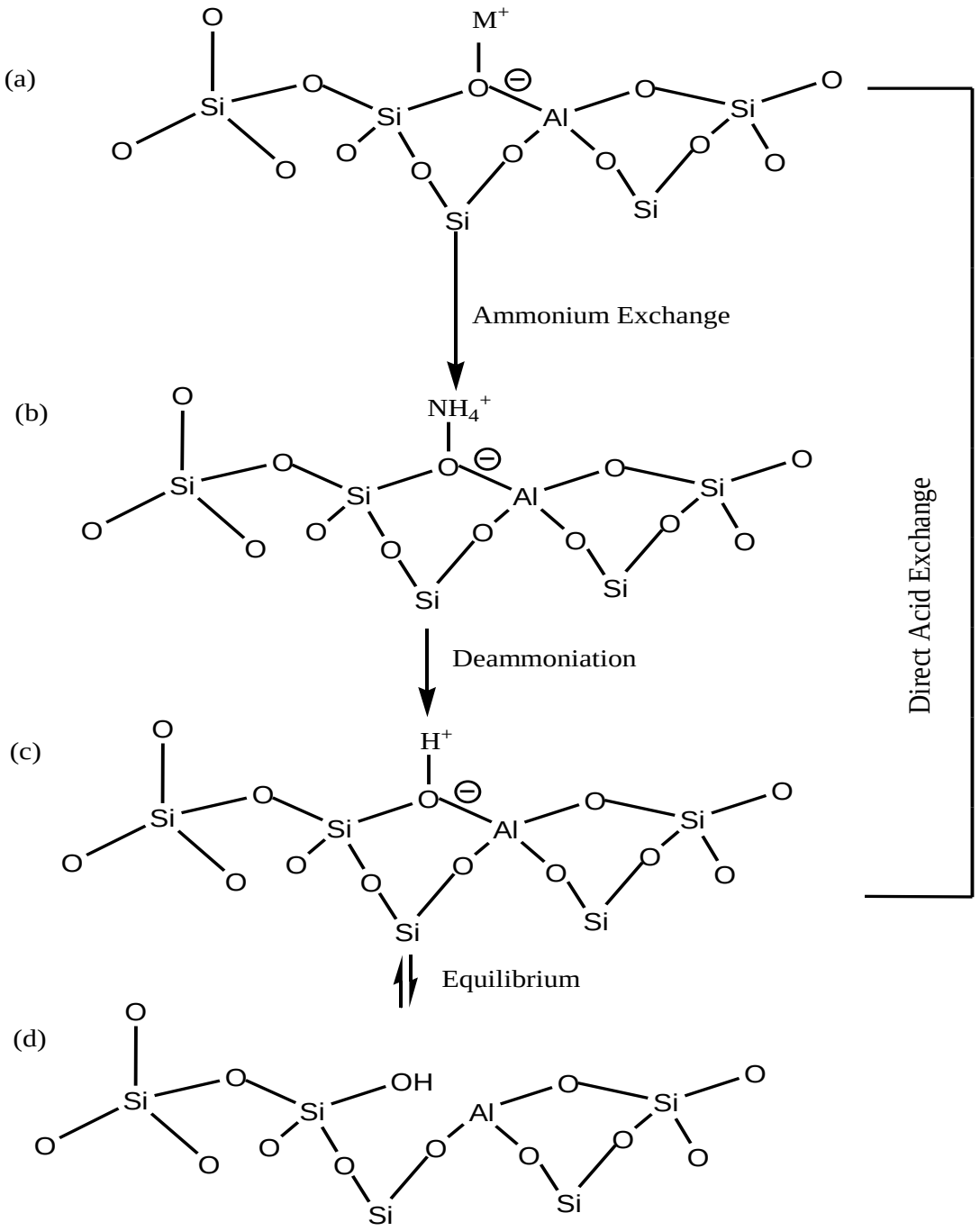

Figure 1-6: Schematic representation of the zeolite framework [37]

1.4.6 Zeolites as Shape Selective Catalyst

Shape selectivity is a unique characteristic of zeolites and related molecular sieves. The intracyrstalline surface of zeolites is an integral part of the crystal structure and, therefore, they are topologically well defined. As a result, zeolites are capable of the passage of organic molecules based on size and steric effects to limit or prevent. The effect is commonly known as shape selectivity. The basic concept of shape selectivity discussed in detail by many authors [38-40]. The shape selective characteristics of zeolite catalysts are due to the restriction of the acid sites in the zeolite pore architecture. The actual pore size within a given structure can be varied within limits of the cations available in the system. Based on the geometric boundary conditions three types of shape selectivity zeolites are attributed [39].

I. Reactant Shape Selectivity

When a mixture of two or more organic molecules used with different size and with zeolite in contact form, smaller molecules are allowed to diffuse into the channels, while the other large molecules are disabled (or screened out) is called reactant shape selectivity of this phenomenon. Chen et al., 1978 [38] have explained reactant shape selectivity based on the Coulombic interaction between the reactants and the zeolite. An important application of reactant shape selectivity practiced in the cracking of linear alkanes by the branched-chain ones, especially in the petrochemical industry.

II. Product Shape Selectivity

Product shape selectivity arises when one or more of the products within the pores or voids of the zeolite diffuse more rapidly than the other products formed, to leave behind the bulky molecules, which will be converted into either less bulky molecules that can diffuse out or subsequently disable catalyst. For example, p-xylene is produced preferably in modified zeolites over the bulky ortho and meta-isomers due to the pore diameter restrictions (See Figure 1-8). Direct confirmation for this type of shape selectivity has been reported by Anderson and Klinowski [41] for the catalytic conversion of methanol to hydrocarbons over ZSM-5.

III. Restricted Transition State Shape Selectivity

Restricted transition state shape selectivity (See Figure 1-8) arises when shape selective restrictions have an influence on the intrinsic kinetics rather than through diffusion limitations. This depends mainly upon the size and shape of the transition state complex made in the course of catalytic conversions inside the cavities of the zeolite. The products that result from less

bulky transition states are favourably formed. It has been found that the restricted transition state selectivity does not always lead the reaction path in zeolites, but electronic as well as thermodynamic effects prevail over steric effects [42].

1.4.7 Thermal Stability

Thermal stability of zeolite is intimately related to SiO_2 / Al_2O_3 ratio. High thermal stability helps to retain structural integrity during long reaction times in the presence of hydrocarbons and water. The regeneration temperature is higher than reaction temperature and the thermal stability plays a crucial role under such circumstances.

1.4.8 Coking of Zeolite

In the course of virtually all catalytic processing of hydrocarbons, coke accumulates on the surface of catalyst and retards its activity. Carbonaceous deposits that accumulate on zeolite catalysts can be classified as either hard or soft coke**.**

Hard coke is generally derived from aromatic hydrocarbons that are present in the feed or that are generated during the reaction. It is typically formed at higher temperatures (e.g. >427 ^{o}C) by the reactions that occur within acidic zeolites. Hard coke formation involves initial adsorption of highly unsaturated hydrocarbons followed by condensation and elimination reaction.

In contrast, soft coke is generally formed by oligomerization or alkylation reactions involving olefins and paraffins or naphthenes. Soft coke is normally formed at low temperatures and usually within the zeolite. Whereas the compounds that constitute soft coke might normally be soluble in hot solvents, the branched nature of these compounds prohibits them from being extracted from the zeolite. Hydrogen to carbon atomic ratios in the soft coke is typically greater than 1.25, while hard coke has typically less than 1.25. Coke forming reactions lead to increased diffusional limitations and pore blocking of the zeolite catalysts [43].

1.4.9 Regenerability

Polyaromatic compounds formed during the hydrocarbon conversion processes adsorb on the catalytic active sites and cause the deactivation of the catalyst. Activity can be regained by oxy-decomposition of the carbonaceous deposits. High thermal stability and shape selective features of the zeolites make them to withstand high regeneration temperatures. Thus, the initial

activity of the zeolite catalyst can be regained by the burning off the coke on the deactivated catalyst.

1.4.10 Zeolites Modification

Zeolites in synthesized form typically contain quaternary amine cations along with residual inorganic cations such as alkali metal cations, most typically sodium. The reactivity and the selectivity of molecular sieve zeolites as catalysts are determined by active site provided by an imbalance in the charge between the silicon and aluminum ions in the framework structure. In order to produce acidic zeolite catalyst, it is necessary to replace the cations in the freshly synthesized material with protons.

The zeolites can be modified suitably by one or more of the following ways:

I. Modification by Isomorphous Substitution

Isomorphous substitution of lattice silicon and aluminum atoms by other elements are carried out either during the hydrothermal synthesis (primary synthesis) [44], or by the post-synthesis (secondary synthesis) methods [45]. In recent years, isomorphous substitution of Si by external elements such as B [44], Fe [46], Ti [47], etc. is widely studied and has been shown in different catalytic properties. Isomorphous substitution modifies the strength of the Brønsted acid sites. The substitution of other ions for Al^{+3} and Si^{+4} in the zeolite frameworks, may change the zeolite properties. The discovery of titanium has substituted ZSM-5 led to remarkable progress in new technology for the production of chemicals, which are obtained as the oxidizing agent by the selective oxidation reactions, in particular with aqueous H_2O_2. Rossin et al., 1987 [48] showed that Co^{2+} can be installed in tetrahedral atomic positions within the framework of ZSM-5. The studies illustrated the possibility backbone atoms as isolated redox centers to use in microporous environments.

There are four types of isomorphous substitution in zeolites according to Barrer's classification:

1. One guest molecule by another (i.e. substitution of NaCl by sodium sulphate transforms sodalite into Nosean.)
2. One cation by another (i.e. treatment of a zeolite with an aqueous solution of the salt containing different cation ~ it is the base of water sweetening.
3. One element by one of its isotopes (i.e. mainly H_2, O_2 and Si)

4. One element in the tetrahedral position by another (i.e. substitution of Si or Al with sterically compatible elements.)

The first one is not essential in catalytic applications. The second is valuable in making bifunctional catalysts. The third one is beneficial in characterizing the zeolite materials. The last one is very essential in substituting different elements into the zeolite framework.

Zeolites modification by isomorphous substitution may give new properties, which may lead to interesting catalytic applications. T-elements can occupy one or more of the following positions in zeolites. Framework sites, exchange positions, defect sites, either inside the pores or on the external sites as metal oxide.

II. Modification by Cation Exchange

Several zeolites are synthesized in a cationic form in which the positively charged cations balance the negatively charged framework system. These extra cations in the framework can be substituted by other cations [36]. The possibility of the replacement of metals in the zeolite framework has been reviewed in many articles [49, 50].

The rate and degree of cation exchange depends on the following factors:

1. The type of cation being exchanged, the size and charge
2. The nature, size and strength of any cation co-ordination complex
3. The temperature of the ion-exchange treatment
4. The thermal treatment of the zeolite, before or after exchange
5. The structural properties of the zeolite and its silica / alumina ratio
6. The locations of the cations in the zeolite structure
7. The concentration of the cation exchange solution
8. The previous treatment of the zeolite

III. Modification by Metal Loading

For several industrial reactions, e.g. such as the hydrogenation or oxidation, it is necessary to have additional components in the catalyst to meet the full or partial catalytic function. Such components are often metals, their oxides or sulphides similar to those used in non- zeolite or amorphous catalyst systems.

Metals which are required for the introduction into the zeolite and / or catalysts include the usual hydrogenation and oxidation components such as Ni, Co, Pt, Ag, Pd, Mo, W, Cr and

the like. The metal loading may be applied by different ways. These include ion exchange the zeolite from the solution, adsorption from the gaseous phase and co-grinding during the catalyst formation of the solid metal component or its solution.

1.4.11 ZSM-5

Zeolite ZSM-5 is a shape-selective microporous material with 10-membered ring pores. ZSM-5 is a member of the pentasil family and its structure was confirmed by Kokotailo et al. 1978 [51]. It consists of a novel configuration of sharing tetrahedra which are organized in groups that attached together of eight secondary building units of five membered rings (See Figure 1-7). These units together form chains, and the composite of these chains leads to the formation of the channel system within the structure. The combination of these building blocks leads to a framework with two intersecting channel systems of sinusoidal and the other is straight.

Sinusoidal channel has near circular opening having a diameter from 5.4 to 5.6 Å and the straight channel elliptical opening has a diameter from 5.2 to 5.8 Å [52]. The nomenclature and structural description of ZSM-5 are given (See Table 1-7).

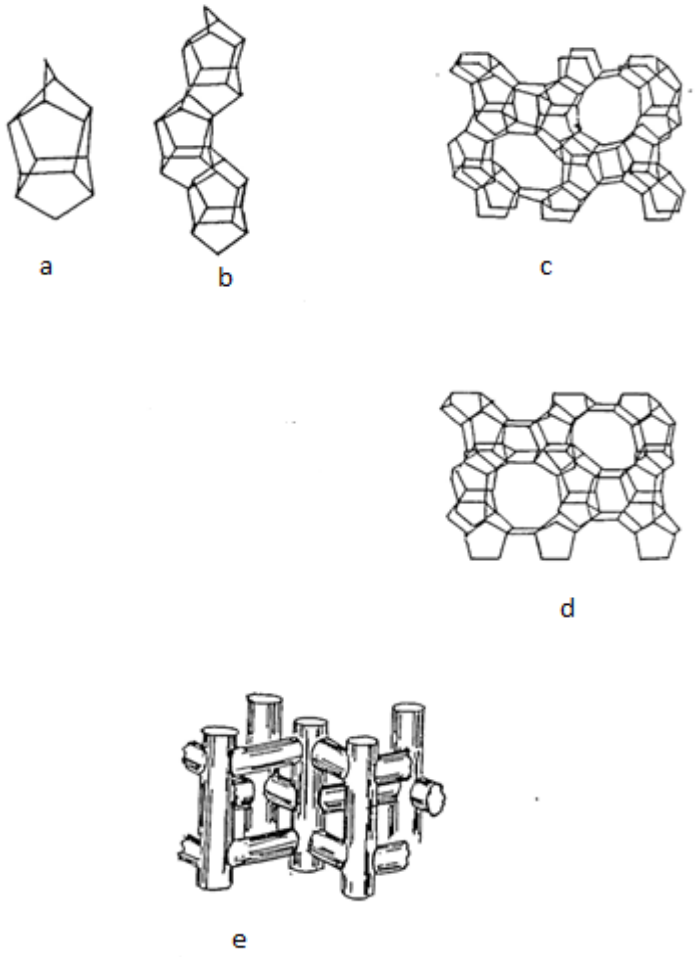

Figure 1-7: Structure of ZSM-5 zeolite [52]

(a) Characteristic configuration of ZSM-5 zeolite (b) Connection of ZSM-5 zeolite (c) Skeletal diagram of 010 face zeolite ZSM-5 (d) Skeletal diagram of 100 face zeolite ZSM-5 (e) Channel structure of zeolite ZSM-5

Table 1-7: Structure of ZSM-5 [53]

Framework Type	MFI
Composition	$\|Na^{+}_{n}\ (H_2O)_{16}\|\ [Al_nSi_{96-n}\ O_{192}]$, n < 27
Secondary building unit	5-1
Unit cell	Orthorhombic, a=20.07Å, b=19.92Å, c=13.42Å α=90° β=90° γ=90°
Framework density	17.9 T/1000 $Å^3$
Channels	{[100] 10MR 5.1 x 5.5 <-> [010] 10MR 5.3 x 5.6} (3-dimensional)

It has been found that the pore structure of the ZSM-5 zeolite pore dimensions is so called medium pore zeolites. This is an important feature of the ZSM-5 structure, which has an impact on its shape selective catalytic properties. If it is converted to the proton form, ZSM-5 can be used as a solid catalyst and a shape-selective matrix in hydrocarbon conversion reaction processes [54]. The greater shape selective properties of ZSM-5 lead to the expansion of industrially important processes.

1.4.11.1 Characterization of ZSM-5 Zeolite

A large number of techniques used for the characterization of zeolites and their precursors. Some of the widespread characterization techniques are important structural identification and acid determination. Structural identification is usually done by XRD pattern and IR- spectrogram.

XRD patterns of synthesized materials are compared with those of ZSM-5 zeolite in the literature. Quantitative measurement of crystallinity of zeolite may also be done by X-ray diffraction technique (three lines corresponding to a 2Θ range from 22.5 to 25.0 degrees have been used for the calculation of the present crystallinity of zeolites ZSM-5). IR spectroscopy has been recognized as a useful tool in the structural investigation of zeolites in recent years. Chao et al., (1981) [55] and Jacobs et al., (1981) [56] had studied the IR spectra of ZSM-5 crystals. Chao et al., (1981) [55] found adsorption bands of external linkages at 400, 545, 800 and 1000-1200 cm^{-1}. The band at 540 cm^{-1} has been assigned by Jacobs et al. (1981) to highly distort five membered double rings present in the ZSM-5 structure. The strong adsorption band in the region 1000-1200 cm^{-1} has been assigned to the internal vibrations of SiO_4 and AlO_4 tetrahedral for ZSM-5 and also for silica and quartz [57]. In addition, IR frequencies of adsorbed probe molecules were used to evaluate Brønsted and Lewis acid sites.

1.4.11.2 Properties of ZSM-5 Zeolite

A. General properties of ZSM-5

ZSM-5 zeolites exhibit some special features:

- ZSM-5 zeolites do not have any super cages with small size windows like other zeolites, and all the pores have uniform dimensions. Because of this molecules larger than the sizes of the channel are not formed (the exception perhaps at the intersections) inside the zeolites.

- High strength of acidity and well separated active sites (high Si/Al ratio) lead to cracking of olefins and olefins intermediates and oligomerization. In the case of zeolite, the cage proximity of acid sites allows the formation of long chain compounds and poly aromatic core molecules [58].
- The pore dimensions of ZSM-5 are suitable for the formation of C_7 and C_8 olefins and their cyclization to corresponding aromatic compounds in the consecutive steps. This unique property of ZSM-5 restricts the formation of di- and tri- cyclic aromatic compounds.

B. Shape Selectivity of ZSM-5

The particular property which makes the ZSM-5 zeolite especially useful for commercial application is its shape selectivity.

The uniform and medium sized pore openings of the ZSM-5, which can determine the fate of reactant molecules and the probability of forming product molecules, made the zeolite of pentasil family suitable for the shape selective catalysis. Zeolite ZSM-5 differs greatly from most other molecular sieves in that its shape selectivity has a very wide dynamic range [59].

Shape selectivity can be classified as (a) reactant selectivity (b) restricted transition state selectivity and (c) product selectivity.

(a) Reactant Selectivity

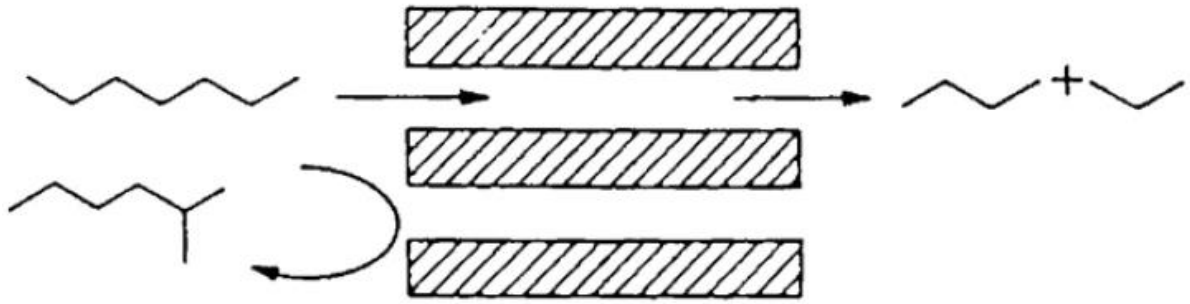

(b) Product Selectivity

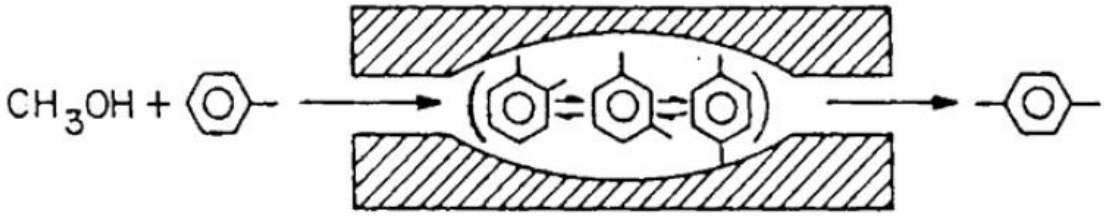

(c) Restricted Transition State Selectivity

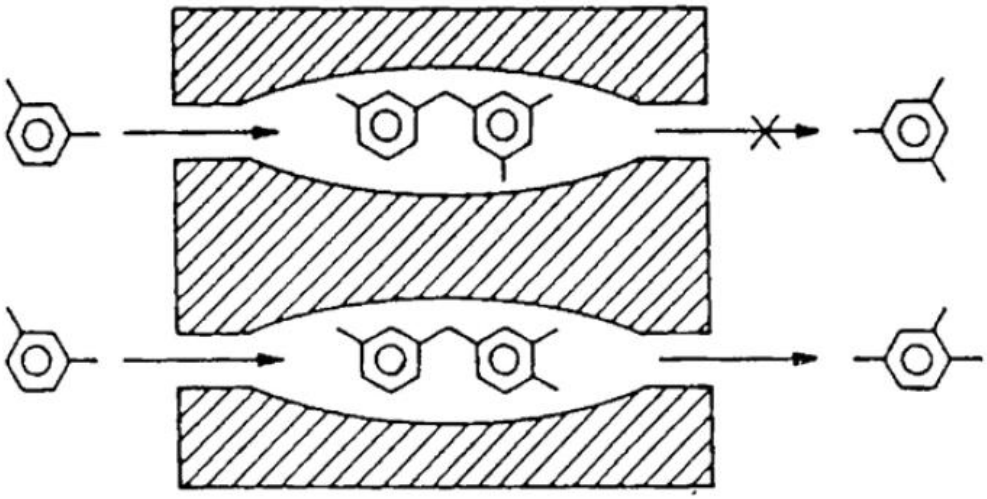

Figure 1-8: Shape selective features of the ZSM-5 zeolite [39]

1.5 Ethylbenzene Production using Alkylation of Benzene

1.5.1 Conventional Processes

In the conventional method, developed in the 1930s, the alkylation is performed at mild conditions (T = 433K) in the existence of a Friedel-Crafts catalyst by reacting benzene and ethylene. The ethylbenzene produced by alkylation of benzene with ethylene, may undertake polyalkylation to other polyethylbenzenes, according to the reactions illustrated in Scheme 1-1.

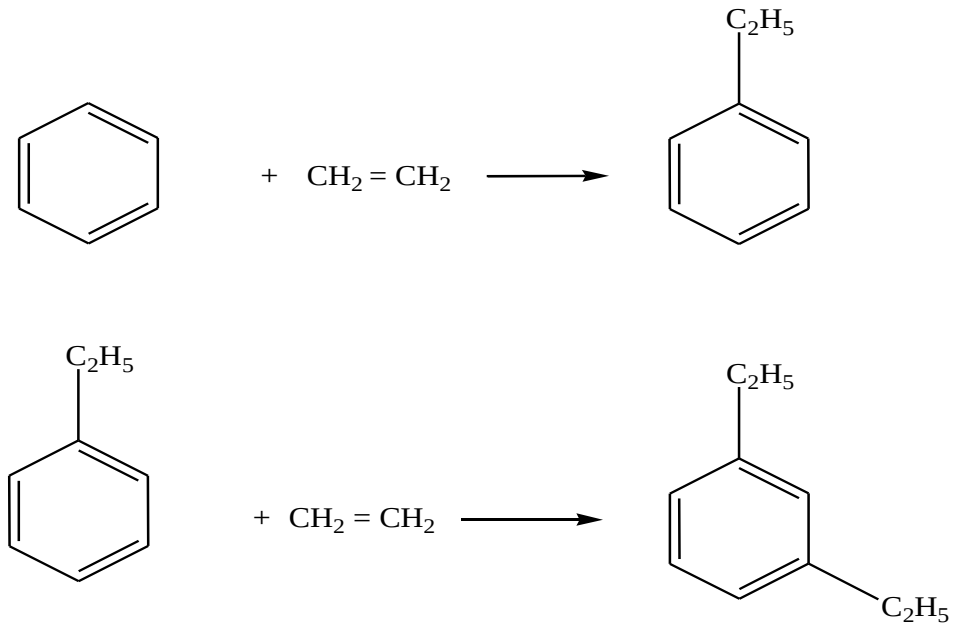

Scheme 1.1

Polyethylbenzenes are reused back to the alkylation process after separation of the product. Here, until the thermodynamic equilibrium is reached polyethylbenzene transalkylation takes place (Scheme 1.2).

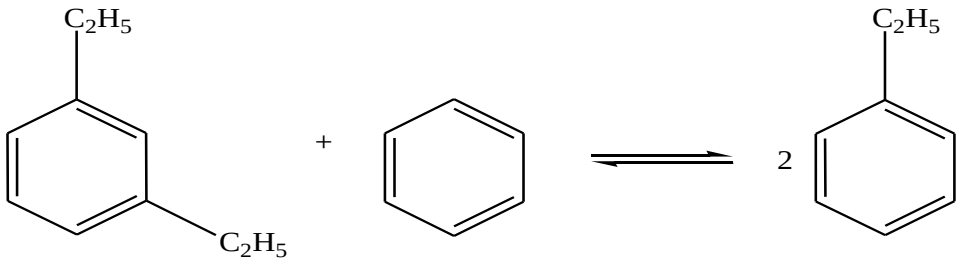

Scheme 1.2

The reaction is carried out in the liquid-phase and, because of the corrosive effect of the catalyst, the process is performed in enamelled or glass lined reactors.

As a possible solution to the problems of corrosion, supported catalysts in the 1960s by UOP for liquid phase (BF_3 / Al_2O_3 in Alkar^{TM} method) and the gas phase (Kieselguhr supported phosphoric acid (SPA)) operations have been proposed. However, due to the partial release of acids, corrosion problems were not completely avoided. Furthermore, these catalysts

are not active in the transalkylation of polyethylbenzenes and cannot be regenerated. For these reasons, such methods do not get great industrial interest.

1.5.2 Solid Acid Catalysts for Alkylation

In the 1940s was the time when the first solid acid catalysts for the alkylation of benzene with ethylene (and propylene) were used in the vapor phase. They were based on amorphous silica-alumina gel, as used in commercial catalytic cracking processes [60].

Starting from the mid-1960s, zeolite catalysts have been evaluated extensively in benzene alkylation with ethylene and in 1966 Venuto et al., (1966) [61] reported that large pore zeolites (REX, HY and REY) are effective catalysts as amorphous silica alumina gels. In addition, as far as REX is concerned, it was found that the catalyst life is better operation found in the liquid phase than in the gas phase, in both the alkylation and transalkylation.

Despite the large amount of research, the first industrial application of a zeolite catalyst occurred in 1976 by Mobil-Badger. This new method was called second generation Mobile-Badger process. Second generation Mobile-Badger process was commercialized in 1980. The alkylation of benzene was carried out in a gas phase fixed bed reactor (for example, T=390-450 °C), using a ZSM-5, a zeolite with medium pore. Similar to $AlCl_3$-HCl method the polyethylbenzene recycled back into the reactor to undertake transalkylation. ZSM-5 has a low coke-forming tendency and thus life cycles between regenerations up to 40-60 days are possible [3]. A second reactor has been commercialized with the third generation process, in the 1990s, where, in the first place for the transalkylation, significantly improve performance (Table 1.8).

Table 1-8: Ethylbenzene production processes [3]

	Process (year)						
	Monsanto – Lummus (<1975)	Mobil Badger Second generation (1980)	Lummus /Unocal/ UOP (1989)	Mobil Badger Third generation (1990)	CDTECH EB (1994)	Mobil-Raytheon EBMax (1995)	Lummus/UOP EBOne (1996)
Alkylation							
T (^{o}C)	160	390-440	240-270	390-440			
Catalyst	$AlCl_3$	ZSM-5	Y	ZSM-5	Y	MCM-22	EBZ-500
Phase	Liquid	Vapour	Liquid	Vapour	-	Liquid	Liquid
Feed ratio	2.5	7.6	7.2	7.6	-	4	4-6
Life (year)	-	0.25	1	1	5	3	2
Transalkylation	No	No	Yes	Yes	Yes	Yes	Yes
Catalyst	-	-	Y	ZSM-5	Y	ZSM-5	EBZ-100
Phase	-	-	Liquid	Vapour	Liquid	Vapour	Liquid
Yield (%)	99.7	98.1	98.2	99.2	99.7	99.5	99.6

1.5.3 Alkylation under Liquid Phase Reaction with Zeolite Catalysts

Lummus/Unocal/UOP first initiated the liquid-phase ethylbenzene process in 1989. The first commercial plant was started up in 1990 using a zeolite catalyst. The liquid-phase process has the benefit of a better thermal control and a longer catalyst life (Table 1.8). The catalyst is based on Y type zeolite, established for the alkylation by Unocal since 1979 [62].

Other large pore zeolites, which are the most suitable in order to overcome the observed diffusion limitations in liquid-phase operation, were regarded as catalyst for ethylbenzene production (for example, L, Omega, Mordenite, ZSM-12, Beta). On account of these investigations in the early 1990s [63], zeolite beta was performed better than Y (Table 1.9). According Bellussi et al., 1995 [64], zeolite Beta is more selective than zeolite Y because of different topologies in the channel systems. In the case of beta zeolite the channel openings (0.57 nm x 0.75 nm x and 0.65 nm x 0.5 nm) are only slightly larger than the size of the benzene molecule and do not allow the formation of these molecules having a critical diameter significantly larger. On the other hand, in the case of Y-zeolite, super cages (diameter = 1.2 nm) are available that enable voluminous byproducts formation. Zeolite beta was also found to be a good catalyst for transalkylation of m-diethylbenzene in the liquid phase. Zeolite beta exhibits better selectivity, the production of less diphenylethanes and xylenes [65].

Recently, zeolite MCM-22 has been shown good performance in the liquid phase alkylation to give alkylation of benzene with ethylene [66]. In particular, MCM- 22 shows that a catalytic activity which is comparable (lower deactivation rate) to USY and about 2.4 times less than zeolite Beta. On the other hand, MCM-22 is much more selective than USY and Beta, in much smaller quantities to produce diethylbenzenes [66].

A new catalyst based on MCM-22 was used recently in a new technology called EBMax^{TM} by Mobile-Raytheon to manufacture ethylbenzene. The alkylation is carried out in liquid phase, while the transalkylation functioned in the gas phase with a ZSM-5 based catalyst in this technology. In 1997 the first industrial use was applied (Table 1.8). In recent times, a new zeolite catalyst (trade name TRANS-4) was designed so that the transalkylation is carried out in the liquid phase. The type of zeolite has not been disclosed.

Since 1989, Lummus/UOP has liquid phase methods that have been improved. Currently the commercialized process called EBOne is emerged. In the alkylation and transalkylation process two different zeolite catalysts (UOP tradename EBZ-500 and EBZ-100) are used. There were no data available on the zeolite used for the preparation of these catalysts

is disclosed, but according to the patent literature is believed to be a modified zeolite beta. The performance of this new process is comparable to those reported for EBMax^{TM} (Table 1.8).

CDTech, a corporation between ABB Lummus Chemical Research and Licensing, established an enhanced technology for ethylbenzene production based on a catalytic distillation process. In the catalytic distillation, reaction and distillation occur in a single column simultaneously with the catalyst contained in bales and in the distillation column reactor stacked. As a result of distillation, the reaction products from the catalytic zone are continuously removed, and a low production of polyethylbenzenes gained. Nevertheless, a transalkylation reactor is required (Table 1.8). Several industrial plants have been recently redesigned or with this new liquid phase implemented technologies. Accordingly, only 24 % of world production is still based on $AlCl_3$-HCl technology. The remainder is almost on zeolite catalysts basis: 40% in the gas phase and 36% in the liquid phase.

Table 1-9: Zeolite performances in benzene alkylation with ethylene [3]

Catalyst	**Conversion (%)**	**Selectivity (%)**			
		Ethylbenzene	Diethylbenzene	Triethylbenzene	Other
Zeolite Y	100	82.0	8.4	0.7	8.8
Zeolite Beta	100	91.1	7.9	0.3	0.7

1.5.4 Benzene Alkylation with Ethanol

The conventional method making ethylbenzene is based on benzene alkylation with ethylene in the existence of an acidic catalyst [67]. Ethylene which used as raw material for ethylation reaction is manufactured from thermal cracking of hydrocarbons such as ethane, naphtha, gas condensates and liquefied petroleum gas [68]. Ren et al. (2006) [68] discovered that the highly endothermic steam cracking process, in which the energy input could be generated by direct burning of fuel, presently accounts for approximately 180-200 $*10^6$ tons of CO_2 emissions worldwide. Though, the energy cost adds approximately seventy percent of the production costs in typical ethane and naphtha based alkenes plants [68]. Accordingly, the process enhancements, especially the replacement of ethene feed, in the current commercial ethylbenzene production would be advantageous in terms of environmental and economic perspectives.

Stable catalyst life for a long period of time and economic importance to those countries where biomass derived alcohol is a supplementary raw material for the production of chemicals in the manufacture of ethylbenzene are factors that make ethanol advantageous. Considering the advantages stated above for using ethanol as alkylating agent for the alkylation of benzene with the usage of zeolite catalysts offers an environmentally friendly method to ethylbenzene production by monitoring pore size for attaining better product selectivity.

Because of their acid-base properties zeolites are attractive materials for alkylation reactions. Brønsted acid sites are needed in order to the alkylation mechanism over acid catalysts proceed via the formation of methoxonium ion [69]. Chandawar et al. (1982) [4] reported a significant improvement in ethylbenzene selectivity by modification of ZSM-5 by phosphorus or boron to reduce the strong acid sites on the surface of the catalyst. Levesque and Dao (1989) [70] also studied the alkylation of benzene with ethanol using steam-treated ZSM-5 zeolite catalysts. They reported that at high benzene/ethanol molar ratio ethylbenzene selectivity increased. Gao et al. (2009) [71] studied the outcome of zinc salt on the synthesis of HZSM-5 for alkylation of benzene with ethanol. They observed that the increase in ethylbenzene selectivity was due to higher Lewis/Brønsted acid ratio and the smaller crystal size.

Besides to the development of catalysts and study of the reaction mechanism, the kinetics of benzene ethylation has been investigated over various types of zeolites. Different models based on reaction mechanisms of Langmuir-Hinshelwood-Hougen-Watson were proposed and a mathematical adjustment to the best model was found. The activation energy determined during ethylation of benzene over $AlCl_3$ impregnated 13X zeolite catalyst was approximately to be 60.03 kJ/mol at 3:1 of constant benzene to ethanol molar ratio. In the same way, Barman et al. (2006) studied kinetic model for benzene alkylation over cerium exchanged NaX zeolite catalyst [72]. The activation energy determined during ethylation of benzene over cerium exchanged NaX zeolite catalyst at 3:1 of constant benzene to ethanol molar ratio was approximately 56 kJ / mol. Ethylbenzene was considered the only product of the alkylation reaction, while other products like diethylbenzene (DEB) were negligible in most of the kinetic studies mentioned above. But most of the researchers had not paid much attention to the modification of the catalysts in benzene/ethanol reaction.

(a) Ethylation Reaction (Primary)

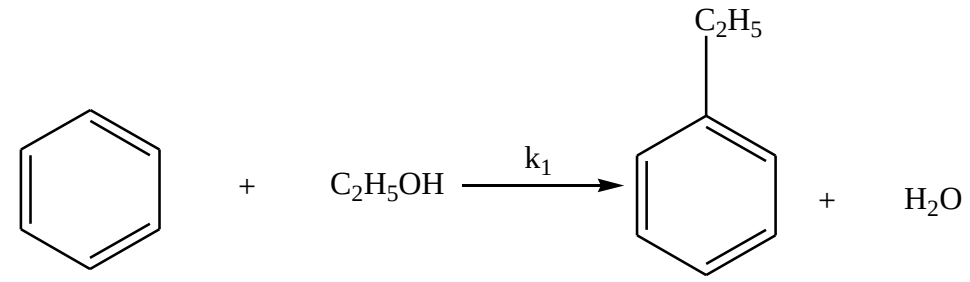

Benzene Ethanol Ethylbenzene

(b) Ethylation Reaction (Secondary)

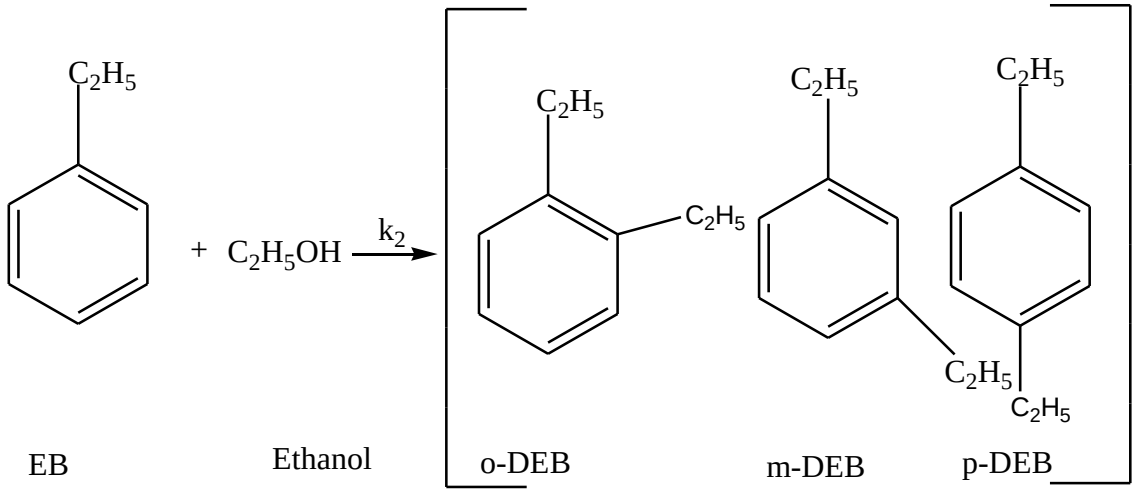

EB Ethanol o-DEB m-DEB p-DEB

Scheme 1.3: Reactions occurring during alkylation of benzene with ethanol [88].

1.6 GAPS TO BE COVERED AND OBJECTIVES

The method of using alkylation of benzene with ethylene over Friedel-Crafts catalysts is a traditional one and make up more than 90% of ethylbenzene manufacture. The use of these catalysts, however, causes many problems such as handling, safety, waste disposal, and corrosion. Therefore, developing simple and environmental friendly techniques have to become more and more imperative with oil crisis coming. Benzene alkylation with ethanol over zeolite catalysts is regarded as promising route for synthesis of ethylbenzene. Especially, as substituent of styrene, ethanol can be obtained from fermentation. Industrialization of this craft would bring energy revolution to the areas where oil is scarce. Recently, several efforts have been put on development of alternative environment-friendly catalyst systems. Zeolite-based catalyst systems are becoming very important in this respect and the conventional catalysts have replaced.

There are many shortcomings concerning its transportation and storage when ethylene is used as the ethylating agent. On the other hand, ethanol has been produced from the fermentation of agriculture wastes and by products on a large scale. The transportation and storage of ethanol are much safer. Direct ethylation of coking benzene with ethanol would be cost-effective.

Economic and environmental issues require high selectivity of catalysts of valuable substances, as this leads to the increased productivity of the process, the purity and quality of the product, reduced cost of the product and the amount of effluents and waste water. It is an important issue to develop clean technologies and highly efficient catalysts for the benzene alkylation for synthesis of valuable petrochemical alkylaromatic derivatives.

Instead of ethylene, the direct use of ethanol as an alkylating agent with benzene for alkylation reaction has several advantages. Stable catalyst life for a long period of time is observed when alcohol, rather than olefin, is used as an alkylating agent. Besides the scientific interest, the direct use of ethanol in the manufacture of ethylbenzene is also of economic importance to those countries where biomass derived alcohol is a supplementary raw material for the production of chemicals.

When ZSM-5 zeolites are modified by the incorporation of magnesium or boron compounds, strong acid sites concentration on the surface is eliminated and that, in addition, a reduction in effective pore size also occurs in the zeolite channels. In the alkylation process, compounds like toluene, xylenes and ethyltoluene are believed to be formed by the further reactions of ethylbenzene on the strong acid sites of the catalyst, lowering the selectivity for the desired ethylbenzene product. Suppression of the strong acid sites should eliminate these secondary products. Moreover, since C_{10+} aromatics (tri-and tetraethylbenzenes) are formed mainly on the outer surface of the zeolite crystals and in the large cavities formed by channel intersections, the elimination of the acid sites on the external surface coupled with the reduction in the effective size of the zeolitic cavities by magnesium or boron compounds should suppress the formation of these C_{10+}aromatics.

The aim was to study selectivity of ethylbenzene through benzene alkylation with ethanol over unmodified as well as modified HZSM-5 catalysts, the development of active and selective zeolite based catalysts for the synthesis of ethylbenzene with high yield and the effect of essential reaction variables such as reaction temperature (300-500 ^{o}C), amount of metal

loading, mole ratio of benzene and ethanol in the feed, effect of different silicon to aluminium ratio HZSM-5 and reaction environment.

To achieve the mentioned aim the following tasks have been set for the present thesis: HZSM-5 zeolite catalyst was modified with boron, magnesium monometallic and boron-magnesium bimetallic by wet impregnation techniques and their selectivity to ethylbenzene was compared with unmodified HZSM-5 catalyst. The developed catalysts were examined for the alkylation of benzene with ethanol using various ratios of benzene to ethanol in the feed. In addition to the above mentioned tasks characterization of unmodified and modified HZSM-5 zeolite catalysts were done using modern Physico-chemical methods of research.

CHAPTER TWO
LITERATURE REVIEW

The alkylation of hydrocarbons with olefins in the presence of $AlCl_3$ catalyst was first reported by M. Balsohn (1879) but C. Friedel and M. Crafts (1930) pioneered much of the early research on alkylation and $AlCl_3$ catalyst. About a century later, the process which employs classical Friedel-Crafts reaction chemistry remained as a major source of ethylbenzene production. Ethylbenzene was first manufactured on a commercial scale in the 1930s by Dow Chemical in the US and by BASF in the Federal Republic of Germany [3]. Since then many studies have been carried out over different catalysts. Although the literature was extensively searched works reported from 1930 onwards have been included in this chapter. Several types of catalysts such as 13X zeolite based, Y zeolite based, mordenite based, silica-alumina and ZSM-5 zeolite based catalysts have been used by a number of researchers for the alkylation of benzene. Recent developments in zeolite catalysis have generated a lot of interests in alkylation of benzene with ethanol due to transportation, storage and environmental issue. To enhance ethylbenzene selectivity, the researchers have used different types of zeolites, particularly ZSM-5 and its modifications. The studies related to catalyst characterization, mechanisms for alkylation reactions, development of environmentally friendly processes and the activities of zeolites etc. In the following section the research work reported in literature on alkylation of benzene and catalysts used for the above stated reaction have been discussed.

Venuto et al. (1965) investigated mechanisms for alkylation reactions. The results indicated that on the basis of product distributions, patterns of substrate reactivity, and advancement and deuterium tracer experiments, alkylation reactions catalysed by acidic faujasites, rare-earth-exchanged X and Y and HY are defined as processes via carbenium ion mechanisms. Sites which are active for alkylation in these three acidic faujasites were visualized as strongly acidic and ultimately protonic. In alkylation with low molecular weight olefins, complex intracyrstalline polymerization hydrogen transfer reactions of the olefin were revealed to be responsible for catalyst aging [61].

Perego and Ingallina (2002) reported massive improvements towards the development of environmentally friendly processes accomplished in the alkylations of aromatics with olefins, since the last four or five decades. Many efforts have been devoted to the exploration of solid catalysts suitable to substitute mineral or Lewis acids and free bases traditionally engaged

as catalysts. According to the authors, the structure of *BEA is the most proper for cumene synthesis, while MWW is the most suitable for ethylbenzene synthesis [3].

Degnan et al. (2001) reported an overview of current industrial alkylation processes for the making of ethylbenzene and cumene. In current years, zeolite catalysts have begun to replace the conventional aluminum chloride and solid phosphoric acid (SPA), Friedel-Crafts catalysts used in ethylbenzene and cumene developments. According to the report of Degnan et al. (2001) approximately 40% of the world's ethylbenzene capacity that still uses $AlCl_3$ is testimony to the productivity and low-cost of this process. To capture this segment of the industry, zeolite catalysts will have to be developed that operate at very low benzene-to-ethylene ratios that make the $AlCl_3$ process economically attractive [67].

Bellussi et al. (1995) investigated the activities of zeolite Beta, Y and solid phosphoric acid. The results indicated that the catalytic performance of zeolite Beta in the liquid phase alkylation of benzene with propylene and ethylene to produce cumene and ethylbenzene, respectively, was higher than that of solid catalysts and zeolite Y. Particle size and composition of the catalyst were factors that affect the catalytic activity of zeolite Beta. Decreasing the framework of aluminium content by direct synthesis or partial substitution of aluminium for boron produced a decrease in both conversion and selectivity in cumene and ethylbenzene synthesis [66].

Corma et al. (2000) studied benzene alkylation with ethene and propene under liquid-phase reaction conditions over zeolites MCM-22, Beta, and ZSM-5. The results indicated MCM-22 to be a good catalyst for benzene alkylation especially with propene, showing high activity, stability and good selectivity. Kinetic experiments showed that alkylation with propene follow an Eley-Rideal type mechanism [73].

Lukyanov and Vazhnova (2008) studied benzene alkylation with ethane into ethylbenzene (EB) at 370^{o}C over two Pt-containing MFI catalysts with the Si/Al ratios of 36 and 140. The reaction temperature and catalysts were nominated based on the analysis of the thermodynamic and kinetic limitations related with this reaction. The experimental results suggested that ethylbenzene formation taking through ethane dehydrogenation into ethene over Pt sites and subsequent benzene alkylation with ethene over acid sites. According to their investigation under selected reaction conditions, the whole process of ethylbenzene formation was driven by the alkylation reaction and several side reactions (including coke formation) were inhibited due to the fundamentally low ethene concentration at 370^{o}C. Also, the low and

moderate acidity of the catalysts allows decoupling of ethylbenzene formation steps and the steps of its subsequent transformation into side products. As a result, both catalysts reveal a remarkably stable performance (during 45-49 hour on stream) with ethylbenzene selectivity in the aromatic products in the range 92.6 and 95.3 mol%, with the highest (benzene-based) ethylbenzene yield of 10.7%. These observed that the ethylbenzene selectivities and yield were essentially higher than those reported previously both for the zeolite and super acidic catalytic systems [74].

Wong et al. (2013) investigated benzene alkylation with ethane into ethylbenzene over a PtH-MFI bifunctional catalyst. Their works demonstrate that the temperature affects in a diverse way the thermodynamic equilibrium of two major reaction steps: (i) benzene alkylation with ethene over acid sites and (ii) ethane dehydrogenation into ethene over Pt sites. It was shown that with increasing temperature, while the ethylbenzene formation rate increased in much lesser extent then ethane dehydrogenation was highly accelerated. As a consequence, high concentration of ethene was observed at high temperatures (450-490 ◦C), while the maximum concentrations of ethylbenzene were very similar at all temperatures. Ethene, which was formed in surplus at high temperatures, was converted via cracking and oligomerization steps into higher alkenes that alkylate benzene (or aromatic products). These alkylation reactions were followed by cyclization and dehydrogenation steps leading to formation of poly aromatics (coke precursors) and later catalyst deactivation. On the other hand, at lower temperatures from 290-410 ◦C ethene reacts preferably with benzene forming ethylbenzene. Hence, side reactions were suppressed and high ethylbenzene selectivity and catalyst stability were observed at these temperatures. Based on the analysis of the catalyst activity, selectivity and stability, it was concluded that 370-410 ◦C can be considered as the optimum temperature range for the direct benzene alkylation with ethane into ethylbenzene. More enhancement of the process may be attained by selective removal of hydrogen from the reactor and by controlling of the ethane/benzene ratio in the feed [75].

Li et al. (2009) studied ethylbenzene synthesis by alkylation of benzene with diethyl carbonate using parent MCM-22 and hydrothermally treated MCM-22. Acidity adjustment of the MCM-22 was performed by hydrothermal treatment of parent MCM-22 by flowing pure steam at high temperature. XRD, SEM and N_2 adsorption/desorption results showed that the crystallinity and pore sizes of MCM-22 were slightly affected at different temperatures by the hydrothermal treatment. NH_3-TPD and FTIR with pyridine adsorption showed only a slight decrease in the Brønsted acid sites, compared with parents MCM-22, with hydrothermal

treatment temperature in the range 500-600 ^{o}C. The strength of the Brønsted acid sites was reduced at hydrothermal treatment temperatures of 700 and 800 ^{o}C. The Lewis acid sites were reduced only to some extent affected by hydrothermal treatment. A significant enhancement in the selectivity of ethylbenzene together with a slight decrease in the benzene conversion was achieved in the catalytic synthesis of ethylbenzene by alkylation of benzene with diethylcarbonate over MCM-22 hydrothermally treated at 600 ^{o}C. A strong decrease in the benzene conversion was detected over MCM-22 hydrothermally treated at 700 ^{o}C. The results showed that the alkylation of benzene with diethylcarbonate happened mainly on Brønsted acid sites, and the effect of the Lewis acid sites on the alkylation process is negligible. Reduction of Brønsted sites of the catalyst can suppress side reactions and improve the selectivity for ethylbenzene. It was that a certain acid strength of the catalyst was found necessary to obtain high benzene conversion and ethylbenzene selectivity [76].

Hu et al. (2014) reported that ethylbenzene formation is tough to be avoided in benzene alkylation with methanol over ZSM-5 catalysts to synthesis toluene and xylene. Moreover, the separation or removal of ethylbenzene from C_8 aromatic yet remains as a major challenge. In their study, they investigated the effect of platinum addition on the catalytic performance of ZSM-5 for benzene alkylation. It was found that the presence of a small amount of platinum in ZSM-5 catalyst would mainly suppress the ethylbenzene formation and lengthen the life-span of the catalyst, which was mainly due to the hydrogenation of ethylene into ethane on platinum particles [77].

Lukyanov and Vazhnova (2008) investigated kinetics of benzene alkylation with ethane into ethylbenzene over bifunctional PtH-MFI catalyst. Benzene alkylation with ethane into ethylbenzene (EB) was studied at 370 ^{o}C over a PtH-MFI bifunctional catalyst of high acidity (Si/Al = 15). Greatly selective and stable catalyst operation was observed at benzene conversions up to 10-12 %, which are close to the thermodynamic equilibrium conversion value of 13.5 %. Kinetic analysis of the experimental data shown that ethylbenzene was formed via two successive reaction steps: (i) benzene alkylation with ethene over acid sites and (ii) ethane dehydrogenation into ethene over platinum sites. These reactions dominate at low contact times and benzene conversions up to 10-12 %. At higher conversions (i.e. higher contact times) other reactions start to compete with the ethylbenzene formation steps leading to a steep drop in the ethylbenzene selectivity and to a reduction in the catalyst stability. The investigation of these side reactions brought about in a better understanding of the requirements for the stable and selective benzene alkylation with ethane into ethylbenzene formation using bifunctional zeolite catalysts [78].

Madeira et al. (2009) studied ethanol transformation into higher hydrocarbons in one step by heterogeneous acid catalysis at 350 ^{o}C and 30 bar total pressure. A comparison was made among three zeolites (HFAU, HBEA and HZSM-5) having the same value of Brønsted acid sites but possessing different pore architectures. The results indicated that due to the deactivation of the strongest acid sites and only a low quantity of C_{3+} hydrocarbons large pore (HFAU and HBEA) zeolites gave mainly increasing yield of ethylene and diethyl ether with time-on-stream. This was described by a faster deactivation of large pore zeolites due to quick coke formation which rapidly reduces strong Brønsted acid sites, required for the transformation of ethylene into higher hydrocarbons. These coke molecules were identified as being poly aromatic compounds. HZSM-5 of medium pore zeolite showed significant formation of C_{3+} hydrocarbons (mostly C_5 - C_{11} compounds) and very small amounts of ethylene and diethyl ether. For this zeolite, after 16 h reaction, there was still complete ethanol transformation into C_{3+} hydrocarbons, even though a 55 % loss of micro porosity and 94 % loss of Brønsted acidity were observed. On HZSM-5 the deactivation was slower and the formation of C_{3+} hydrocarbons was detected even when the catalyst was saturated with coke molecules (high activity for the hydrogen transfer reactions). It could be possible, that for this zeolite, reaction occurred at the pore mouth of the channel [79].

Wichterlova et al. (1991) reported that the alkylation of toluene with ethylene to produce p-ethyltoluene can be conducted selectively on small crystals ($\leq$ 1 μm) of unmodified H-ZSM-5 zeolites to a level higher than that corresponding to the thermodynamic equilibrium composition. According to their investigation a comparison of the ethyltoluene isomers formed with H-Y and H-ZSM-5 zeolites at different conversions and temperatures indicated that p-ethyltoluene was favourably formed in the channel intersections of the H-ZSM-5 zeolite, even during the initial alkylation step. The final ethyltoluene isomer composition was a result of competition between the rates of alkylation and isomerization and subsequent diffusional transport of individual isomers through the zeolites channels. Zeolite coking caused an apparent increase in the p-ethyltoluene selectivity; however, a more dramatic decrease in toluene conversion resulted in the formation of a considerably lower amount of p-ethyltoluene. This was caused by a partial blocking of the zeolite channel system [80].

Madeira et al. (2012) considered the catalytic activities of Si/Al ratios ranging from 16 to 500 HZSM-5 zeolites for ethanol transformation into hydrocarbons. HZSM-5 (Si/Al = 40) was found to be the most stable and selective catalyst due to the amount of radicals, which are active sites for ethanol conversion into higher hydrocarbons and finest balance between the

number of Brønsted acid sites. However, a change in radical species nature occurred with time on stream (TOS) which could be accountable for the deactivation of all catalysts leading to a decrease of C_{3+} hydrocarbons yield [81].

Sun et al. (2009) studied some post-treatment effects, including hydrothermal treatment, calcination and La_2O_3 modification on the catalytic activities of a nanoscale HZSM-5 zeolite for ethylation of benzene coking. The nanoscale HZSM-5 zeolite catalysts prepared were evaluated in a fixed-bed down flow reactor and treated by hydrothermal treatment, calcination and La_2O_3 modification in series. The results showed that both the hydrothermal treatment and the calcination resulted in a drastic decrease in the total amount of acid sites, while the subsequent modification La_2O_3 out a slight increase in the number of acid sites only. These finishing operations resulted in a decrease of Brønsted/Lewis ratio of nanoscale HZSM-5 zeolites. The hydrothermal treatment by La_2O_3 modification followed created new large micropores on the nanoscale HZSM-5 zeolites, resulting in the coexistence of micropores and mesopores. The increase in the catalyst life can be attributed both to the modified calcined-hydrothermal treated HZSM-5 (La-C-HT-HZSM-5) catalyst suppressing carbon deposit formation and partially receiving the carbon deposit formed in lanthanum low acid and intricate pore structure. The prepared La-C-HT-HZSM-5 catalyst revealed good catalytic stability within 1,500 hours' time-on-stream in the ethylation of coking benzene with ethylene under reaction conditions [14].

Bokade et al. (2004) reported alkylation and disproportionation of ethylbenzene (EB) in the presence of aromatics like *m*- and *p*-xylene isomers over a pore-size regulated HZSM-5 catalyst. The industrial feed having different compositions of xylene isomers and ethylbenzene were used for the experimentation. Hence, they were expected to hinder the flow of reactant molecules both within zeolite channels and on the external surface of zeolite channels. It was detected that regardless of the different compositions of feed concentration of the xylene mixture isomers were together in the product [82].

Sugi et al. (2006) studied the La_2O_3 and CeO_2 modifications of H-ZSM-5 zeolites to advance the shape-selectivity in the alkylation of mononuclear aromatic hydrocarbons and related reactions. The results showed that the selectivities of p-diethylbenzene (p-DEB) among diethylbenzene isomers were upgraded without substantial loss of catalytic activity by the modification with these oxides in the ethylation of ethylbenzene (EB). It was shown that the La_2O_3 modification improved the selectivity of p-DEB more effectively than the CeO_2 modification. They reported that the improvement of the selectivities over these oxides is due

to the prevention of the isomerization of p-DEB at external acid sites. The para-selectivity for La_2O_3-modified H-ZSM-5 zeolites is improved due to ‘‘product selectivity’’ resulting from the favoured diffusion of para-diethylbenzene by the adjustment of pore entrance as well as by the deactivation of external acid sites. The improvement in the formation of less bulky xylene isomers was also observed in the isomerization of xylene isomers and the disproportionation of toluene over La_2O_3- and CeO_2-modified H-ZSM-5 zeolites [83].

Odedairo and Al-Khattaf (2010) investigated the activities of zeolite catalysts based on ZSM-5, TNU-9, SSZ-33 and mordenite for benzene ethylation with ethanol at three different reaction temperatures (250, 275 and 300 ◦C) and for reaction times of 3, 5, 7, 10, 13, 15 and 20 s. The results showed that the SSZ-33 catalyst comprising 12-12-10-ring channels gave the highest benzene conversion, which was due to high acidity of this zeolite together with increased mass transport through large pores. The present conversion of benzene follows the order: mordenite < ZSM-5 < TNU-9 < SSZ-33. TNU-9 zeolite catalyst acts like the 10-ring ZSM-5 with respect to ethylbenzene selectivity, while the behaviour of SSZ-33 is close to that of a large pore zeolite with potential cage effects. It was reported that the present EB selectivity follows the order: mordenite < SSZ-33 < TNU-9 < ZSM-5, which suggested that this order is not directly related to the benzene conversion [84].

Ding et al. (2007) investigated the pore structure and acidity of nanoscale ZSM-5 zeolite catalysts. Alumina and rare earth were used as binders and prepared catalysts treated by pure steam to compare their performance. The catalytic activities of the catalysts were investigated using alkylation of ethylbenzene, toluene with ethanol and methanol as probe reactions respectively. The results showed that treated nanoscale ZSM-5 catalysts maintained a good crystallinity up to 800 °C. While the abilities for adsorption of cyclohexane and normal hexane declined on the dealuminated nanoscale ZSM-5 catalyst samples. Amount of both the tetrahedrally coordinated framework aluminum and that of the octahedral coordinated non framework aluminum reduced and the average pore diameter improved. For the catalysts treated at 700 ^oC, the catalytic activity for the alkylation of toluene with methanol as well as the selectivity of p-xylene was improved. Although the amount of total acid reduced significantly and strong acid sites almost disappeared. The alkylation activity was very low when the hydrothermal treatment temperature was 800 ^oC. Correspondingly, the activity of the catalysts for the alkylation of ethylbenzene with ethanol reduced with higher treatment temperatures [85].

Kim et al. (1993) reported that anti mono silicate and gallosilicate catalysts, modified with a small amount of boron oxide for the alkylation of ethylbenzene with ethanol showed perfect para-selectivity. In addition, the alkylation activities of these zeolites were compared with the modified high H-ZSM-5, which also has perfect para- selectivity. The improvement of the para-selectivity as a result of the modification was to reduce the effective pore size and due to the reduction of the acid strength of zeolites MFI [86].

Xue et al. (2014) investigated the selective para-diethylbenzene synthesis by alkylation of ethylbenzene with diethyl carbonate using B_2O_3/HZSM-5 catalysts. The characterization results showed that the 15% B_2O_3/HZSM-5 catalyst prepared by using triethyl borate as the precursor demonstrated a high catalytic performance in alkylation of ethylbenzene with diethyl carbonate along with an outstanding shape-selectivity. This could be attributed to the large molecular size of triethyl borate that would lead to the formation of boron oxide on the external surface and preserve the acid sites in the micro pores of HZSM-5 zeolite. In contrast, the B_2O_3/HZSM-5 catalysts prepared by using trimethyl borate or boric acid led to the strong reduction of the catalytic activity, which was attributed to the decrease in the amount of the total acid sites caused by the partial blockage of the pores of HZSM-5 zeolite [87].

Odedairo and Al-Khattaf (2010) investigated benzene ethylation over fresh ZSM-5 based catalyst in a riser simulator that can represent the operation of a fluidized-bed reactor. The kinetic study was carried out experimental runs for reaction times of 3, 5, 7, 10, 13, and 15 s at four different temperatures (300, 325, 350 and 400 ◦C). Mole ratio of benzene to ethanol (B/E) was varied from 1:1 upto 3:1. For the different temperatures, benzene conversion, ethylbenzene and diethylbenzene yield were found to increase with reaction temperature and time. Over the fresh catalyst at 400 ◦C, the maximum benzene conversion of 16.95% in which the major products were ethylbenzene, diethylbenzene and other hydrocarbon as by-products was obtained. Quasi-steady-state approximations with catalyst deactivation function based on two different models were used to model the experimental results. By using non-linear regression analysis kinetic parameters for benzene ethylation and ethylation of ethylbenzene with ethanol were estimated. The apparent activation energy of ethylbenzene ethylation was found to be lower than the value for benzene ethylation. Furthermore, the effect of benzene to ethanol ratio (B/E) on the activation energies and products distribution was also investigated [88].

Chandawar et al. (1982) reported the alkylation of benzene with ethanol over pure and modified (with phosphorous and boron) HZSM-5 zeolites. The results indicated that the ethyl

group in ethylbenzene was formed from ethanol without the intermediate formation of ethylene. According to the investigation made by the authors' modification of HZSM-5 with phosphorous increased the selectivity towards formation of ethylbenzenes. This was attributed to the elimination of the strong acid sites in HZSM-5 by added phosphorous [4].

Vijayaraghavan and Raj (2004) studied ethylation of benzene with ethanol in the vapour phase over $AlPO_4$-5, MAPO-5, MnAPO-5 and ZAPO-5. The products were ethylbenzene (EB), 1,4-diethylbenzene (PDEB), 1,3-diethylbenzene (MDEB) and poly alkyl benzenes (1,2,4- and 1,3,5-triethylbenzene, and 1,2,4,5-tetraethylbenzene). MnAPO-5 was found to be more active in comparison to the other catalysts. Maximum conversion (47%) was noted at 400^oC over MnAPO-5. Although isomorphic substitution in MnAPO-5 is nearly the same as in MAPO-5 and ZAPO-5, the increase in conversion was credited to the presence of unpaired electrons in the d-subshell of manganese. The selectivity of the products was found to decline with time-on-stream but the selectivity to ethylbenzene revealed an increase after 2 h on stream. MnAPO-5 registered nearly 14% yield of ethylbenzene and 17% yield of diethylbenzene, whereas the yield of other products was found to be 16% at maximum conversion [8].

Zhang et al. (2013) studied the activities of mesoporous MCM-22 zeolites with Si/Al ratios of 15-45, which were hydrothermally synthesized by carbon black particles through a hard template technique. The physicochemical properties of mesoporous MCM-22 were characterized by SEM, XRD, N_2 adsorption, XPS, TEM, NH_3-TPD, ICP and TGA-DTA techniques. The existence of mesopores was advantageous to increase the accessibility of zeolitic acid sites and for reduction of the mass transfer limitations of bulky molecules. Mesoporous MCM-22 exhibited higher selectivity to ethylated benzenes, higher ethylene conversion and better stability than conventional MCM-22, possibly serving as a solid-acid catalyst in petrochemical industry when applicable to liquid-phase ethylation of benzene with ethylene [89].

Bhandarkar and Bhatia (1994) studied the selective formation of para-ethyltoluene using toluene and ethanol using modified as well as unmodified shape-selective HZSM-5 catalysts. The reaction was carried out in a fixed-bed reactor in the temperature range 300-500 ^oC and atmospheric pressure. The effect of steaming temperature, reaction temperature, toluene to ethanol mole ratio, conversion, selectivity and activity over both unmodified and modified HZSM-5 zeolites were investigated. Inorganic additives such as magnesium, phosphorus and

boron were used to modify the parent zeolite HZSM-5 using ion-exchange and impregnation techniques.

The Langmuir-Hinshelwood-Hougen-Watson approach (LHHW) and the Eley-Rideal mechanism were used to propose reaction models based on analysed data obtained from experiment. The modification of HZSM-5 showed an increase in activation energy from 61.78 (unmodified HZSM-5) to 97.03 kJ/mol (Mg-HZSM-5). The increase in apparent activation energy of the modified catalyst was attributed to the lower acid strength and not to the decreased number of acid sites responsible for the alkylation reaction [90].

Levesque and Dao (1989) studied alkylation of benzene to produce ethylbenzene using an aqueous solution of ethanol of concentration similar to a fermentation broth. From the results steam-treated ZSM-5 zeolite catalyst was found to be effective and selective in the manufacture of ethylbenzene. Ethylbenzene and ethylene were the main products formed in alkylation reaction. Although diethylbenzene and other light olefins were made in small quantity as secondary reaction products. This alkylation reaction represented an interesting approach for the preparation of important and useful hydrocarbons using aqueous ethanol produced by fermentation [91].

Corma et al. (2009) investigated alkylation of benzene with ethanol and benzene with isopropanol or propylene based on the catalytic behaviour of two multipore zeolites containing channels of different sizes, SSZ-33 (10 windows × 12 member ring) and ITQ-22 (8 × 10 ×12 member ring pores). The results were compared to that of zeolites with intersecting channels of the same size, ZSM-5 (10 × 10 member ring channels) and Beta (12 × 12 member ring channels).

The investigation showed that for the alkylation of benzene with ethanol in gas phase, ITQ-22 behaved like 10 member ring ZSM-5 with respect to ethylbenzene selectivity, while the behaviour of SSZ-33 is closed to that of a 12 member ring zeolite such as Beta. For the alkylation of benzene with isopropanol or propylene in gas and liquid phase, Beta and ITQ-22 gave similar selectivity values, which were much better than those obtained with ZSM-5. Meanwhile, SSZ-33 gave intermediate selectivity between that of 10 member ring ZSM-5 and 12 member rings Beta zeolite. ITQ-22, therefore, showed a unique behaviour as a multipurpose alkylation catalyst, characteristically different from those of previously studied zeolites. The catalytic behaviour of ITQ-22 had been rationalized not only in terms of the topology of the channels but also took into account the location of the protons. A computational study showed

preferential Aluminum location at the 10 member ring, near the intersection with the 12 member rings channels, and at the intersections between 10 and 12 member rings channels [92].

Villarreal et al. (2002) reported that for the synthesis of methylstyrene the products of toluene alkylation (*p*-ethyltoluene (*p*-ET) and *m*-ethyltoluene (*m*-ET)) were used. The polymers made from methylstyrene have benefits in comparison with polystyrene: higher glass transition temperature and lower density. One to use toluene as a substitute of benzene in petrochemical synthesis moreover enabled due to the production of polymethylstyrenes. A new process of selective production of *p*-ET and *m*-ET mixture, suitable for polymerization, had been developed as a result of the syntheses of high-silica zeolites (HSZs) of the type ZSM-5. In their paper, the optimal conditions of alkylation of toluene by ethanol using pentasil zeolites as catalysts were stated [93].

Raimondo et al. (1997) investigated the alkylation of benzene by methanol, ethanol, iso-propanol and n-octanol over USY, H-ZSM-5, mordenite and Theta-1 and the acidity/porosity relations obtained compared with those in an alumina-pillared saponite (ATOS) and an alumina-pillared montmorillonite (BP-PILC). Pseudo first order alkylation rates follow the order: BP-PILC < ATOS < Theta-1 < USY < mordenite < H-ZSM-5, which for the zeolite was not that expected on the basis of acidity. Conversely, ethanol conversion in H-ZSM-5s with Si/A1 ratios 5/35 - 5/400 does not follow expected acidity trends and methanol consumption during alkylation could be used to construct an acidity scale.

It was shown that the determining factor was the reaction occurred via electrophilic attack of intermediate matrix-attached oxonium ion at incoming benzene molecules and that pore size, rather than acidity. Whereas both pore sizes in PILCs were too large, which hinder efficient alkylation the smaller channels of H-ZSM-5 were the most favourable because they allow close approach between oxonium ion and benzene [94].

Vijayaraghavan et al. (2006) studied the vapour and liquid phase alkylation of various reactions over MnAPO-11 and MnAPO-5. The studies recommended that a strong deactivation of the catalyst occurred with increase in bulkiness of the reactants. Results showed that the liquid phase reactions showed good conversion and extended catalyst life; whereas the vapour phase reactions resulted in faster deactivation of the catalyst which carried out at high temperatures (350 and 400 ^{o}C) [95].

Sridevi et al. (2001) investigated zeolite in the form of extrudates which were impregnated with 15% $AlCl_3$ and characterized by qualitative methods the commercially available 13X (NaX). Experimental runs for the kinetic study were carried out with constant benzene to ethanol molar ratio of 3:1, varying the space velocity under isothermal conditions in the reactor and at three different temperatures 400, 425, and 450^oC. Experiments were carried out to select the zone in which the mass transfer resistances were insignificant. Based on Langmuir–Hinshelwood–Hougen–Watson different models for reaction mechanisms were proposed and a mathematical fit for the best model was found. By using Arrhenius relationship the frequency factor and activation energy were evaluated. By non-linear regression analysis the model parameters were estimated [96].

Zhang et al. (2012) studied the catalytic activities of MCM-56 analogues which were post synthesized via a mild acid treatment technique from hydrothermally synthesized MCM-22 lamellar precursors with Si/Al ratios of 15-45. The physicochemical properties of MCM-56 were characterized by SEM, XRD, N_2 adsorption, 29Si and 27Al MAS NMR, XPS, NH_3-TPD and pyridine adsorption IR techniques. The postsynthesized MCM-56 showed a broad X-ray diffraction of emerged 1 0 1 and 1 0 2 reflections and possessed a structural disorder along the layer stacking direction in comparison to MCM-22 with 3-dimensional MWW topology. MCM-56 analogues had a larger external surface than MCM-22 composed of partially delaminated MWW nanosheets. The MCM-22 and MCM-56 catalysts were employed in the liquid-phase alkylation of benzene with ethylene. MCM-22 exhibited a lower yield of ethylated benzenes and a lower catalytic stability than MCM-56 analogues. MCM-56 analogues proved that to serve as promising solid-acid catalysts for processing bulky molecules in petrochemical industry [97].

Ogunbadejo et al. (2015) investigated with varying SiO_2/Al_2O_3 ratio 80, 280, and 2000 the making of para-ethyltoluene (p-ET) from the alkylation of toluene with ethanol over three MFI zeolites. The ethylation reaction was conducted at a temperature range of 300-400 ^oC, molar feed ratio of toluene to ethanol at 1:1 and reaction times of 5-20 s in a batch fluidized-bed reactor. With temperature over all the MFI zeolites except for MFI-80, showed a maximum conversion of 29 % at 300 ^oC toluene conversion increased. The product distribution showed ethyltoluene as major product with a maximum yield of 26 % over MFI-80. Constant toluene conversion of 14 % and 100 % ethanol conversion, para-selectivity top-ET was 100 % over MFI-2000 compared with 27 % and 48 % over MFI-80 and MFI-280, respectively at 400 ^oC. The high para-selectivity over MFI-2000 was recognized due to the combined effects of higher

SiO_2/Al_2O_3 ratio, very weak acid sites and larger crystal size (longer diffusion length). The experimental data were analyzed for each MFI zeolite and based on the Langmuir–Hinshelwood model suitable reaction mechanism for toluene ethylation was proposed. The activation energy for the formation of p-ET over MFI-280 and MFI-2000 was 30 and 65kJ/mol, while the heat of adsorption of ethanol was 19 and 29 kJ/mol, respectively [98].

Odedairo and Al-Khattaf (2013) investigated that opportunities for a more environmental friendly gasoline by removing considerable portions of benzene by alkylation of benzene with light alcohols. The performances of mordenite and ZSM-5 zeolites as catalysts were tested in the alkylation reaction of benzene with different light alcohols such as methanol, ethanol and isopropanol. The experiments were carried out with a 1/1 mol ratio of benzene/alcohol for 3, 5, 7, 10, 13, 15 and 20 s at 200, 250, 300, 350 and 400 ◦C in a fluidized-bed reactor. They reported that nature of the alcohol molecule and the reaction temperature and the Brønsted to Lewis acid ratio of the catalysts, played an important role in the alkylation reactions. According to results, for benzene alkylation with methanol to toluene and xylene, both mordenite and ZSM-5 are active and selective catalysts, while for benzene ethylation to ethylbenzene, ZSM-5 exhibits higher ethylbenzene selectivity than mordenite. Isopropanol offers greater difficulty to be activated as compared to the other alcohols at higher temperatures, while the lower temperature favours benzene isopropylation to cumene over both catalysts. By studying the alkylation of benzene with alcohols of different chain length, it had been found that as the optimum temperature for alkylation reaction decreased the alkyl size i.e. methyl, ethyl, and propyl increased [99].

Galadima and Muraza (2015) reported that the alkylation of benzene to mono and multi-alkylated benzenes is recently considered as a vanguard technology by the petroleum refineries for the reduction of benzene from gasoline feedstock. Its benefits over the other reduction technologies include limiting the consumption of hydrogen and retention of octane properties. The technology is therefore broadly considered at the global scale. The choice of most appropriate reaction conditions and catalyst are very important. The catalyst suitable for this reaction must be highly regenerable, active, resistance to deactivation by coking or poisons and selective [100].

Bhat and Halgeri (1993) studied ethylbenzene dealkylation, accompanied by xylene isomerisation over MFI zeolite. The effects of the presence of paraffinic compounds on the dealkylation and variation in ethylbenzene concentration in the isomer feed have been considered. In addition to that the undesired dealkylation of ethylbenzene during its alkylation

was reported. The results showed that the extent of dealkylation depends on the weight hourly space velocity, temperature and mole ratio of alkyl benzene to alcohol [101].

Li et al. (2009) studied catalytic ethylbenzene synthesis by alkylation of benzene with diethyl oxalate over HZSM-5 with Si/Al ratios from 50 to 250. The investigations revealed a significant decrease in acidic strength and the number of acidic sites with increasing Si/Al ratio from 50 to 250. With increasing Si/Al ratio from 50 to 200, the ethylbenzene selectivity and benzene conversion increased. With a further increase in Si/Al ratios, a slight decrease in the selectivity for ethylbenzene and conversion of benzene was noticed, indicating that a proper acidic strength was required in this reaction [102].

Vazhnova et al. (2013) reported that the deactivation of the highly acidic PtH-MFI catalyst in the reaction of benzene alkylation with ethane in ethylbenzene took through two modes. The first mode corresponds to the selective deactivation of the platinum sites, which was highly active in the hydrogenolysis reactions. This deactivation occurred during the first 4 hours of the catalyst operation which resulted in the significant improvement of the catalyst selectivity toward ethylbenzene. The second, much slower, deactivation process was observed during ten hours and was responsible for the deactivation of platinum and acid sites with similar rates. This deactivation mode leads to the re-distribution of the reaction products in a way that was very similar to the effect of contact time on the product distribution. The analysis of the IR spectra of the fresh and coked catalyst samples revealed that coke species were formed both inside and outside of the zeolite channels. It was shown that these coke species directly blocked the catalyst brønsted acid sites but did not block the zeolite channels up to the coke content of 5-6 wt. % in the catalyst. The coke located on the external surface has a major effect on the large platinum particles (10 nm) present in the catalyst, as follows from the IR study of the CO adsorption. Their work also indicated that there were at least two different platinum sites in the platinum particles, possibly responsible for the different reaction types, namely dehydrogenation and hydrogenolysis. These two different platinum sites were affected by coke deposits differently, and therefore, their deactivation could clarify the observed two modes of the catalyst deactivation [103].

Ebrahimi et al. (2011) simulated industrial ethylbenzene production unit and the results were compared against five days experimental data. According to the prevailing state of unit, that is recycled ratio of benzene, benzene selectivity and energy consumption, the device is not working under its optimum conditions for minimum cost of ethylbenzene production. In the current design, high amount of benzene recycle (6:1) results in an additional cost due to the

fractionation of ethylbenzene to have from benzene. A new approach has been proposed to modify the benzene alkylation process and reduce the unit energy consumption. In the redesigned program, two double alkylation reactors converted to four single-bed reactors. The amount of injected ethylene, reaction temperature and return flow were controlled as adjustable parameters to optimize the process. In the modified method, the reflux ratio was reduced to 1.87 and increases the benzene selectivity. The optimized method showed a significant decrease in the energy consumption of the device compared to the current process. Also, the mass fraction of ethylbenzene was achieved to 99.12% of its purity has before entering to the transalkylation for further purification. Therefore, if the illustrated purity for the final application is acceptable, the transalkylation of the new design could be eliminated [104].

Li et al. (2009) studied the catalytic synthesis of ethylbenzene. According to their report, strong acidic sites may lead to an excessive decomposition of diethyl carbonate. Their results strongly suggest that the alkylation of benzene with diethyl carbonate over HZSM-5 is a suitable path for the synthesis of ethylbenzene. Among the catalysts tested, HZSM-5 with a Si/Al ratio of 200 had the greatest benzene conversion and ethylbenzene selectivity due to its optimal acid strength. Catalyst activity increased significantly as the temperature is improved from 340 ^{o}C to 380 ^{o}C and the highest benzene conversion was obtained at 380 ^{o}C. With increase in feed ratio (benzene: DEC) and WHSV the selectivity for ethylbenzene can be improved [105].

Xue et al. (2010) investigated selective synthesis of ethylbenzene by vapor phase alkylation of benzene with diethyl carbonate over MCM-22 modified by MgO. From their investigation, characterization results show that the number of Brønsted acid sites on MCM-22 reduced significantly after MgO modification, which resulted in a decrease in activity. However, they reported that the selectivity for ethylbenzene was improved greatly over MCM-22 modified by magnesium oxide, which can be recognized to the effective suppression of subsequent alkylation of ethylbenzene by the reduction in Brønsted acid sites [106].

Zaidi and Pant (2005) studied catalytic activity of copper oxide impregnated HZSM-5 in methanol conversion to liquid hydrocarbons. Several CuO/HZSM-5 catalysts have been studied in a small scale fixed bed reactor for the conversion of methanol to gasoline range hydrocarbons. Catalysts were prepared by using wet impregnation technique. The CuO loading over HZSM-5 (Si/Al=45) catalyst was investigated in the range of 0 to 9 wt%. The investigation reveals that incorporation of CuO onto HZSM-5 zeolite significantly improved conversion and yields of liquid hydrocarbon product. The major products of the reactions were ethylbenzene, toluene, xylene, isopropyl benzene, ethyl toluene, trimethyl benzene and tetra

methyl benzene. The maximum methanol conversion and yield of hydrocarbon product was obtained at a CuO loading of 7wt% [107, 108].

Eswaramoorthi and Dalai (2006) studied modification of SBA-15 with boron. Isomorphous substitution of boron in SBA-15 framework was effectively carried out for the first time by direct synthesis method. The decrease in d-spacing and unit cell parameter compared to siliceous SBA-15 showed the integration of boron in the framework. The scanning electron microscope images of B-SBA-15 and siliceous SBA-15 indicated that the morphology was changed when the boron was integrated in the SBA-15 framework [109].

Srivastava and Nigam (1982) presented a closed-form analytical solution for the problem of homogeneous and heterogeneous reactions in a tubular flow reactor. A technique was developed where the Galerkin method was applied in the Laplace transform domain. The technique delivered a simple solution which does not require numerical effort such as that required in the circumstance of the conventional variable separable method. Legitimately comparable results were obtained [110].

CHAPTER THREE
EXPERIMENTAL DETAILS

This chapter describes the methods used for preparation of boron and magnesium (monometallic and bimetallic catalysts) supported on ZSM-5 zeolite catalysts as well as various techniques used for catalyst characterization. The experimental setup, experimental procedure and product analysis have also been discussed in detail.

3.1 MATERIALS

The chemicals and gases used in the experiments were obtained from different manufacturers and suppliers. ZSM-5 zeolite in protonic and powder form with SAR-90 and NaZSM-5 with SAR=31 were obtained from Sud-Chemie India Pvt. Ltd. Benzene used in the experiments was > 99 % pure. Boric acid (99.5 % pure) and benzene for the present study were obtained from RFCL limited, New Delhi, India. Pure ethanol (99.9 %) was supplied by Merck KGaA, Germany. Magnesium nitrate (99 % pure) and ammonium nitrate extra pure (98 %) were supplied by HiMedia laboratories Pvt. Ltd. Mumbai, India.

3.2 CATALYST PREPARATION

Sodium ZSM-5 zeolite in the form of powder with SAR-31 obtained from Sud-Chemie India Pvt. Ltd was transformed to protonic form by repeated exchange using 1 M solution of ammonium nitrate four times and each time for 6 hour by using fresh solution of ammonium nitrate at 55 ^{o}C under reflux and stirring. After that zeolite was separated from ammonium solution, washed and dried for 12 hours at 120 ^{o}C. The catalyst was then calcined at 550 ^{o}C for 5 hour. Magnesium nitrate and boric acid were impregnated in the same weight percent of respective metal contents (8 %) using their aqueous solutions on the HZSM-5 zeolite. The contents were heated at 55 ^{o}C overnight under total reflux and stirring. The solutions were subsequently filtered. The filtered solid was dried at 120 ^{o}C overnight and calcined at 550 ^{o}C for 5 hour in a muffle furnace. From atomic absorption spectroscopy and inductive coupling plasma results the impregnations of Mg and B were 5 % and 4 %, respectively. The zeolite powder so obtained was pelletized at 10 tonne / cm^2 pressure, broken into small pieces and used for the studies in the size range 0.3 - 0.5 mm.

HZSM-5 SAR = 90 obtained from Sud-Chemie India Pvt. Ltd was in protonic form, so no further transformation activities were done to transform it to protonic form except catalyst was calcined (activated) at 550 ^{o}C for 5 hours to be activated. Boron or magnesium monometallic and boron-magnesium bimetallic catalysts were prepared by incipient wetness impregnation method. In this method, desired amount of metal precursors (H_3BO_3 and $Mg(NO_3)_2 \cdot 6H_2O$) were dissolved in deionised water and calculated amount of HZSM-5 zeolite catalyst was added to this solution under stirring. Total metal loading was kept constant for both monometallic and bimetallic catalysts as 5, 10, 15 wt%. After doing this the rest of procedures were similar to that of NaZSM-5 form of zeolite catalyst as stated above.

3.3 CATALYST CHARACTERIZATION

The catalysts were characterized by various methods including surface area measurement, X-ray diffraction, temperature programmed desorption, inductive coupled plasma-mass spectroscopy, scanning electron microscopy and transmission electron microscopy.

N_2 adsorption-desorption isotherm measurements were performed at -196 ^{o}C using a Micrometrics Accelerated Surface Area and Porosimetry (ASAP-2020) system. Prior to the analysis, the samples were degassed at 250 ^{o}C for 8 h under vacuum. The surface area of all the samples were analysed employing the multi point Brunauer-Emmett-Teller (BET) method by using adsorption data at the relative pressure (P/P_o) range of 0.05-0.3. Pore size distribution were determined by using Barret-Joyner-Halenda (BJH) method considering the desorption branch.

X-ray diffraction (XRD) analysis was performed in order to determine the phase structure of the catalyst and crystallinity. The spectra were recorded with a Bruker AXS D8 advance diffractometer using Cu-Kα monochromatized radiation source (λ=1.5418 Å), Ni filter and 40 kv at the two theta interval of 5-50^{o} with scan speed of 1 ^{o}/min. The average crystallite size of the catalysts were determined using Scherrer formula ($D=0.90\lambda/\beta \, Cos\Theta$, where β is the full width at half-maximum height (FWHM) and Θ is the diffraction angle from the line width of the respective XRD peaks. The phases present were identified by comparison of the XRD peaks of the catalysts with the standard data files provided by Joint Committee on Powder Diffraction Standards (JCPDS).

The acidic properties of catalysts were measured by ammonia temperature – programmed desorption (NH_3-TPD). NH_3-TPD measurements in the temperature range from room temperature to 650 ^oC were performed in Micromeritics ChemiSorb 2720 equipped with a TCD. Prior to each experiment, zeolite catalyst samples were put in a quartz cell with U shape and pretreated, insitu, for 1 h at 250 ^oC in a flow of nitrogen (>99 %) of 20 ml/min. After cooling to 25 ^oC, adsorption of ammonia was carried out in a flow of ammonia and helium mixture of 40 ml/min. After the catalyst surface became saturated it was kept for some time to remove the excess of ammonia. The temperature-programmed desorption was carried out with a linear heating rate of approximately 10 ^oC/min from 25 ^oC to 650 ^oC in a flow of helium (>99 %) of 20 ml/min. The NH_3 that desorbed was measured by a thermal conductivity detector.

Total B and Mg metal contents in prepared catalysts were determined by inductive coupled plasma –mass spectrometer (ICP-MS). Approximately 15 mg of catalyst and 2 ml of aqua regia (0.5 ml nitric acid and 1.5 ml of hydrochloric acid) were placed together in a 15 ml glass vial fitted with a Teflon lined cap, and digested in an oven at 100 ^oC for 2 hr. Then the samples were prepared by dilution with Millipore water to required concentrations (< 1 ppm). Perklin-Elmer Elan DRC-e ICP-MS was used for the elemental analysis.

To explore the morphology and composition of the catalysts, scanning electron microscopy (SEM) images were collected using Quanta scanning electron microscope (Model 200 PEG, USA) equipped with energy dispersive X-ray spectra (EDX). Catalyst sample was dispersed uniformly on the sample holders and coated with gold using sputter coater (Edwards S150) and then SEM images were taken at an acceleration voltage of 20 kV under vacuum. The morphologies of prepared catalysts were also analysed by transmission electron microscopy (TEM). TEM investigations were carried out using a Tecnai G^2 20 S-Twin (FEI Netherland) microscope equipped with EDAX. The samples were prepared by dispersing in absolute ethanol using an ultrasonic bath and evaporating a drop of resultant suspension onto the carbon coated copper grid.

Infrared spectra were obtained at 4 cm^{-1} resolution on Nicolet 6700 series FTIR Spectrometer. The infrared cell used was fitted with KBr windows. A sample of the zeolite powder was accurately weighed and mixed with around 300 mg KBr and then passed into a 10 mm diameter wafer at 15 tonnes/cm^2 pressure. This wafer was placed in the IR cell. The IR cell spectra were recorded at room temperature in air. Background IR correction for air was also made.

Thermo-gravimetric analysis was conducted in order to determine the thermal stability of the zeolite framework and weight loss occurring from zeolite lattice during heating. TGA were conducted on SII 6300 EXSTAR using air as carrier gas at 200 ml/min on a 10 mg of sample. The TGA of modified and unmodified HZSM-5 heated from ambient temperature to 1000 ^{o}C in temperature progression of 10 ^{o}C / min have been done.

3.4 CATALYTIC PERFORMANCE

3.4.1 Experimental Set-up

Alkylation of benzene with ethanol was carried out in a fixed bed, continuous down flow tubular quartz (0.6 cm I.D and 66 cm long) reactor placed inside a microprocessor controlled furnace (Metrex Scientific Instruments Pvt.Ltd, New Delhi). The same reactor tube was used in all the experiments. The reactor was preceded by a preheater and followed by a condenser. The reactor was equipped with a programmable temperature controller (PID) and the schematic diagram of the process is shown in Figure 3.1.

3.4.2 Experimental Procedure and Product Analysis

In a typical run, about 0.7 g of catalyst (which occupied about 6 cm height of the reactor) was charged into the reactor and the reaction was carried out at atmospheric pressure using unmodified as well as modified HZSM-5 catalysts. The catalyst was activated for one hour in an atmosphere of nitrogen before the experimental runs were started. The benzene and ethanol mixtures of 2:1 and 4:1 by volume ratio (1:1 and 3:1 mole ratio respectively) was introduced with the help of a metering pump at a rate of 0.4 ml/min and vaporized in the pre-heater before contacting the catalyst. The reactant vapours along with nitrogen entered the reactor, which was electrically heated. The flow rate of the carrier gas nitrogen was 0.5 litres per minutes. The products vapour, along with unreacted reactants, were condensed in the condenser and the liquid samples collected were analyzed in a gas chromatograph and mass spectroscopy with a 30 m x 0.32 mm (0.25 µm film thickness) Elite-1 capillary column (Perklin Elmer) using a flame ionization detector (FID). The program used was as follows. Initial oven temperature was 70 ^{o}C which was held for 2 min. After that the temperature was increased to 200 ^{o}C with a ramp rate 10^{o}C/min. Again it stayed at 200 ^{o}C for 1 min. The Detector and Injection temperatures were 250 ^{o}C. Flow rate of air, hydrogen and nitrogen were 350, 25 and 35 ml/min, respectively. Nitrogen was used as carrier gas and the split ratio was 1:50.

From gas chromatography results, the selectivity and yield of diethylbenzene in the product was calculated. The conversion of benzene was also noted for modified as well as unmodified HZSM-5 catalysts. Each experiment has been done three times and the average value has been taken. For experimental error greater than $\pm 5\%$, the experiment has been redone.

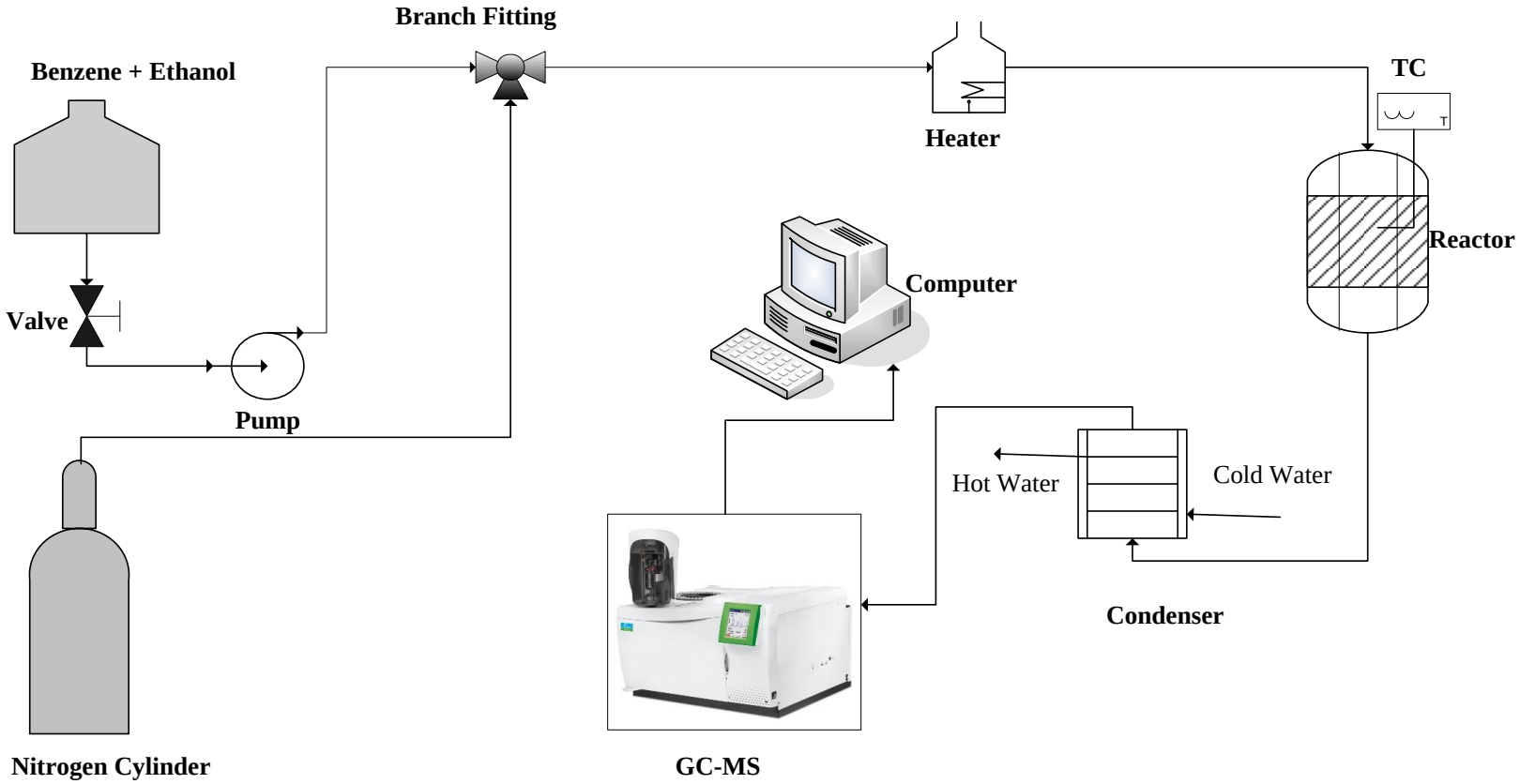

Figure 3-1: Schematic Diagram of Temperature Controlled Down Flow Tubular Reactor Used for Alkylation of Benzene with Ethanol

CHAPTER FOUR
RESULTS AND DISCUSSION

The work described in the present chapter explores the potential of boron, magnesium (monometallic) and boron-magnesium (bimetallic) supported HZSM-5 zeolite as catalysts for the selective alkylation of benzene with ethanol to produce ethylbenzene. The effects of support and boron-magnesium weight ratio on the catalytic activity and product selectivity have been investigated in detail. The physico-chemical characteristics of the catalysts were correlated with the catalytic performance. Furthermore, effect of various reaction parameters such as reaction temperature, benzene to ethanol ratio, silicon to aluminium ratio and metal loading were investigated to maximize benzene conversion and ethylbenzene selectivity. The stability of the catalysts was also investigated.

4.1 Selective Alkylation of Benzene with Ethanol Over Modified HZSM-5 Zeolite Catalysts (SAR=31) to Produce Ethylbenzene

Our objective was to develop a novel catalyst which could provide high benzene conversion and ethylbenzene yield at mild reaction conditions. For preliminary experiments, B or Mg monometallic and B-Mg bimetallic catalysts supported on HZSM-5 zeolite catalyst with SAR=31 were synthesized by incipient wetness impregnation method and examined for alkylation of benzene with ethanol. The catalytic experiments were carried out in a fixed bed continuous down flow tubular quartz (0.6 cm I.D and 66 cm long) reactor placed inside a microprocessor based temperature controlled furnace at 300-500 ^{o}C and at atmospheric pressure in the presence of nitrogen as carrier gas. The catalytic activity and products selectivity obtained for all catalysts were compared.

4.1.1 Effect of Physico-chemical Properties

4.1.1.1 BET Surface Area

Table 4.1 shows the surface area and pore volume of unmodified and modified HZSM-5 zeolite catalysts. The surface area of HZSM-5 (SAR=31) was 349 m^2/g. It can be found from Table 4.1 that the surface area of support was reduced significantly after metal impregnation. Among the modified support catalysts, the surface area of Mg(5%)-HZSM-5 catalyst was highest (308 m^2/g) and the surface area of B(4%)-Mg(5%)-HZSM-5 catalyst was the lowest

(270 m^2/g). Total pore volume of the unmodified HZSM-5 zeolite catalysts was also reduced after modification. This may be due to the deposition of metal cations used for modification.

Table 4-1: BET surface area of different types of HZSM-5 (SAR=31) catalysts

Type of catalyst	BET surface area (m^2/g)	External surface area (m^2/g)	Total pore volume (cm^3/g)	Average pore width (4V/A by BET) (Å)
Unloaded HZSM-5	349	134	0.22	25.05
Mg(5%)-HZSM-5	308	105	0.20	25.44
B(4%)-HZSM-5	278	58	0.18	25.46
Mg (5%)-B (4%) HZSM-5	270	74	0.17	25.75

4.1.1.2 XRD Analysis

XRD analysis was carried out using powder diffractometer (Bruker D8) at Institute Instrumentation Centre (IIC), Indian Institute of Technology Roorkee. Cu-Kα (λ=1.5417 Aº, 40 kv and 30 mA) was used as anode material and the range of scanning angle (2θ) was kept between 5º to 120º with scan speed of 2θ= 1º/min. The powder XRD patterns (Figure 4.1) of all the four samples exhibited well-resolved diffraction peaks, which were characteristic of the MFI framework structure. The high intensity of peaks in the XRD patterns indicated that the zeolite samples were highly crystalline materials and the highest diffraction peaks have been seen at 2θ = 23º. There was no mismatch in the pattern of peaks for a, b and d in Figure 4.1, so no other phase formation was found. However, a new peak appeared in the case of (c) around 28º, which is due to the formation of B_2O_3 as a new phase. Although the peaks were shifted towards higher 2θ values, may be due to the internal stress or due to the change in inter planar distance. Greater shift was found for boron modified. The reason was due to the incorporation of the metal cation into the framework and formation of new phase. All the modified samples were found to be highly crystalline. The XRD patterns were used to calculate the average crystal size and the relative crystallinity of the different zeolites. The average crystal sizes were estimated using the Scherrer equation.

$$D = \frac{k\lambda}{\beta \mathrm{Cos}\theta} \text{ ---------- (4.1)}$$

Where D is the crystal size, k is a constant (0.99), λ is the X-ray wavelength (λ= 0.1542 nm), β the peak width at a half-height (in radians) and θ the Bragg's angle of diffraction.

The relative crystallinity of the modified zeolites was calculated by comparing the average intensities of the most intense peaks with that of the parent zeolite, HZSM-5, assuming 100% of crystallinity for the starting material. The calculations were made according to the standard methods ASTM D 5758 for ZSM-5 zeolite.

$$\%\text{XRD Relative Crystallinity of HZSM\_5} = \frac{\text{Hs}}{\text{Hr}} * 100\% \text{ ---------- (4.2)}$$

Where, H_s = peak height for the sample, and H_r = peak height for the reference sample.

As we can see from Table 4.2 the crystal size of the modified and unmodified HZSM-5 were the same but the relative crystallinity was highest for 4%B-HZSM-5 while the lowest crystallinity was for 4%B-5%Mg-HZSM-5.

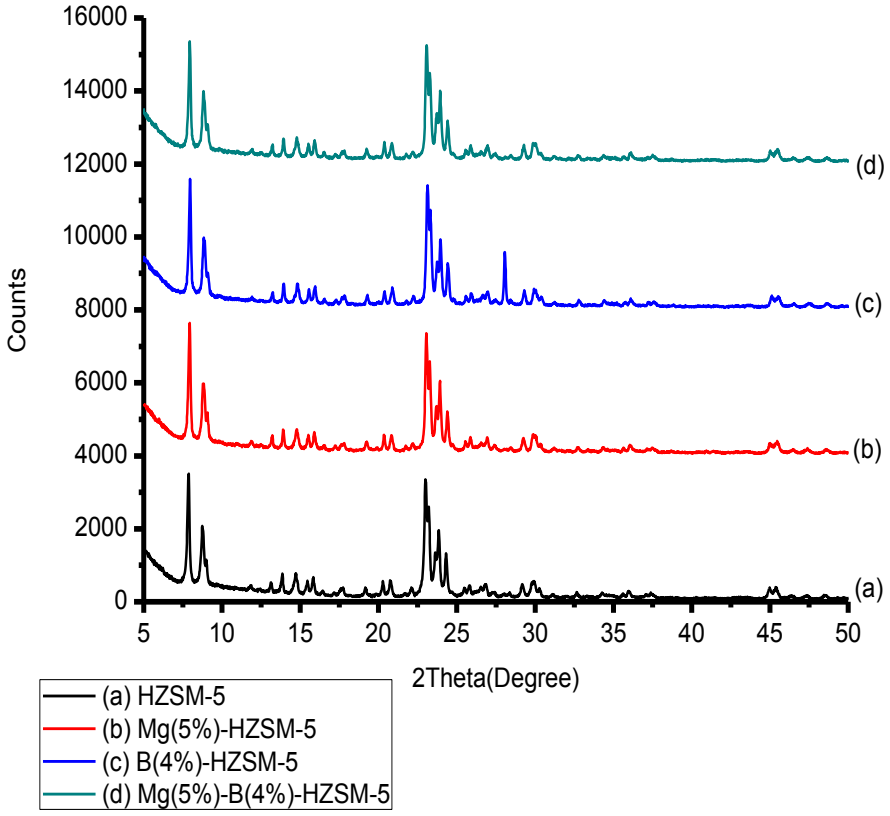

Figure 4-1: X-ray diffraction patterns of unmodified and modified HZSM-5 (SAR=31)

Table 4-2: Relative crystallinity and crystal size of modified and unmodified HZSM-5

No.	Type of catalyst	Crystal size (Å)	Relative crystallinity (%)
1	HZSM-5	180	100
2	5%Mg-HZSM-5	180	97.7
3	4%B-HZSM-5	180	98.2
4	4%B-5%Mg-HZSM-5	180	93.1

4.1.1.3 FE-SEM and TEM

The morphology of the zeolite samples was evaluated by Transmission Electron Microscopy (TEM) and Field Emission- Scanning Electron Microscope (FE-SEM) using a TEM TECNAI G^2 20 S-TWIN and ULTRA plus, respectively. Transmission Electron Microscopic images of the samples are shown in Figure 4.2. TEM results show modified zeolite to be in good agreement with XRD results as there were no major changes in the structure (morphology). In this way, it was possible to confirm that the particle sizes and morphologies remained unchanged during the impregnation treatments. The zeolite was able to keep its structure even after loading with boron and magnesium. Further the TEM imaging shows rough surface and irregular shape of the crystal. The presence of boron and magnesium on the surface of zeolite crystallites was identified by using EDAX. The elemental chemical analyses performed by Atomic Absorption Spectroscopy (AAS) (Avanta M) and Inductive Coupling Plasma Mass Spectroscopy (ICP-MS) (Perkin Elmer) also support the EDAX results shown in Figure 4.4 below.

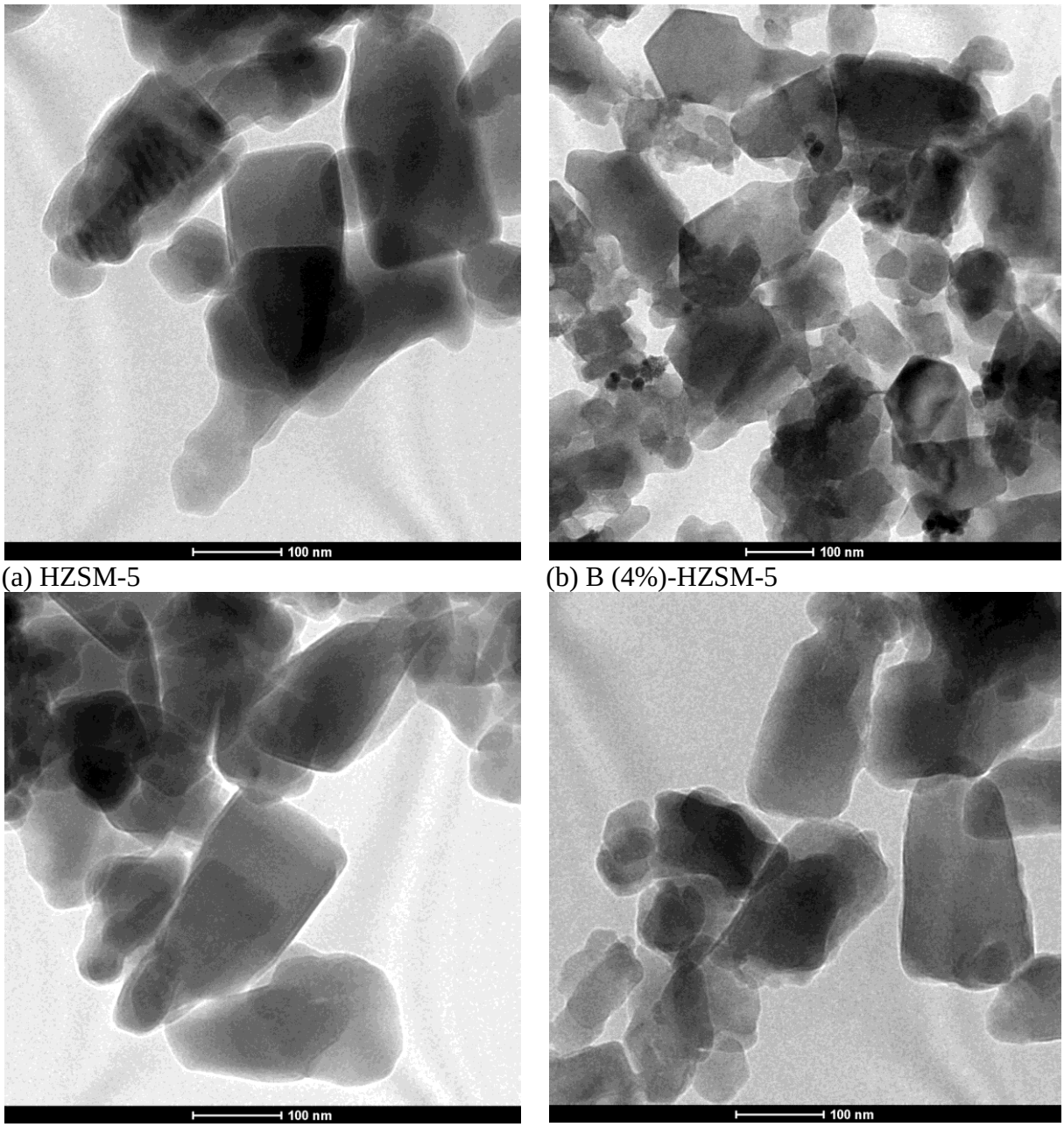

(a) HZSM-5 (b) B (4%)-HZSM-5

(c) Mg(5%)-B(4%)-HZSM-5 (d) Mg(5%)-HZSM-5

Figure 4-2: Transmission Electron Microscopic results of unmodified and modified HZSM-5

Scanning electron micrograph (Figure 4.3) of all the samples indicates the morphology of the parent and modified HZSM-5 zeolite crystals. It can be seen that the individual particles form larger and irregular aggregates, being therefore difficult to determine the mean size of the primary particles from the SEM image. The FE-SEM photographs reveal a change in the morphology of HZSM-5 upon modification with boron and magnesium. A comparison of the activities between modified and unmodified HZSM-5 reveals that the appearance of cavities and cages facilitates the alkylation reaction and shape selectivity of the catalyst after its modification.

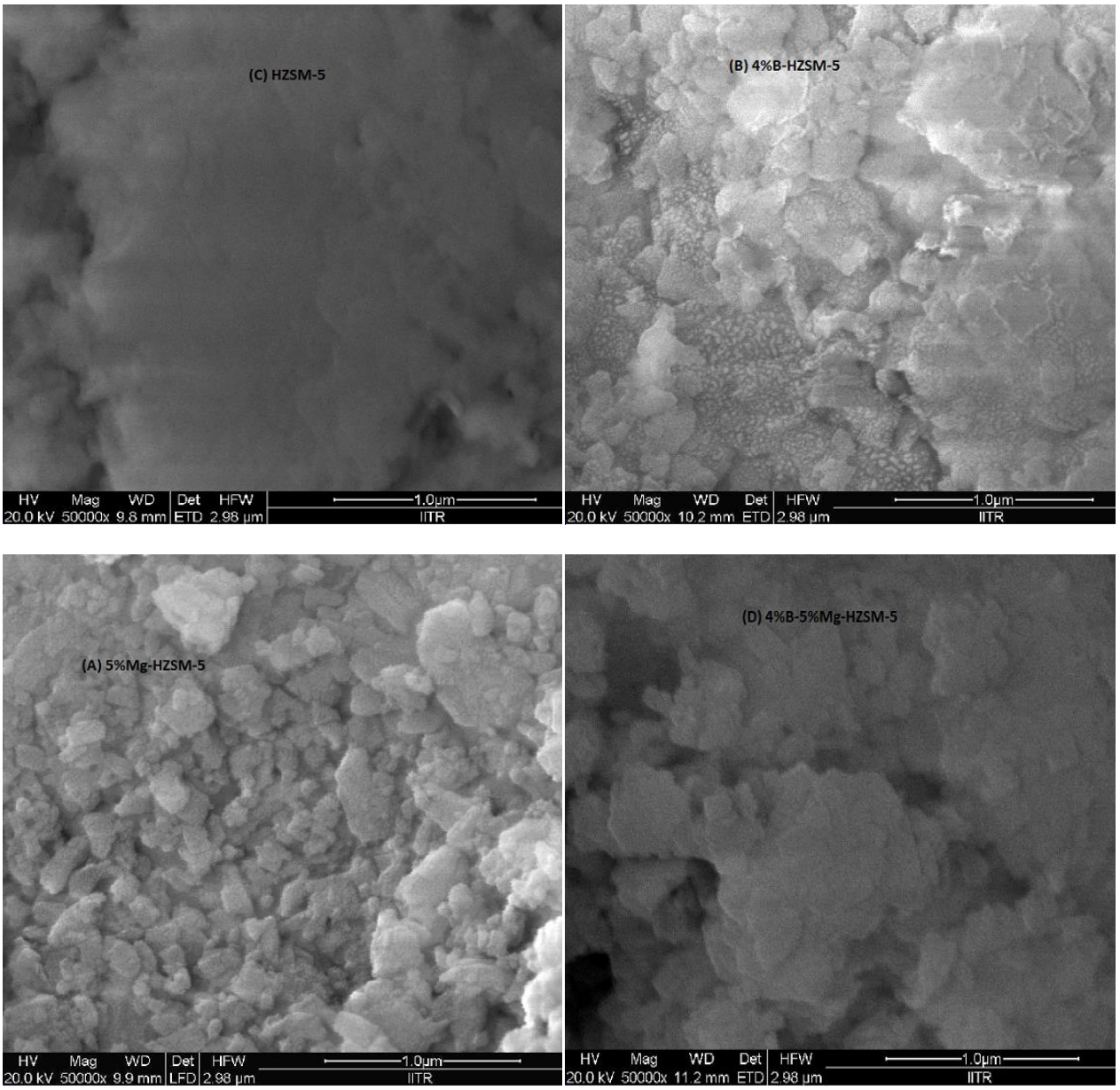

Figure 4-3: Scanning Electron Microscopic results of unmodified and modified HZSM-5

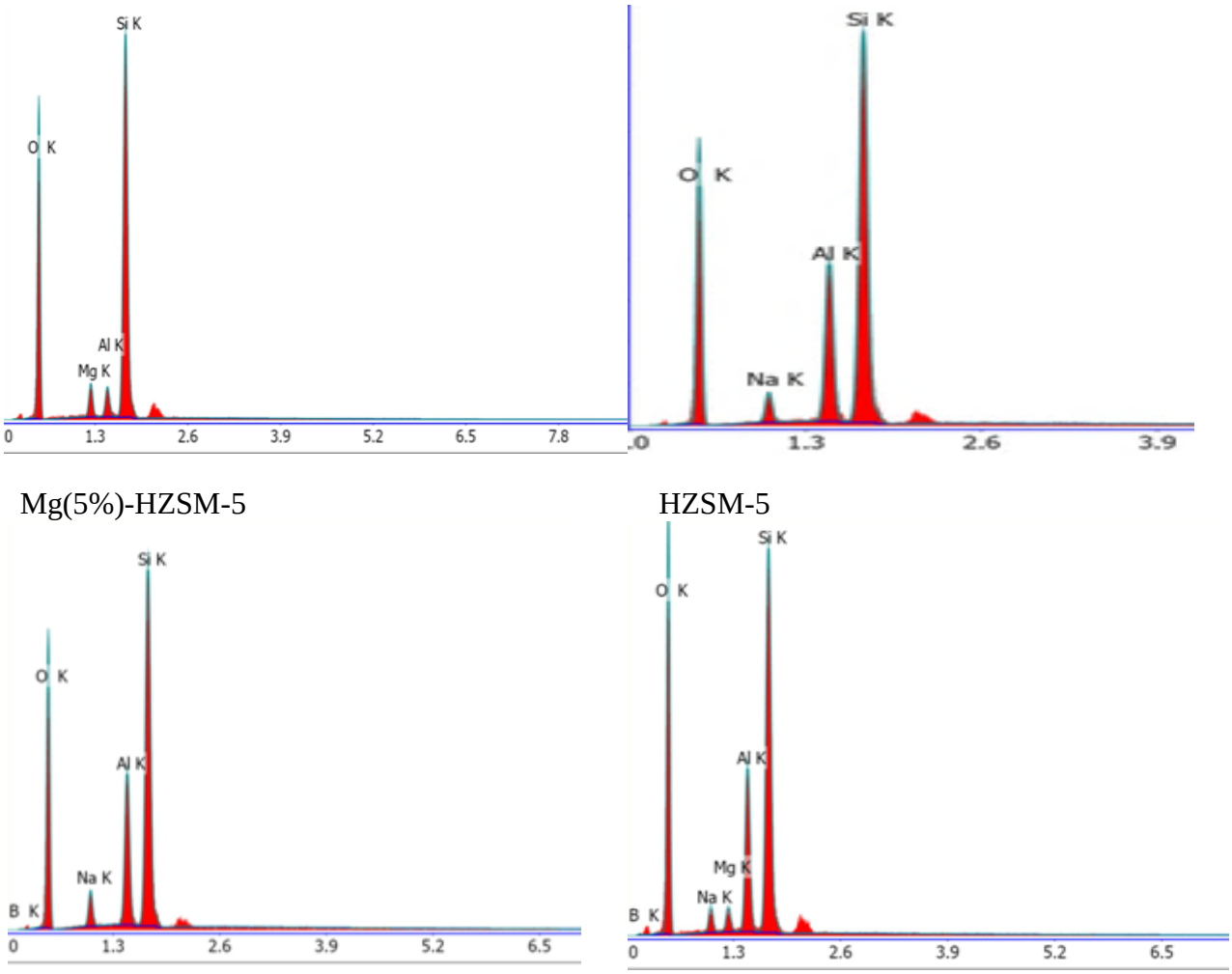

Figure 4-4: EDAX results of unmodified and modified HZSM-5

4.1.1.4 Thermo- gravimetric Analysis

Thermo- gravimetric analysis (TGA) was conducted in order to determine the thermal stability of the zeolite framework and weight loss occurring (from zeolite lattice) during heating. TGA were conducted on SII 6300 EXSTAR using air as carrier gas at 200 ml/min on a 10 mg of sample. Figure 4.5 presents the TGA of unmodified and modified HZSM-5 (Si/AL ratio = 31) heated from ambient temperature to 1000 ^{o}C in the temperature progression of 10 ^{o}C/min. The portion of the curves up to 200 ^{o}C is normally linked to the weight loss due to moisture content of the catalyst, whereas, the portion of the curves from 200 to 1000^{o}C is assigned to the weight loss due to removal of hydrocarbon, moisture contained inside the pores and coke. 4%B-HZSM-5 catalyst has the lowest weight loss up to 550 ^{o}C but beyond this temperature huge weight loss occurred. From ambient temperature to 1000 ^{o}C, the highest weight loss was seen for 4%B-HZSM-5 followed by 5%Mg-HZSM-5, 4%B-5%Mg-HZSM-5

and HZSM-5 respectively. The weight loss of 4%B-HZSM-5 between 650-900^{o}C is due to melting of B_2O_3 which had appeared as a new phase. The percent weight loss of all the catalysts is given in table (3) below.

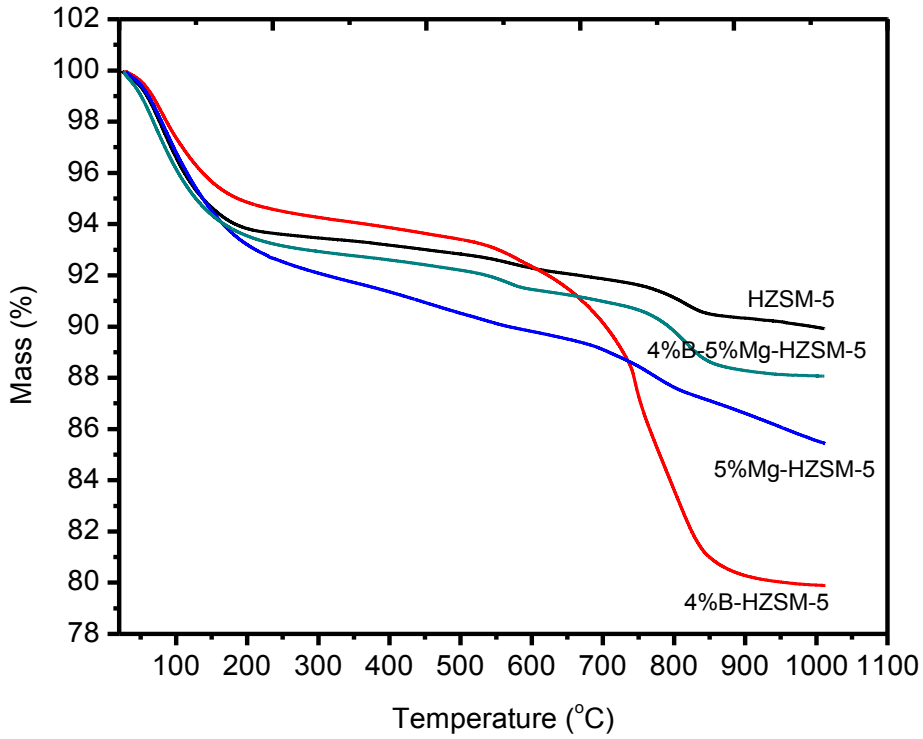

Figure 4-5: TGA graph of HZSM-5, 4%B-HZSM-5, 5%Mg-HZSM-5 and (4%B-5%Mg) HZSM-5

Table 4-3: Percent weight loss of modified and unmodified HZSM-5 by TGA test (from ambient to 1000 ^{o}C)

No.	Name of catalyst	TGA percent weight loss (%)
1	HZSM-5	10.1
2	B(4%)-HZSM-5	20.1
3	Mg(5%)-HZSM-5	14.5
4	Mg(5%)-B(4%)-HZSM-5	11.9

The percent weight loss for modified and unmodified HZSM-5 by TGA test revealed that there was greater weight loss happened to the modified catalyst. However, when the catalyst was modified by bimetallic element the weight loss become reduced**.**

4.1.1.5 FTIR Analysis

Infrared spectra were obtained at 4 cm^{-1} resolution on Nicolet 6700 series FTIR Spectrometer. The infrared cell used was fitted with KBr windows. A sample of the zeolite powder was accurately weighed and mixed with around 300 mg KBr and then passed into a 10 mm diameter wafer at 15 tonnes/cm^2 pressure. This wafer was placed in the IR cell. The IR cell spectra were recorded at room temperature in air. Background IR correction for air was also made.

The IR structural studies of zeolite were carried out in the infrared region of wave number 400 to 4000 cm^{-1}, because fundamental vibrations of SiO_4, AlO_4 or TO_4 units are contained in this region. In the KBr pellet technique a small amount of the solid sample is mixed with powdered KBr and pressed into pellet.

The band at (i) 545 cm^{-1} is assigned to the highly distorted double five membered rings present in the ZSM-5 structure, (ii) 3739, 3660 and 3609 cm^{-1} are assigned to weak, medium and strong Brønsted acid sites , respectively, (iii) 1700 cm^{-1} to water bond, (iv) 800 cm^{-1} to Al-O bond and (v) 1350 cm^{-1} to Si-O-Si bond, etc. The values of the wave numbers mentioned above against particular characteristics may shift a little after the ion exchange process.

Table 4-4: The approximate IR band corresponding to a functional group present in the HZSM-5

Functional group	Wavenumber	Functional group	Wavenumber
Si-OH	3745 cm^{-1}	Si-O-Si	1140 cm^{-1}
Si-OH-Al	3610 cm^{-1}	Si-O-Al	1075 cm^{-1}
Al-OH	3600 cm^{-1}	Al-O	760 cm^{-1}
H-OH	1660 cm^{-1}		

The FTIR test showed that there was strong acid site around 3500 cm^{-1} while weak acid site observed 1200 cm^{-1}. The area of the peaks indicates the concentration of strong and weak acidic sites. These results agree with the NH_3-TPD result and the experimental result obtained. For bimetallic modified catalyst the good result obtained was due to the weak acidic sites on

the surface for unmodified HZSM-5 reduced and strong acidic sites inside the pores increased (see Figure 4.6).

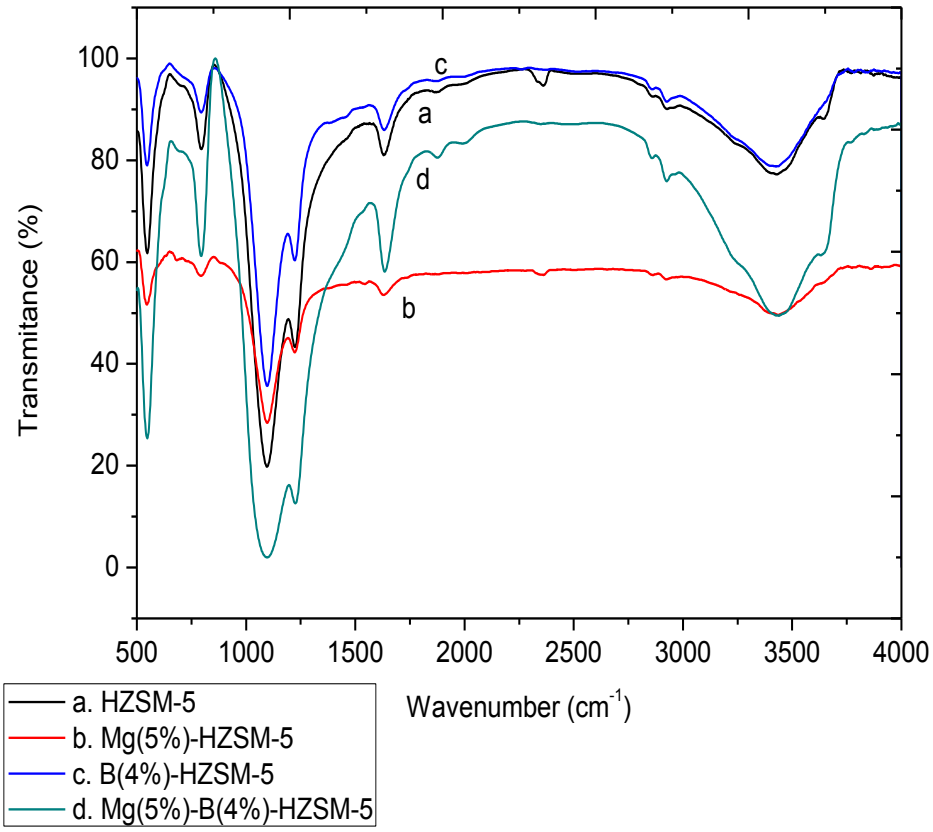

Figure 4-6: FTIR spectra of modified and unmodified HZSM-5 zeolites in the region of framework vibrations

4.1.1.6 Temperature Programmed Desorption of Ammonia (NH_3-TPD)

NH_3-TPD measurements in the range from room temperature to 650^oC were performed in a micromeritics ChemiSorb 2720. Zeolite samples were put in a U shape quartz cell and pretreated, insitu, for 1 h at 250 ^oC in a flow of nitrogen (>99%) of 20 ml/min. After cooling to 25^oC, adsorption of ammonia was carried out in a flow of ammonia and helium mixture of 40 ml/min. After the catalyst surface became saturated, it was waited for some time to remove the excess of ammonia. The temperature-programmed desorption was carried out with a linear heating rate of approximately 10 ^oC/min from 25 ^oC to 650 ^oC in a flow of helium (>99%) at 20 ml/min. The NH_3 that desorbed was measured by a thermal conductivity detector and the electrical signals from the detector and from the thermocouple (that measures the temperature

inside the cell with the catalyst) were digitised by a CR3A chromatographic integrator and transmitted to a computer.

The temperature programmed desorption of a basic molecule such as ammonia (NH_3-TPD) is one of the most commonly used methods used for measuring the surface acidity of porous materials such as zeolites, clays or mesoporous silica [111].

The acid strength can be determined by measuring the heat of adsorption or desorption of a suitable probe molecule. Ammonia meets the requirements of such a probe. Firstly, it is small enough to enter all the zeolite pores. Secondly, it can react with both the Brønsted and Lewis acid sites [112].

From the NH_3-TPD experiments (Figure 4.7) it could be concluded that two types of acid sites are present in H-ZSM-5: weak acid sites corresponding with desorption at low temperature and strong acid sites corresponding with desorption at high temperature. The amount of this weak acid and strong acids is listed in Table 4.5.

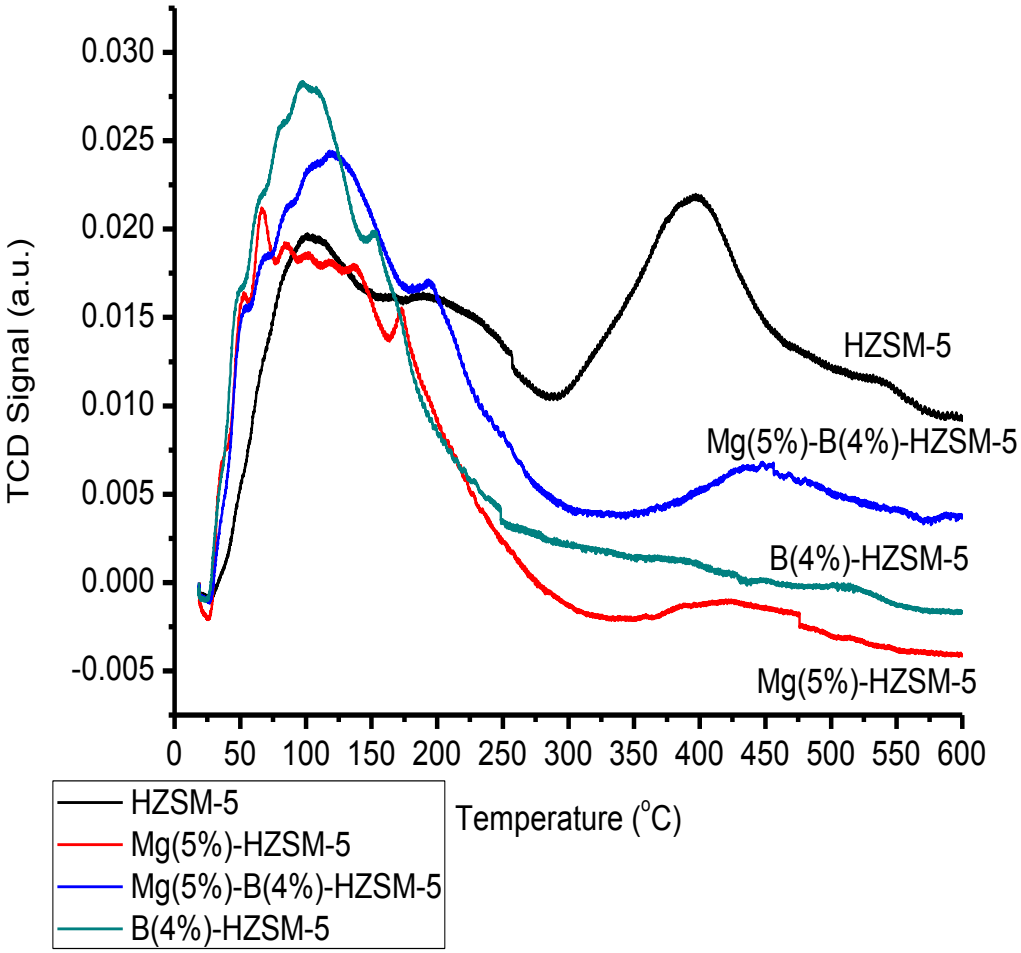

Figure 4-7: Ammonia Temperature Programmed Desorption (NH_3-TPD) of Modified and Unmodified HZSM-5

Table 4-5: Ammonia Temperature Programmed Desorption (NH_3-TPD) of Modified and Unmodified HZSM-5 (SAR=31)

No.	Type of catalyst	Concentration of weak acid sites (mmol/g)	Concentration of strong acid sites (mmol/g)
1	HZSM-5	5.388	2.706
2	Mg(5%)-HZSM-5	0.447	1.947
3	B(4%)-HZSM-5	1.305	2.458
4	Mg(5%)-B(4%)-HZSM-5	1.538	3.771

4.1.2 Performance of Modified and Unmodified HZSM-5 Catalysts

Benzene alkylation with ethanol can be considered as an electrophilic substitution on the aromatic ring over acidic zeolites. It is commonly considered as proceeding via a carbenium ion-type mechanism [113]. The ethylation of benzene with ethanol has been proposed to take place by the reaction of the activated alkene (formed by dehydration of the alcohol) on the acid sites of the zeolite [73, 114]. Scientists and researchers have developed different catalysts in order to make ethanol dehydration more industrial friendly to enhance ethylene yield and lower reaction temperature. Phosphoric acids, oxides, zeolites, and hetero poly acids have been used as catalysts used for acid catalysed alcohol dehydration. Among the zeolite catalysts, ZSM-5 zeolite is most widely studied, due to its capability of catalysing the reaction at lower temperatures, which made it commercially valuable and promising [115].

The disproportionation of toluene to benzene and xylene is known to be catalysed by acidic catalysts such as HZSM-5 and HY/β-AlF_3/Cu [116, 117]. Various types of zeolites, such as mordenite, USY, Beta, MCM-22 and ZSM-5 catalysts have also shown good catalytic activity and stability in ethylbenzene disproportionation/alkylation using different types of reactor and reaction conditions. The disproportionation of ethylbenzene gives rise to diethylbenzene and benzene [114].

In the present study, a comparison between the performances of unmodified and modified HZSM-5 for the alkylation reaction of benzene with ethanol was carried out. Experiments were carried out in a fixed catalytic bed down flow reactor at a constant feed (benzene and ethanol mixture, 2:1 by volume) rate of 0.4 ml/min and a carrier gas (N_2) flow 0.5

litres per minute (lpm). The WHSV of benzene and ethanol mixture as feed was 32.6 h^{-1} using nitrogen as carrier gas and to activate catalyst. The products of the reactions were analyzed by gas chromatograph. Liquid products contained benzene, ethanol, toluene, ethylbenzene, p-xylene, m-xylene, o-xylene, diethylbenzene and triethylbenzene. The gaseous products contained negligible amount of hydrocarbon gases (ethane, methane, ethylene, etc.). The following equations were used to check the activity of the catalysts:

$$\text{Benzene conversion } (\%X_B) = \frac{\text{Moles of benzene converted}}{\text{Moles of benzene in the feed}} \times 100 \qquad (4.3)$$

$$\text{Ethylbenzene yield } (\%Y_{EB}) = \frac{\text{Moles of ethylbenzene obtained}}{\text{Moles of beneze converted}} \times 100 \qquad (4.4)$$

$$\text{Ethylbenzene selectivity } (\%S_{EB}) = \frac{\text{Moles of ethylbenzene (desired product) formed}}{\text{Moles of all products formed}} \times 100 \qquad (4.5)$$

4.1.2.1 Unmodified HZSM-5 Zeolite Catalyst

From Table 4-6 it can be seen that the product contains xylenes mixture, ethyl benzene, diethylbenzene, triethylbenzene, unconverted benzene and ethanol. Again it can be seen from Figure 4-8 that with the increase in reaction temperature from 300 to 400 ^{o}C the conversion of benzene increases and starts to decline beyond that. The benzene conversion passes through a pronounced maximum at 400 ^{o}C. However, the selectivity of ethylbenzene increases starting from 350 ^{o}C while the highest yield of ethylbenzene was obtained at 450 ^{o}C.

Table 4-6: Effect of reaction temperature on catalytic performance of HZSM-5 catalyst for alkylation of benzene with ethanol

Products (mol %)	**Temperature (^{o}C)**				
	300^{o}C	350^{o}C	400^{o}C	450^{o}C	500^{o}C
Ethanol	18.83	15.68	11.41	9.84	13.54
Benzene	41.57	33.78	30.52	32.39	41.39
Toluene	0.71	0.56	0.68	0.84	0.47
Ethylbenzene	22.71	23.29	28.92	33.62	30.97
Para-Xylene	1.55	2.82	1.48	0.78	0.29
Meta-Xylene	0.66	1.36	1.05	0.86	0.36
Ortho-Xylene	0.95	1.44	1.17	0.73	0.32
Diethylbenzene	3.79	7.23	8.13	7.32	3.35
Triethylbenzene	6.68	10.01	14.97	12.81	7.21
Others	2.51	3.81	1.67	0.81	2.11

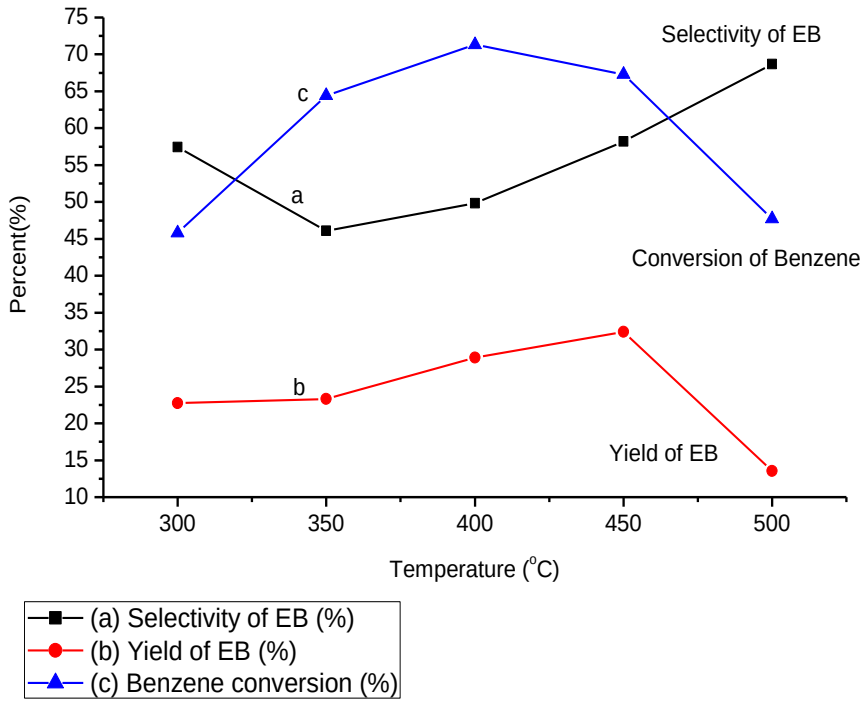

Figure 4-8: Effect of reaction temperature on catalytic performance of HZSM-5 catalyst for alkylation of benzene with ethanol for selectivity and yield of ethylbenzene

4.1.2.2 Modified HZSM-5 Zeolite Catalyst

A) Magnesium Modified HZSM-5 Zeolite Catalyst

The results of the alkylation of benzene with ethanol using Mg(5 %)-HZSM-5 as a catalyst is presented in Table 4-7 and Figure 4-9. The products were toluene, xylenes, diethylbenzene, triethylbenzene and ethylbenzene. At reaction temperatures of 400 ^{o}C, Mg(5%)-HZSM-5 shows highest conversion of 71.7 %.

Ethylbenzene (EB), diethylbenzene (DEB) and triethylbenzene (TEB) were obtained as major products in the alkylation of benzene with ethanol over Mg(5%)-HZSM-5 catalyst. Negligible amounts of xylene, toluene and gaseous hydrocarbons were also detected.

Figure 4-9 summarizes the product selectivity during the alkylation of benzene with ethanol over this catalyst. Ethylbenzene was obtained as the most predominant product over this catalyst and might be attributed to its free diffusion without steric hindrance through the pores of the catalysts. Formation of ethylbenzene represents the primary alkylation step, while

the alkylation reaction of ethylbenzene with ethanol led to the formation of diethylbenzene, representing the secondary alkylation reaction. Ethylbenzene selectivity over Mg(5%)-HZSM-5 decreases with increase in benzene conversion and vice versa.

Table 4-7: Effect of reaction temperature on catalytic performance of 5%Mg-HZSM-5 catalyst for alkylation of benzene with ethanol

Products (mol %)	**Temperature (^{o}C)**			
	350^{o}C	400^{o}C	450^{o}C	500^{o}C
Ethanol	2.84	2.18	1.98	3.58
Benzene	35.84	27.72	32.55	40.46
Toluene	1.4	0.84	0.66	0.66
Ethylbenzene	29.13	31.60	33.55	33.95
Para-Xylene	2.24	1.86	1.24	0.58
Meta-Xylene	1.94	1.60	1.13	0.53
Ortho-Xylene	1.26	1.24	0.84	0.45
Diethylbenzene	11.3	14.31	10.75	5.75
Triethylbenzene	11.88	16.44	15.27	10.46
Others	2.18	2.20	2.05	3.59

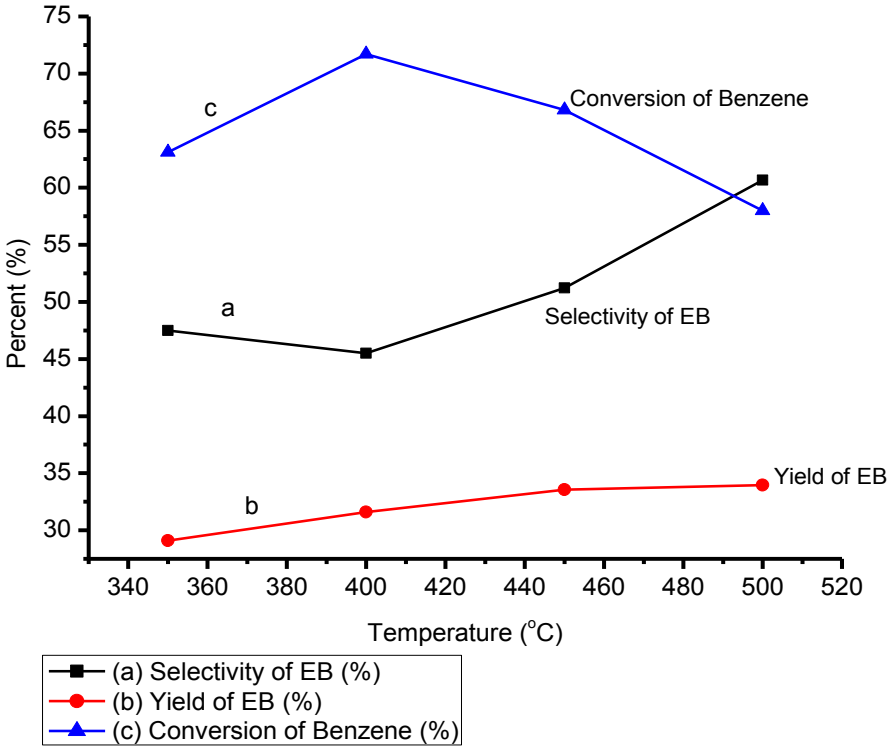

Figure 4-9: Effect of reaction temperature on catalytic performance of 5%Mg-HZSM-5 catalyst for alkylation of benzene with ethanol for selectivity and yield of ethylbenzene

B) Boron Modified HZSM-5 Zeolite Catalyst

When ethanol is contacted with benzene in the presence of solid acid catalyst, the alkylating agent can follow (a) alkylation with benzene to produce ethyl benzene (b) ethylbenzene reacts with ethanol to produce diethylbenzene and (c) diethylbenzene reacts with excess ethanol to produce triethylbenzene. Table (4-8) and Figure 4-10 show the effect of reaction temperature on catalytic performance of B(4%)-HZSM-5 catalyst for alkylation of benzene with ethanol. Table 4-8 shows the formation of xylenes, diethylbenzene, triethylbenzene and ethylbenzene in the products. The highest conversion of benzene was obtained at 400 ^{o}C while the selectivity of ethylbenzene increased with a decrease in benzene conversion.

Table 4-8: Effect of reaction temperature on catalytic performance of 4%B-HZSM-5 catalyst for alkylation of benzene with ethanol

Products (mol %)	**Temperature (^{o}C)**			
	350^{o}C	400^{o}C	450^{o}C	500^{o}C
Ethanol	16.48	10.09	-	-
Benzene	55.57	34.02	38.96	46.35
Toluene	-	-	-	-
Ethylbenzene	22.28	31.31	38.32	38.06
Para-Xylene	5.66	2.58	1.57	0.67
Meta-Xylene	-	-	-	-
Ortho-Xylene	-	-	-	-
Diethylbenzene	-	6.42	5.35	2.94
Triethylbenzene	-	15.58	15.80	9.75
Others	-	-	-	2.23

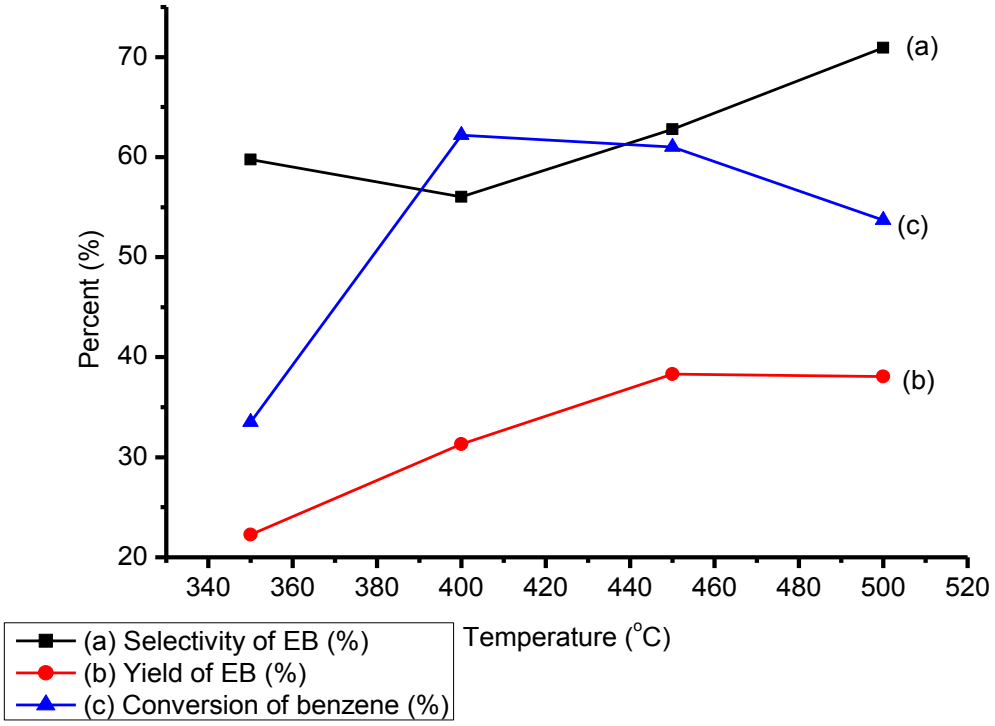

Figure 4-10: Effect of reaction temperature on catalytic performance of 4%B-HZSM-5 catalyst for alkylation of benzene with ethanol showing selectivity and yield of ethylbenzene.

C) Boron and magnesium bimetallic modified HZSM-5 zeolite catalyst

The effect of reaction temperature on conversion of benzene as well as ethanol (limiting reactant) for the alkylation reaction over Mg(5%)-B(4%)-HZSM-5 for benzene to ethanol ratio (v/v) 2:1 is shown in Table 4.9 and Figure 4.11. In the temperature range of 300-500 ^{o}C, the conversion of benzene is found to be increasing up to 400^{o}C, which thereafter starts decreasing. The decline in conversion of benzene is probably due to the decomposition of alkylating reagent (ethanol) at higher temperatures. Furthermore, above reaction temperature of 400 ^{o}C, reversible reactions (transalkylation reaction and ethylbenzene disproportionation) are likely to play an important role, thereby decreasing conversion of benzene. According to Mogahid Osman et al., 2013, the catalytic experiment in the CREC Riser Simulator shows that low temperature favours the EB ethylation reaction while higher temperature is favourable for disproportionation.

The effect of reaction temperature on selectivity of ethylbenzene over Mg(5%)-B(4%)-HZSM-5 catalyst for the above stated ratio of feed is also shown in Figure 4.11. Both the selectivity and yield of ethylbenzene is found to increase with increase in temperature. It

appears that with increase in temperature the diffusion rates are increased and, thereby, the selectivity and para selectivity is also increased. Ethylbenzene was the major product.

Table 4-9: Effect of reaction temperature on catalytic performance of Mg(5%)-B(4%)-HZSM-5 catalyst for alkylation of benzene with ethanol

Products (mol %)	**Temperature (°C)**				
	300°C	350°C	400°C	450°C	500°C
Ethanol	3.00	1.82	1.89	5.09	2.93
Benzene	47.02	34.49	32.97	41.99	46.34
Toluene	0.35	0.81	0.70	0.37	0.76
Ethylbenzene	31.06	34.45	37.72	37.39	36.92
Para-Xylene	6.77	4.93	2.51	0.43	0.47
Meta-Xylene	1.03	2.01	1.43	-	-
Ortho-Xylene	0.94	1.33	0.91	-	-
Diethylbenzene	2.81	8.46	9.06	3.05	2.69
Triethylbenzene	4.80	10.45	11.87	6.99	5.18
Others	1.81	1.24	0.94	4.69	4.70

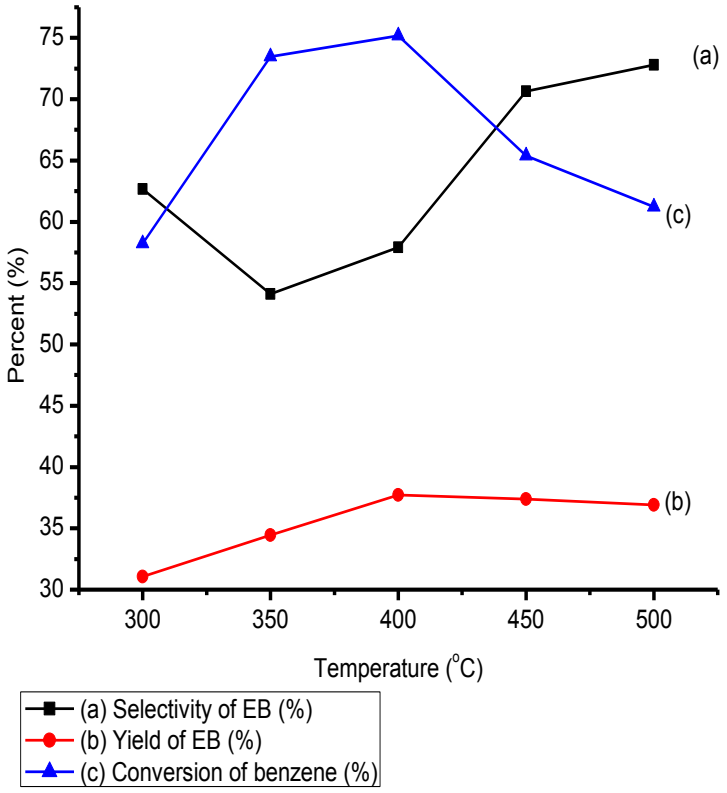

Figure 4-11: Effect of reaction temperature on catalytic performance of Mg (5%)-B (4%)-HZSM-5 catalyst for alkylation of benzene with ethanol for selectivity and yield of ethylbenzene

4.1.2.3 Performance Comparison of Modified and Unmodified HZSM-5 Catalysts

As it is shown below in Figure 4.12, the highest selectivity of ethylbenzene was obtained with boron modified HZSM-5 for the temperature range below 390 ^{o}C. Above this temperature the highest selectivity of ethyl benzene was obtained by using bimetallic (B and Mg) modified HZSM-5. Generally, it is observed that the selectivity of ethyl benzene over Mg (5%)-B (4%)-HZSM-5 and B(4%)-HZSM-5 were higher than unmodified HZSM-5. Mg(5%)-HZSM-5 had lower ethylbenzene selectivity than unmodified HZSM-5 above 360 ^{o}C.

From Figure 4.13, the highest yield of ethylbenzene (37.7%) was obtained by Mg (5%)-B (4%)-HZSM-5 for the temperature range below 440 ^{o}C. While above 440 ^{o}C the highest yield (38.32 %) was obtained by B(4%)-HZSM-5. The unmodified HZSM-5 had the lowest yield (32.39 %) compared to the modified ones. As shown in Figure 4.14 and 4.15, in terms of benzene and ethanol conversions, Mg (5%)-B (4%)-HZSM-5 was the best. B(4%)-HZSM-5 showed lower benzene conversion while Mg(5%)-HZSM-5 showed better benzene conversion relative to unmodified HZSM-5.

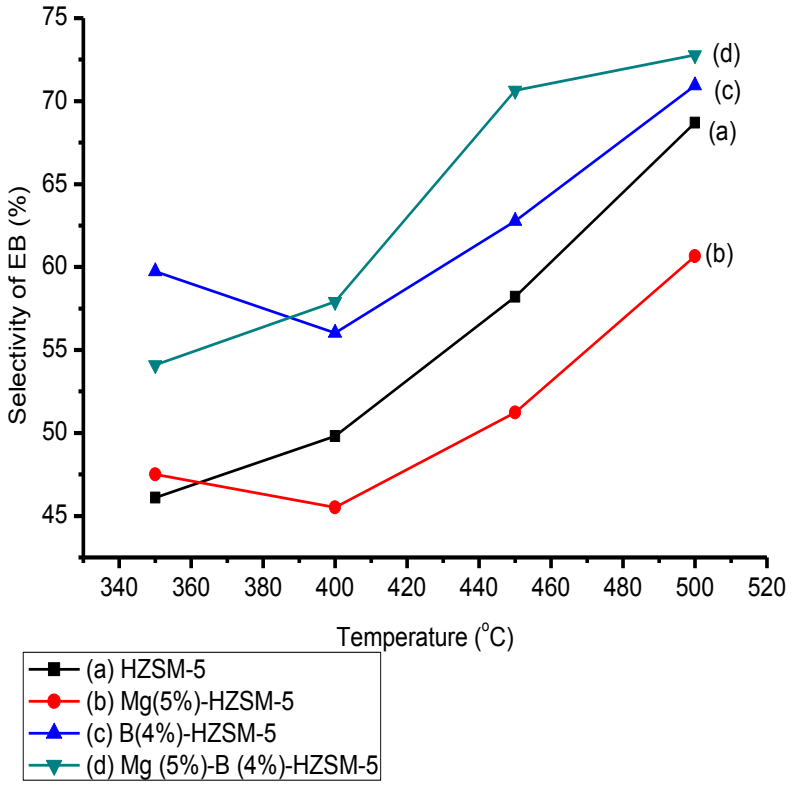

Figure 4-12: Selectivity of Ethylbenzene (%) for modified and unmodified HZSM-5

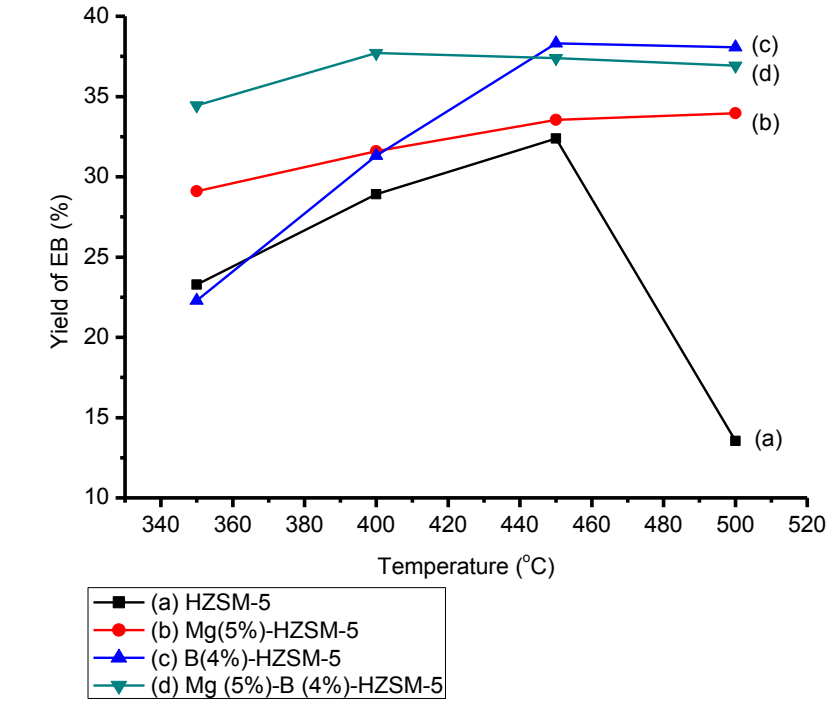

Figure 4-13: Yield of Ethylbenzene (%) for modified and unmodified HZSM-5

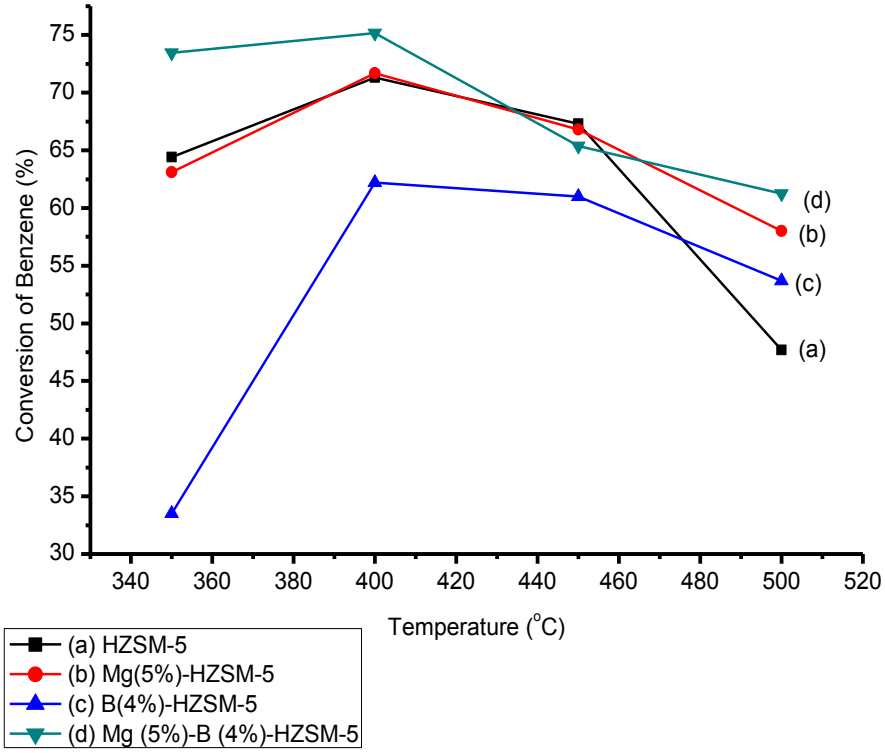

Figure 4-14: Conversion of benzene (%) for modified and unmodified HZSM-5

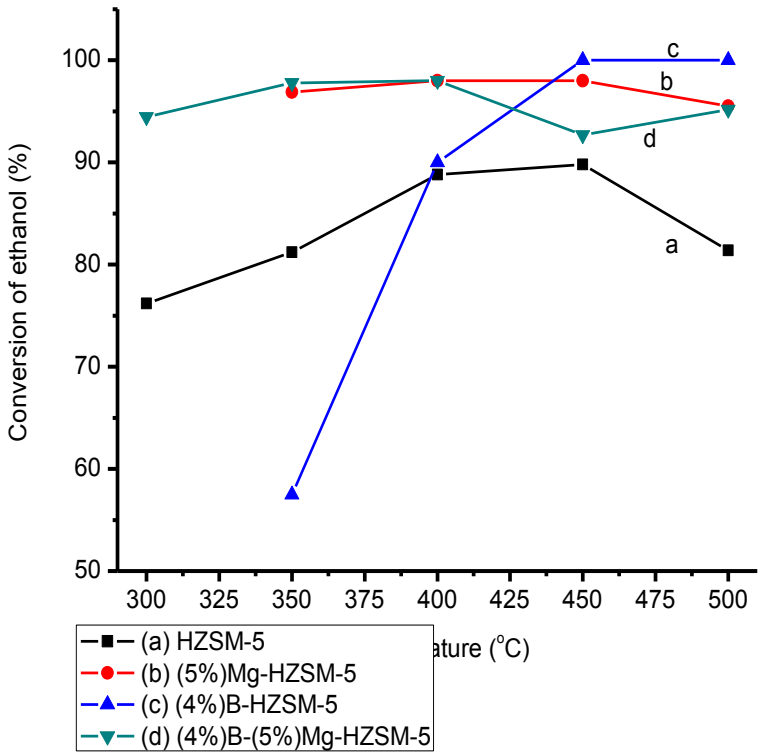

Figure 4-15: Conversion of ethanol (%) for modified and unmodified HZSM-5

Summary:
From the experimental results presented above we observed the following

- Ethylbenzene is the primary product while diethylbenzene, triethylbenzene, toluene and xylene mixtures also exist in the product.
- Highest selectivity of ethylbenzene (72.79%) and higher conversion of benzene (75.17%) was obtained by bimetallic catalyst (Mg(5%)-B(4%)-HZSM-5) at 500^{o}C and 400^{o}C respectively. This is due to pore size reduction form BET surface area result and also reduction of weak acids on the surface and increase of strong acids sites inside the pores of the catalysts which observed from NH_3-TPD results.
- Boron modified showed lower benzene conversion (62.2%) while magnesium modified showed approximately the same benzene conversion (71.7%) when compared to unmodified HZSM-5 (71.3%).
- The existence of abundant ethanol may facilitate the alkylation of benzene to produce ethylbenzene and then further alkylation to diethylbenzene and tri ethylbenzene. Therefore, it would be essential to do further investigation.

4.2 Selective Alkylation of Benzene with Ethanol over Modified HZSM-5 Zeolite Catalysts (SAR=90)

In this section, the performance of HZSM-5 zeolite catalysts (SAR=90) modified with boron, magnesium and magnesium-boron have been compared. Our objective in this section was to develop a novel catalyst which can provide high benzene conversion and ethylbenzene yield at mild reaction condition (temperature range 300-500 ^{o}C and at atmospheric pressure). For preliminary experiments, B or Mg monometallic and B-Mg bimetallic catalysts supported on HZSM-5 zeolite catalyst with SAR=90 were synthesized by incipient wetness impregnation method and examined for alkylation of benzene with ethanol. Total metal loading of 5, 10, and 15 % was used for catalyst synthesis. The catalytic experiments were carried out in a fixed bed continuous down flow tubular quartz (0.6 cm I.D and 66 cm long) reactor placed inside a microprocessor controlled furnace reactor in the temperature range 300-500 ^{o}C and atmospheric pressure in the presence of nitrogen gas. The catalytic activity and products selectivity obtained for all catalysts were compared.

4.2.1 Selective Alkylation of Benzene with Ethanol over Magnesium Modified HZSM-5 Zeolite Catalysts (SAR=90)

4.2.1.1 Effect of Physico-chemical Properties

4.2.1.1.1 XRD

X-ray powder diffraction was employed to determine the value of relative crystallinity (RC). The commercial zeolite, HZSM-5 was assumed to have 100% crystallinity. The determination of the value was based on the area of the characteristic peaks in the 2Θ range of from 22.5^{o} to 25^{o}. XRD analysis was carried out using powder diffractometer (Bruker D8) at Institute Instrumentation Centre (IIC), Indian Institute of Technology Roorkee. Cu-Kα (λ=1.5417 Å, 40 kv and 30 mA) was used as anode material and the range of scanning angle (2θ) was kept between 5º to 50º with scan speed of 2θ= 1º/min. The powder XRD patterns (Figure 4.16) of all the four samples exhibited well-resolved diffraction peaks, which were characteristic of the MFI framework structure. The high intensity of peaks in the XRD patterns indicated that the zeolite samples were highly crystalline materials and the highest diffraction peaks have seen at 2θ = 23^{o}. There was no mismatch in the pattern of peaks for (a), (b) and (c) in Figure 4.16, so no new phase formation found.

However, a new peak appeared for (d) at around 28^{o} in the XRD pattern. This was due to the formation of MgO as a new phase. Although the peaks were shifted towards lower 2θ

values, may be due to the internal stress or due to the change in inter planar distance. The reason may be due to the deposition of the metal cation on to the surface of catalyst. All the modified samples were found to be highly crystalline. The XRD patterns were used to calculate the average crystal size and the relative crystallinity of the different zeolites. The average crystal sizes were estimated using the Scherrer equation (Eq. 4.1).

The relative crystallinity of the modified zeolites was calculated by comparing the average intensities of the most intense peaks with that of the parent zeolite, HZSM-5, assuming 100% of crystallinity for HZSM-5. The calculations were made according to the standard methods ASTM D 5758 for ZSM-5 zeolites (Eq. 4. 2).

As we can see from Table 4.10 the crystal size of the modified and unmodified HZSM-5 were the same but the relative crystallinity was highest for 5%Mg-HZSM-5 while the lowest relative crystallinity was for 15%Mg-HZSM-5. This is due to point of zero charge property of HZSM-5.

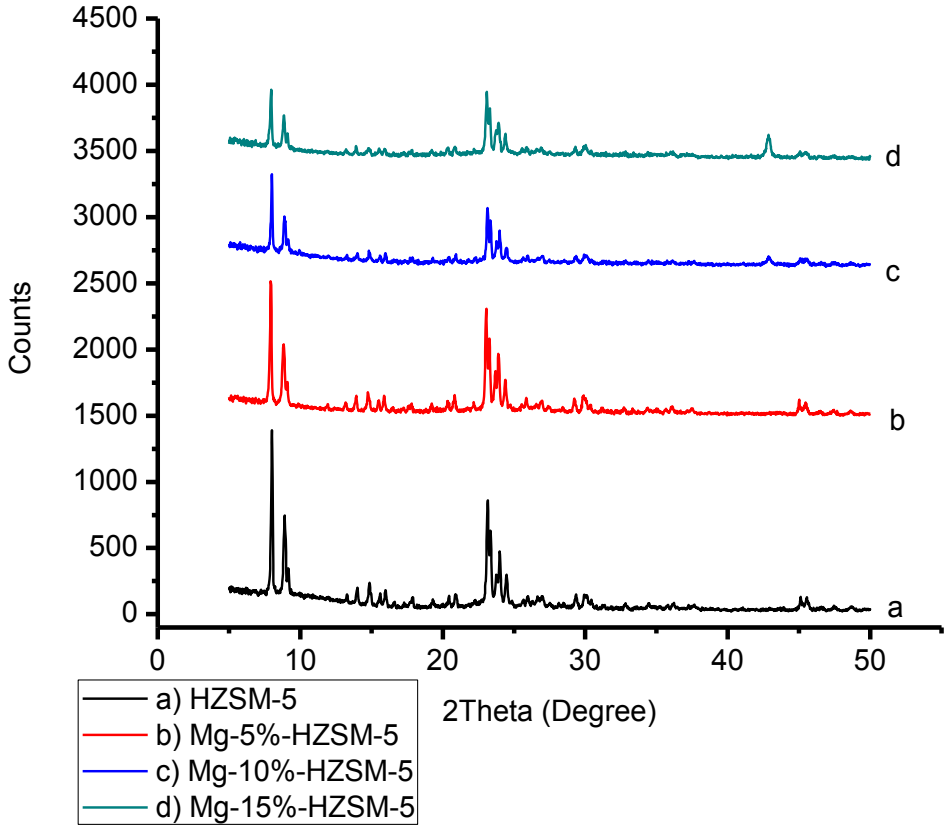

Figure 4-16: X-ray diffraction patterns of unmodified and magnesium modified HZSM-5

Table 4-10: Relative crystallinity and crystal size of modified and unmodified HZSM-5

No.	Type of catalyst	Crystal size (Å)	Relative crystallinity (%)
1	HZSM-5	12.9	100
2	5%Mg-HZSM-5	12.9	93.7
3	10%Mg-HZSM-5	12.9	58.0
4	15% Mg-HZSM-5	12.9	51.3

4.2.1.1.2 Thermogravimetric Analysis

Thermogravimetric analysis was conducted in order to determine the thermal stability of the zeolite framework and weight loss occurring from zeolite lattice during heating. TGA were conducted on SII 6300 EXSTAR using air as carrier gas at 200 ml/min on a 10 mg of sample.

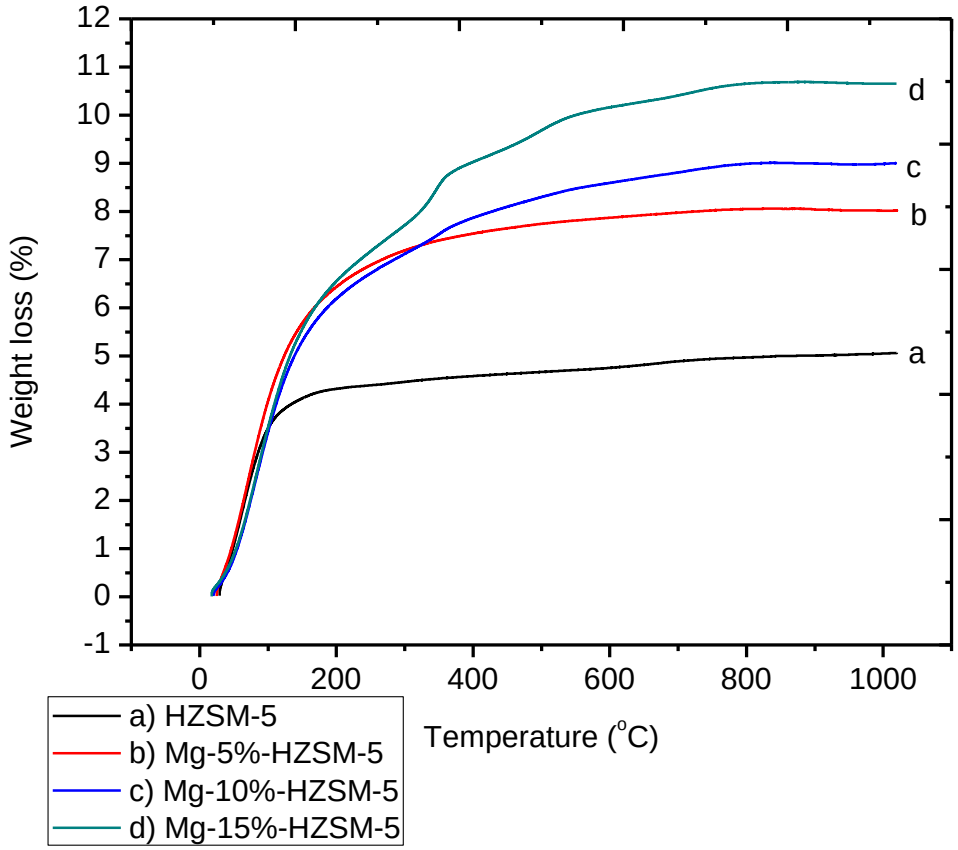

Figure 4-17: TGA graph of HZSM-5, 5%-HZSM-5, 10%Mg-HZSM-5 and 15%Mg-HZSM-5

Figure 4.17 presents the TGA of unmodified and modified HZSM-5 (Si/AL ratio = 90) heated from ambient temperature to 1000 ^{o}C in temperature progression of 10 ^{o}C/min. The portion of the curves up to 200 ^{o}C is normally linked with the weight loss due to moisture content of the catalyst, whereas, the portion of the curves from 200 to 1000 ^{o}C is assigned to the weight loss due to removal of hydrocarbon, moisture contained inside the pores and coke. HZSM-5 catalyst has the lowest weight loss. From ambient temperature to 1000 ^{o}C, the highest weight loss was seen for 15%Mg-HZSM-5 followed by 10%Mg-HZSM-5 and 5%Mg-HZSM-5 respectively.

4.2.1.1.3 Fourier Transform Infrared (FTIR)

For framework studies, Fourier transform infrared (FTIR) was performed using Perkin Elmer 1600 spectrophotometer. Spectrum was recorded in the range 400 cm^{-1} - 1500 cm^{-1}. The KBr wafer technique was used in this study. For sample preparation, the samples were mixed with KBr. About 1-3 g mixture of samples and KBr were placed in the die and pressed at 10 ton pressure.

Infrared spectra of the zeolites taken in the middle range region (400-1400 cm^{-1}) gave clue to the structural characteristics of the zeolites. The IR spectra of commercial HZSM-5 and modified HZSM-5 with different amount of magnesium are given in Figure 2. The characteristic bands at 450 cm^{-1} (T-O band), 550 cm^{-1} (double ring), 795 cm^{-1} (symmetric stretching), 1000 cm^{-1} and 1220 cm^{-1} (both are T-O-T bond) are all exist in the samples confirming the presence of structural features of ZSM-5. This is in agreement with the work done by Narayanan et al., 1998 [118]. The main asymmetric stretching of band at 1100 cm^{-1} varies in frequency. This is due to the number of Al atoms in the framework structure. Breck, 1974 stated that the frequency of main asymmetric stretch of the tetrahedra, which is a peak at 1100 cm^{-1}, varies with the number of Al atoms in the framework structure [36].

To analyse the hydroxyl (OH) groups of the catalysts, the IR analysis for the near range frequency was performed. Figure 4.18 shows the near range spectra for the synthesis catalyst.

Two peaks have been observed in each spectrum. The first peak around 3609.5 cm^{-1} was assigned for aluminum framework hydroxyl bridge [Si-(OH)-Al] bond while the second peak, around 3743 cm-1 was assigned to the silanol [Si-(OH)] bond. The presence of hydroxyl groups in the catalysts is important as it will affect the acidity of the catalysts. Peak at 3609 cm^{-1} closely related to Brønsted acid sites. The results indicated that the modification of SiO_2/ Al_2O_3 ratio in HZSM-5 can affect the acidity of the catalysts. The same results were also obtained by Segawa et al., 1998 and Ivanov et al., 1999 in their works [120, 121]. The results also proved that the decrease in acid sites is proportional to the increase of SiO_2/ Al_2O_3 ratio, as

proposed by Costa, (2000) [122]. Szostak (1989) also stated that varying the SiO_2/ Al_2O_3 ratio in the series of zeolites can alter acid strength [119]. Furthermore, Chu et al. (1985) and Topsoe et al. (1981) indicated that the acidity is associated with the aluminum atom in the crystalline framework [123, 124]. Acidity decreases as aluminum is removed from the crystal and increases as aluminum is inserted into the framework.

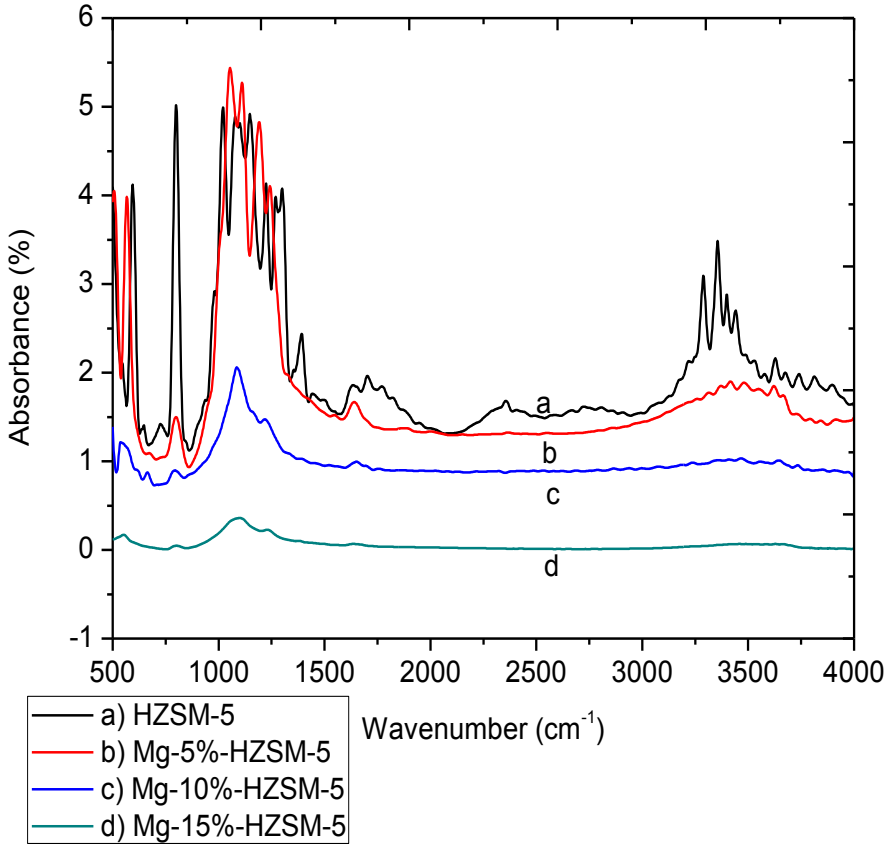

Figure 4-18: FTIR graph of HZSM-5, 5%-HZSM-5, 10%Mg-HZSM-5 and 15%Mg-HZSM-5

4.2.1.1.4 Temperature Programmed Desorption of Ammonia (NH_3-TPD)

NH_3-TPD measurements in the range from room temperature to 650 ^oC were performed in a micromeritics ChemiSorb 2720 apparatus. Zeolites samples were put in a quartz cell with U shape and pretreated, insitu, during 1 h at 250 ^oC in a flow of nitrogen (>99%) of 20 ml/min. After cooling to 25 ^oC, adsorption of ammonia was carried out in a flow of ammonia and helium mixture of 40 ml/min. After the catalyst surface became saturated some time was waited to remove the excess of ammonia. The temperature-programmed desorption was carried out with a linear heating rate of approximately10 ^oC/min from 25 ^oC to 650 ^oC in a flow of helium (>99%) of 20 ml/min. The NH_3 that desorbed was measured by a thermal conductivity detector. The electrical signals from the detector and from the thermocouple (that measures the

temperature inside the cell with the catalyst) were digitised by a CR3A chromatographic integrator and transmitted to a computer.

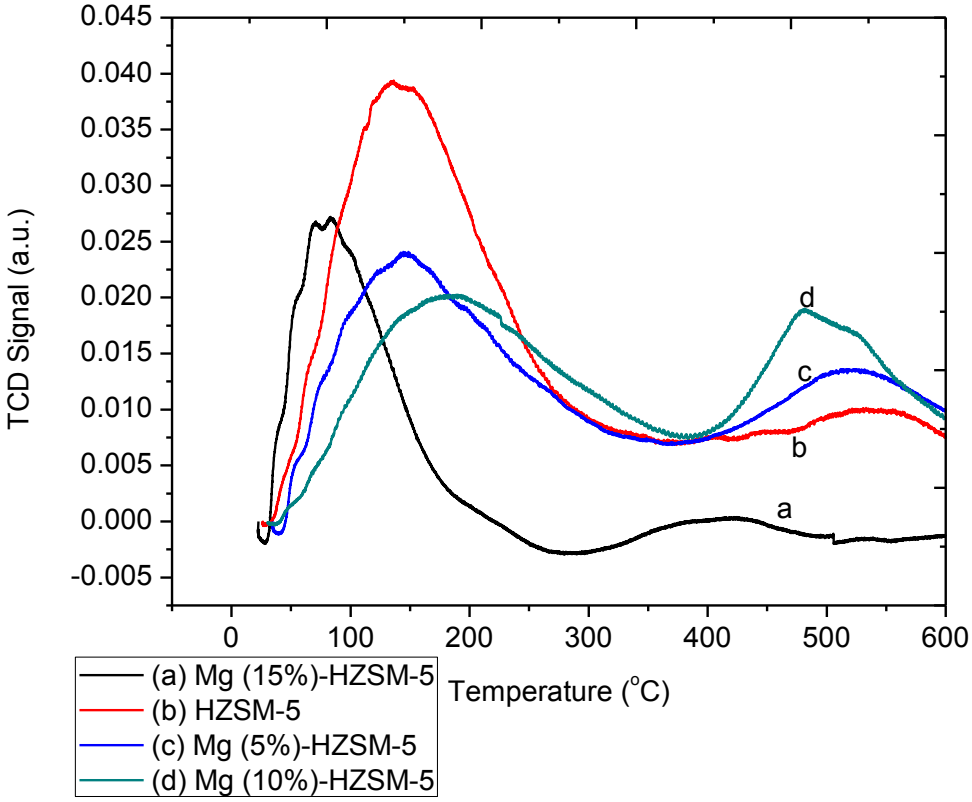

Figure 4-19: Ammonia Temperature Programmed Desorption (NH_3-TPD) of magnesium modified and unmodified HZSM-5

Table 4-11: Ammonia Temperature Programmed Desorption (NH_3-TPD) of modified and unmodified HZSM-5

No.	Type of catalyst	Weak acid sites (mmol/g)	Strong acid sites (mmol/g)
1	HZSM-5 (SAR=90)	2.21	6.80
2	Mg-5%-HZSM-5	1.62	6.3
3	Mg-10%-HZSM-5	1.62	5.97
4	Mg-15%-HZSM-5	1.950	2.472

The decrease and increase of either strong or weak acid sites depend on the point zero charge concepts. Therefore, the proton ion on HZSM-5 will be exchanged by metal cations upto only zero potential limits. Beyond that either the metal cations or metal oxides act as Lewis acid which are act as weak acid sites.

4.2.1.2 Performance of magnesium modified HZSM-5 catalysts

In this section, the performance of 5, 10 and 15% magnesium modified HZSM-5 zeolite catalyst were compared. The alkylation of benzene with ethanol was carried out over modified HZSM-5 zeolite catalysts (calcined) with different benzene to ethanol ratio. Experiments were carried out in a fixed catalytic bed down flow reactor at a constant feed (benzene and ethanol mixture of 2:1 and 4:1 ratios by volume) rate of 0.4 ml/min and a carrier gas (N_2) flow 0.5 litres per minute (lpm). The WHSV of benzene and ethanol mixture as feed was 32.6 h^{-1}. Nitrogen was used as carrier gas to activate the catalyst. The products of the reaction were analyzed by gas chromatograph. Liquid products contained benzene, ethanol, toluene, ethylbenzene, p-xylene, m-xylene, o-xylene and diethylbenzene. The gaseous products contained negligible amount of hydrocarbon gases (ethane, methane, ethylene, etc.).

Figure 4.20 through 4.25 present the performance of 5, 10 and 15% magnesium loading on HZSM-5 catalyst in terms of benzene conversion, ethylbenzene selectivity and yield at different reaction temperatures. Tables 4.12 through 4.16 present products of the reaction in the presence magnesium modified HZSM-5 catalysts.

Table 4-12: Effect of reaction temperature on catalytic performance of (Mg) 5% - HZSM-5 (SAR = 90) catalyst for alkylation of benzene with ethanol in the ratio 2:1

Products (mol %)	**Temperature (^oC)**				
	300	350	400	450	500
Ethanol	6.02	2.30	1.37	0.84	10.40
Benzene	28.50	30.10	38.19	30.80	30.54
Toluene	3.76	2.50	8.20	0.60	6.10
Ethylbenzene	36.72	38.33	39.34	40.87	38.43
p-Xylene	0.10	0.28	0.41	0.18	0.05
m-Xylene	0.35	0.42	0.74	1.65	0.69
o-Xylene	0.01	0.01	0.01	0.01	0.14
1,2-Diethylbenzene	0.37	0.48	0.25	0.53	0.15
1,4-Diethylbenzene	14.00	13.45	7.99	16.13	10.49
Others	10.17	12.13	3.50	8.39	3.01

Figure 4.20 shows the performance of 5%Mg-HZSM-5 catalyst for benzene to ethanol ratio 2:1 by volume. It is observed that the highest yield of ethylbenzene (40.87%) is seen at 450 ^oC while the highest ethylbenzene selectivity (65.07%) is observed at 500 ^oC.

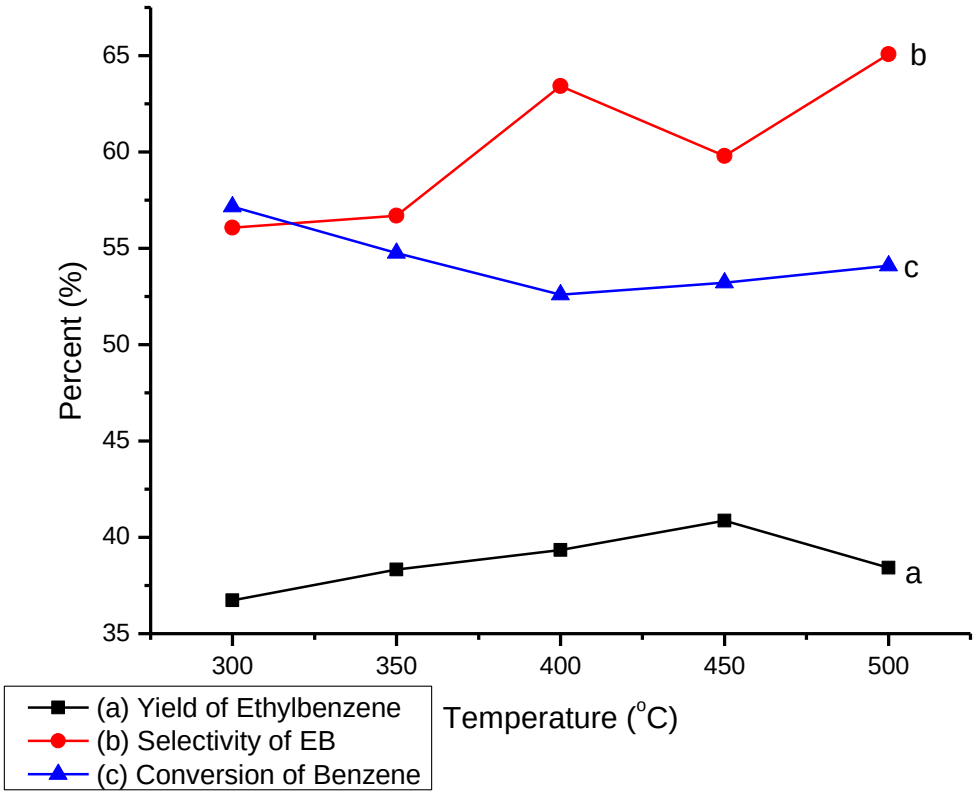

Figure 4-20: Effect of reaction temperature on catalytic performance of (Mg) 5% - HZSM-5 (SAR = 90) catalyst for alkylation of benzene with ethanol in the ratio 2:1

Table 4-13: Effect of reaction temperature on catalytic performance of (Mg) 5% - HZSM-5 (SAR = 90) catalyst for alkylation of benzene with ethanol in the ratio 4:1

Products (mol %)	**Temperature (°C)**				
	300	350	400	450	500
Ethanol	6.70	1.42	1.72	7.17	9.70
Benzene	27.79	32.19	26.04	28.11	26.80
Toluene	2.80	2.58	6.47	1.53	1.32
Ethylbenzene	37.62	39.43	39.45	41.00	37.92
p-Xylene	0.28	0.20	0.26	0.23	0.34
m-Xylene	0.20	0.44	1.08	0.20	0.29
o-Xylene	0.01	0.01	0.01	0.01	0.01
1,2-Diethylbenzene	0.36	0.38	0.86	0.32	0.93
1,4-Diethylbenzene	13.00	13.43	19.38	12.41	16.82
Others	11.24	9.92	4.73	9.02	5.87

Figure 4.21 displays the performance of 5%Mg-HZSM-5 catalyst for benzene to ethanol ratio 4:1 by volume. It is observed that the highest yield of ethylbenzene (41.00%) is seen at 450 °C

while the highest ethylbenzene selectivity (63.35%) was observed at 450 ^{o}C. The highest conversion of benzene is found to be 67.46% at 400 ^{o}C.

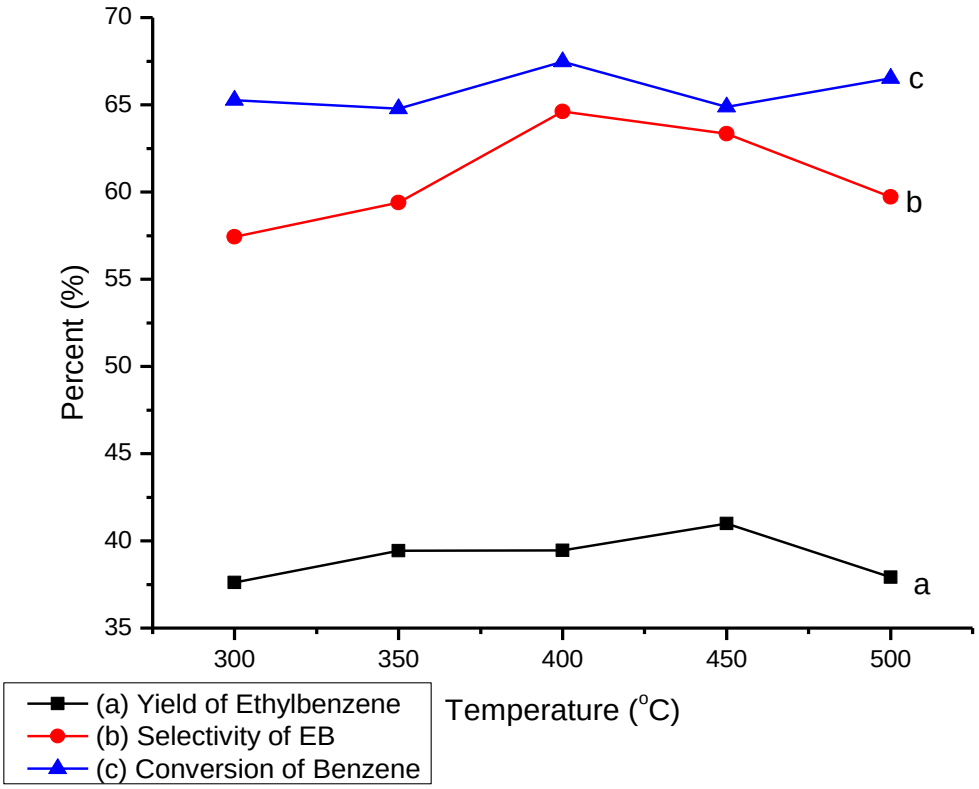

Figure 4-21: Effect of reaction temperature on catalytic performance of (Mg) 5% - HZSM-5 (SAR = 90) catalyst for alkylation of benzene with ethanol in the ratio 4:1

Table 4-14: Effect of reaction temperature on catalytic performance of (Mg) 10% - HZSM-5 (SAR = 90) catalyst for alkylation of benzene with ethanol in the ratio 2:1

Products (mol %)	**Temperature (^{o}C)**				
	300	350	400	450	500
Ethanol	2.65	3.10	1.37	2.10	2.50
Benzene	29.00	34.78	38.19	28.39	24.42
Toluene	7.80	8.00	8.20	8.49	5.68
Ethylbenzene	34.58	35.89	38.34	38.05	36.35
p-Xylene	0.38	0.40	0.41	0.51	0.61
m-Xylene	0.29	0.56	0.74	0.49	0.47
o-Xylene	0.01	0.01	0.01	0.01	0.01
1,2-Diethylbenzene	0.15	0.34	0.25	0.39	0.66
1,4-Diethylbenzene	6.45	7.43	8.99	14.70	21.92
Others	18.69	9.49	3.50	6.87	7.38

Figure 4.22 depicts the performance of 10%Mg-HZSM-5 catalyst. For benzene to ethanol ratio 2:1 by volume, we observed that the highest yield of ethylbenzene (38.34%) is seen at 400 ^{o}C while the highest ethylbenzene selectivity (63.43%) is observed at 400 ^{o}C. The highest conversion of benzene is found to be 63.40% at 500^{o}C.

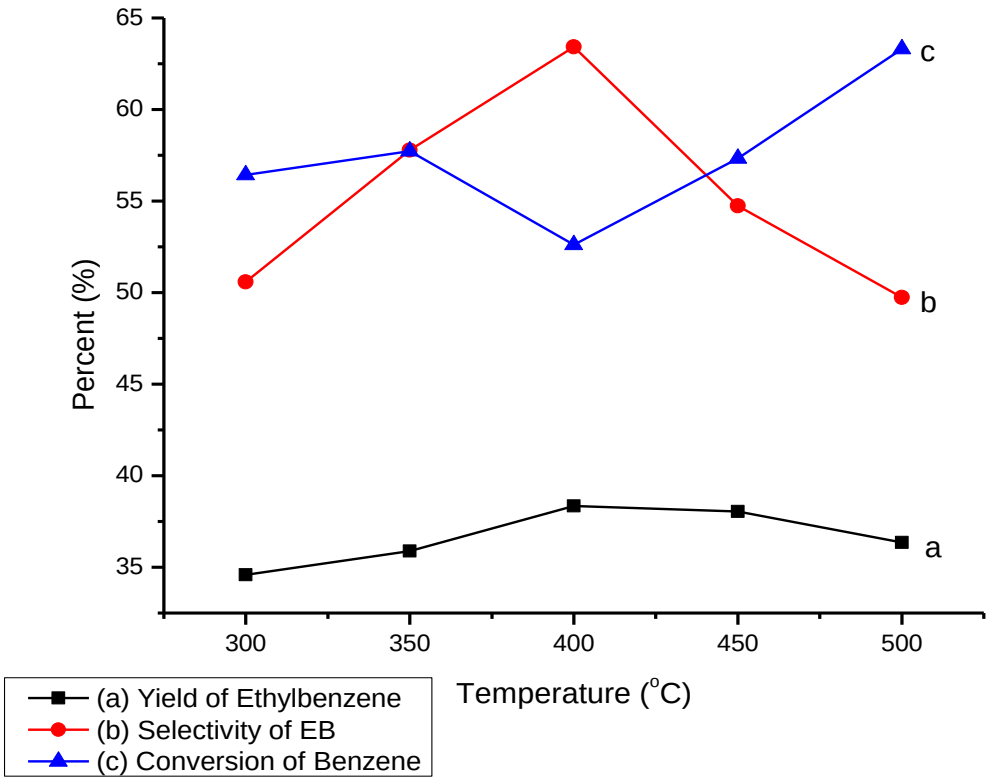

Figure 4-22: Effect of reaction temperature on catalytic performance of (Mg)10% - HZSM-5 (SAR = 90) catalyst for alkylation of benzene with ethanol in the ratio 2:1

Table 4-15: Effect of reaction temperature on catalytic performance of (Mg) 10% - HZSM-5 (SAR = 90) catalyst for alkylation of benzene with ethanol in the ratio 4:1

Products (mol %)	**Temperature (^{o}C)**				
	300	350	400	450	500
Ethanol	6.72	1.37	1.62	11.17	9.72
Benzene	28.79	36.19	24.04	30.11	26.80
Toluene	2.76	2.59	6.57	1.43	1.32
Ethylbenzene	35.62	39.43	40.45	42.42	38.92
p-Xylene	0.18	0.28	0.46	0.13	0.34
m-Xylene	0.30	0.42	1.08	0.20	0.29
o-Xylene	0.01	0.01	0.01	0.00	0.01
1,2-Diethylbenzene	0.38	0.48	0.76	0.42	0.93
1,4-Diethylbenzene	12.00	13.44	17.72	6.41	14.82
Others	13.24	5.79	7.29	7.71	6.85

Figure 4.23 illustrates the performance of 10%Mg-HZSM-5 catalyst for benzene to ethanol ratio 4:1 by volume. It is observed that the highest yield of ethylbenzene (42.42%) is seen at 450 ^{o}C while the highest ethylbenzene selectivity (66.54%) is observed at 450 ^{o}C. The highest conversion of benzene is found to be 69.96% at 400 ^{o}C.

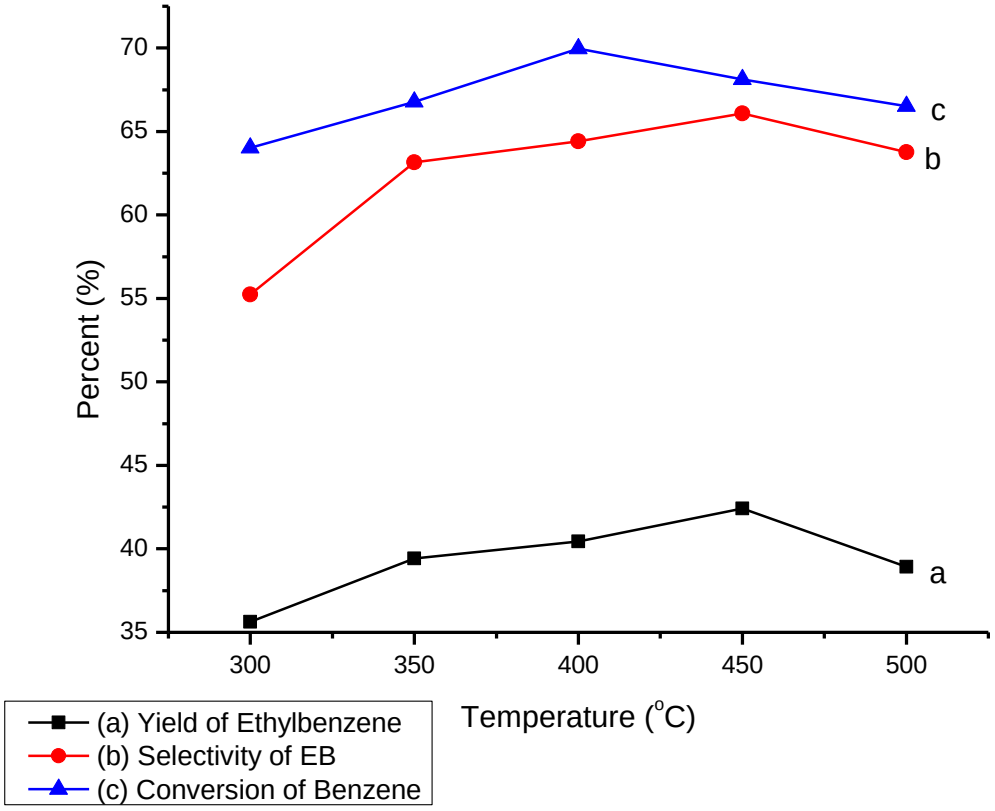

Figure 4-23: Effect of reaction temperature on catalytic performance of (Mg) 10% - HZSM-5 (SAR = 90) catalyst for alkylation of benzene with ethanol in the ratio 4:1

Table 4-16: Effect of reaction temperature on catalytic performance of (Mg) 15% - HZSM-5 (SAR = 90) catalyst for alkylation of benzene with ethanol in the ratio 2:1

Products (mol %)	**Temperature (^{o}C)**				
	300	350	400	450	500
Ethanol	21.69	7.04	4.96	0.97	14.40
Benzene	33.90	43.97	21.99	25.90	36.54
Toluene	0.02	0.05	0.43	0.52	0.10
Ethylbenzene	31.15	34.85	35.79	39.58	35.43
p-Xylene	0.00	0.02	0.18	0.19	0.05
m-Xylene	0.00	0.04	0.28	1.07	0.00
o-Xylene	0.01	0.00	0.01	0.01	0.14
1,2-Diethylbenzene	0.00	0.04	0.42	0.63	0.15
1,4-Diethylbenzene	10.13	2.22	30.30	26.68	7.49
Others	3.1	11.77	5.64	4.45	5.70

Figure 4.24 illustrates the performance of 15%Mg-HZSM-5 catalyst for benzene to ethanol ratio 2:1 by volume. It is observed that the highest yield of ethylbenzene (39.58%) is seen at 450 ^{o}C while the highest ethylbenzene selectivity (71.14%) is observed at 350 ^{o}C. The highest conversion of benzene is found to be (66.95%) at 400^{o}C.

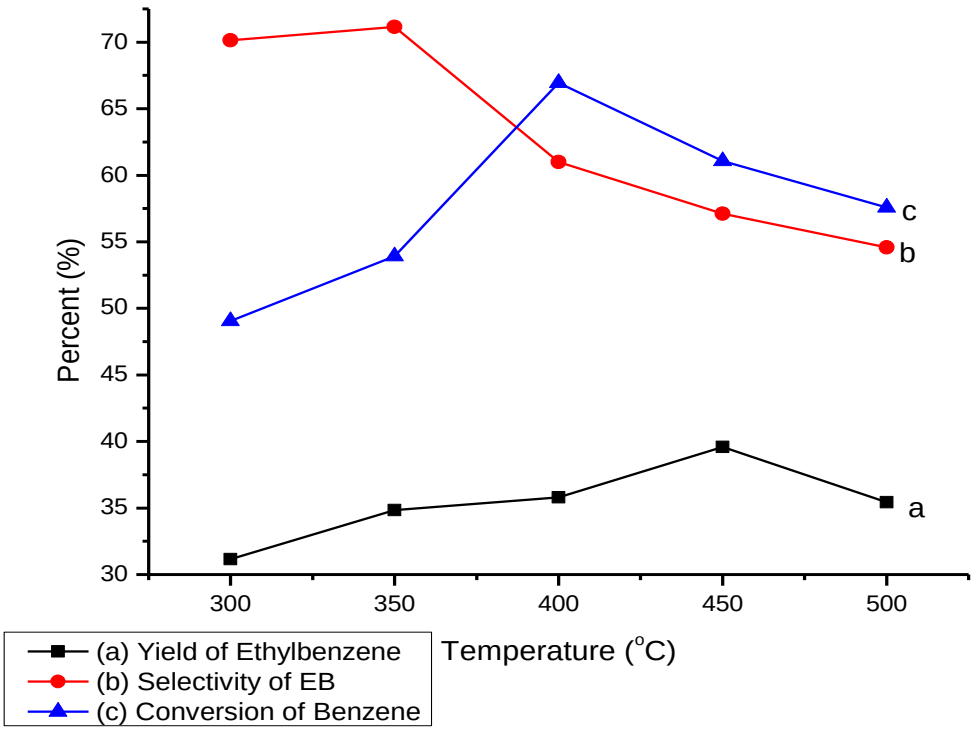

Figure 4-24: Effect of reaction temperature on catalytic performance of (Mg) 15% - HZSM-5 (SAR = 90) catalyst for alkylation of benzene with ethanol in the ratio 2:1

Table 4-17: Effect of reaction temperature on catalytic performance of (Mg) 15% - HZSM-5 (SAR = 90) catalyst for alkylation of benzene with ethanol in the ratio 4:1

Products (mol %)	**Temperature (^{o}C)**				
	300	350	400	450	500
Ethanol	14.40	15.02	6.86	1.78	0.80
Benzene	36.54	34.80	23.19	22.55	27.80
Toluene	0.10	0.12	0.27	0.66	0.70
Ethylbenzene	35.43	36.58	37.18	37.63	41.87
p-Xylene	0.05	0.08	0.13	0.21	0.18
m-Xylene	0.00	0.13	0.37	0.73	1.65
o-Xylene	0.14	0.00	0.01	0.01	0.00
1,2-Diethylbenzene	0.15	0.28	0.68	0.60	0.53
1,4-Diethylbenzene	7.49	9.24	26.95	30.21	22.13
Others	5.70	3.75	4.36	5.62	4.34

Figure 4.25 demonstrates the performance of 15%Mg-HZSM-5 catalyst for benzene to ethanol ratio 4:1 by volume. It is observed that the highest yield of ethylbenzene (41.87%) is seen at 500 ^{o}C while the highest ethylbenzene selectivity (67.59%) is observed at 300 ^{o}C. The highest conversion of benzene is found to be (71.82%) at 450 ^{o}C.

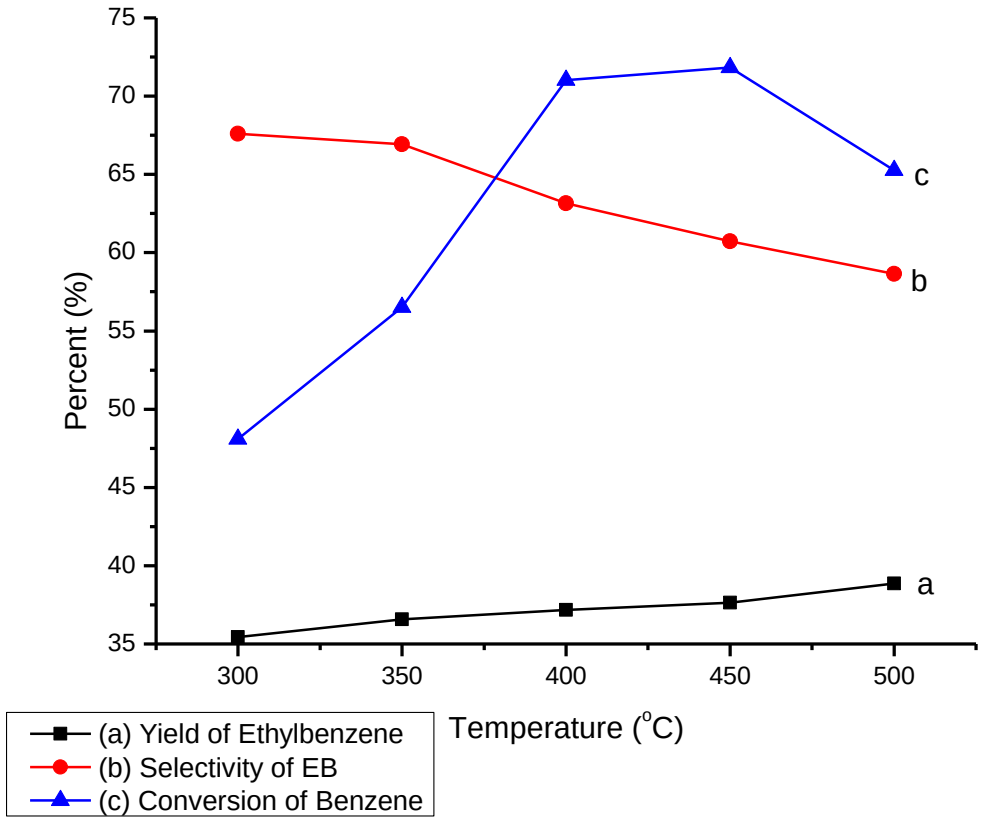

Figure 4-25: Effect of reaction temperature on catalytic performance of (Mg) 15% - HZSM-5 (SAR = 90) catalyst for alkylation of benzene with ethanol in the ratio 4:1

Summary:

Ethylbenzene was the primary product while diethylbenzene, triethylbenzene, toluene and xylene mixtures also exist in the product. The highest selectivity of ethylbenzene (71.14%) was obtained by 15%Mg-HZSM-5 while the lowest ethylbenzene selectivity (63.43%) was obtained by 10%Mg-HZSM-5 for 2:1 benzene to ethanol ratio by volume. For benzene to ethanol ratio 4:1 also the highest selectivity for ethylbenzene (67.59%) was observed by 15%Mg-HZSM-5 while the lowest selectivity of ethylbenzene (63.35%) was obtained by 5%Mg-HZSM-5. In terms of ethylbenzene yield, all HZSM-5 catalysts modified by magnesium resulted approximately in the range of 38-42%. The highest conversion of benzene (71.82%) was obtained by 15%Mg-HZSM-5.The existence of excess ethanol may facilitate the alkylation of

benzene to produce ethylbenzene and then further alkylation to diethylbenzene and tri ethylbenzene. Therefore, it would be desirable to use lower ethylating agents.

4.2.2 Selective Alkylation of Benzene with Ethanol over Boron Modified HZSM-5 Zeolite Catalysts (SAR=90)

4.2.2.1 Effect of Physico-chemical Properties

4.2.2.1.1 XRD

XRD analysis was carried out using powder diffractometer (Bruker D8) at Institute Instrumentation Centre (IIC), Indian Institute of Technology Roorkee. Cu-Kα (λ=1.5417 Å, 40 kv and 30 mA) was used as anode material and the range of scanning angle (2θ) was kept between 5º to 50º with scan speed of 2θ= 1º/min. The powder XRD patterns (Figure 4.26) of all samples exhibited well-resolved diffraction peaks, which were characteristic of the MFI framework structure. The high intensity of peaks in the XRD patterns indicate that the zeolite samples were highly crystalline materials and the highest diffraction peaks was seen at 2θ = 23º. By using X'Pert High Score Plus software, these zeolites belong to Ref. Code = 00-033-1161 material.

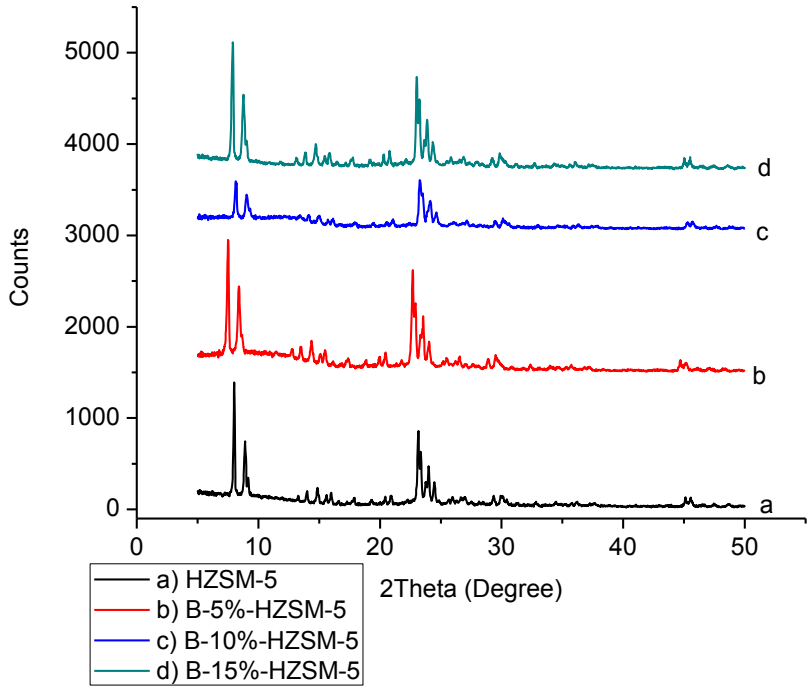

Figure 4-26: X-ray Diffraction patterns of unmodified and boron modified HZSM-5 (SAR=90)

As we can see from Table 4.18 the crystal size of the modified and unmodified HZSM-5 were the same but the relative crystallinity was highest for 5%B-HZSM-5 while the lowest relative crystallinity was for 10%B-HZSM-5.

Table 4-18: Relative crystallinity and crystal size of boron modified and unmodified HZSM-5

No.	Type of catalyst	Crystal size (Å)	Relative crystallinity (%)
1	HZSM-5	12.9	100
2	5%B-HZSM-5	12.9	132.2
3	10%B-HZSM-5	12.9	120.6
4	15% B-HZSM-5	12.9	50.1

4.2.2.1.2 Thermogravimetric Analysis

Thermo- gravimetric analysis was conducted in order to determine the thermal stability of the zeolite framework and weight loss occurring from zeolite lattice during heating. TGA were conducted on SII 6300 EXSTAR using air as carrier gas at 200 ml/min on a 10 mg of sample. Figure 4.27 presents the TGA of modified and unmodified HZSM-5 (SAR=90) heated from ambient temperature to 1000 ^{o}C in temperature progression of 10^{o}C/min. The portion of the curve upto 100 ^{o}C is normally linked with the weight loss due to moisture content of the catalyst, whereas, the portion of the curve from 100 to 1000 ^{o}C is assigned to the weight loss due to removals of hydrocarbon, moisture contained inside the pores and coke.

Table 4-19: Percent weight loss of boron modified and unmodified HZSM-5 zeolite catalysts from ambient temperature to 1000 ^{o}C

No.	Name of catalyst	Weight loss (%)
1	HZSM-5 (SAR=90)	5.1
2	B-5%-HZSM-5	5.6
3	B-10%-HZSM-5	8.6
4	B-15%-HZSM-5	9.5

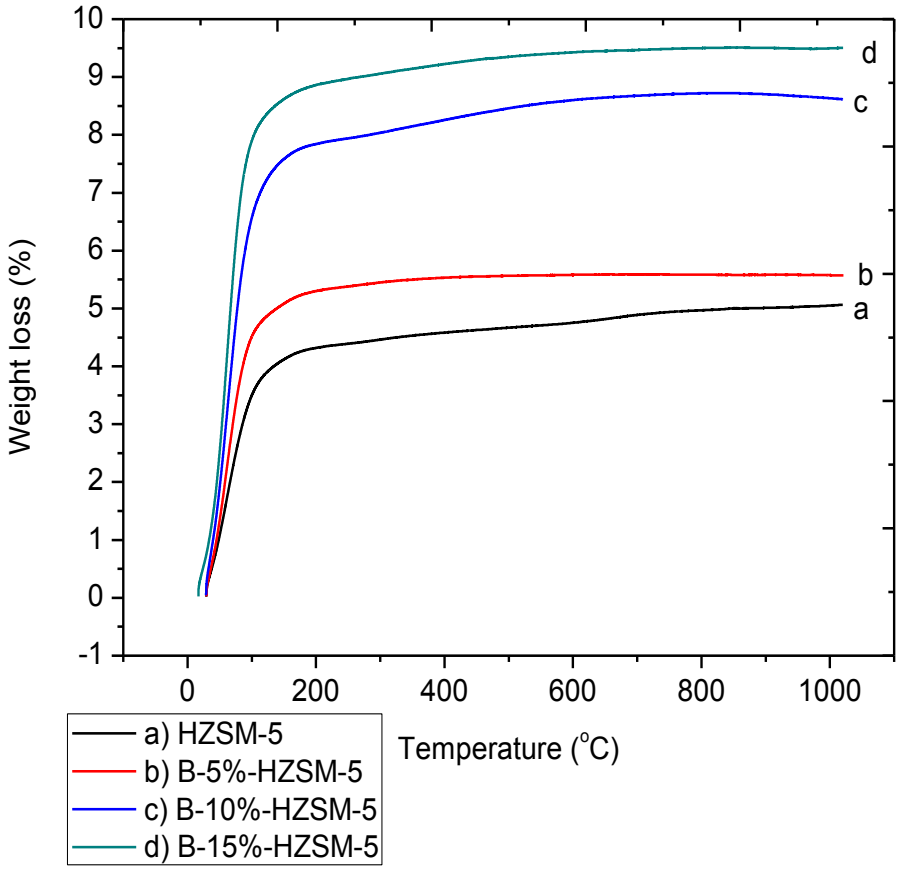

Figure 4-27: TGA graphs of boron modified and unmodified HZSM-5 zeolite

4.2.2.1.3 FTIR Analysis

Infrared spectra were obtained at 4 cm^{-1} resolution on Nicolet 6700 series FTIR Spectrometer. The infrared cell used was fitted with KBr windows. A sample of the zeolite powder was accurately weighed and mixed with around 300 mg KBr and then passed into a 10 mm diameter wafer at 15 tonnes/cm^2 pressure. This wafer was placed in the IR cell. The IR cell spectra were recorded at room temperature in air. Background IR correction for air was also made.

The IR structural studies of zeolite have been carried out in the infrared region of wave number 400 to 4000 cm^{-1}, because fundamental vibrations of SiO_4, AlO_4 or TO_4 units are contained in this region. In the KBr pellet technique a small amount of the solid sample was mixed with powdered KBr and pressed into pellet.

The band at (i) 545 cm^{-1} is assigned to the highly distorted double five membered rings present in the ZSM-5 structure, (ii) 3739, 3660 and 3490 cm^{-1} are assigned to weak, medium and strong Brønsted acid sites , respectively, (iii) 1700 cm^{-1} to water bond, (iv) 800 cm^{-1} to Al-O bond and (v) 1350 cm^{-1} to Si-O-Si bond, etc.

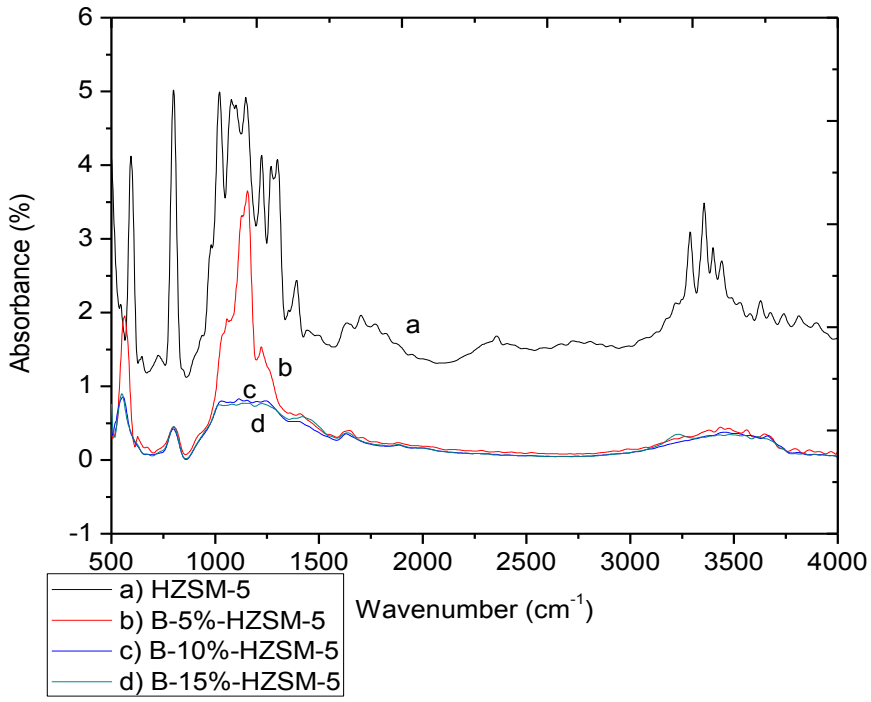

Figure 4-28: FTIR Spectra of boron modified and unmodified HZSM-5 zeolite

4.2.2.1.4 FE-SEM

The morphology of the zeolite samples was evaluated by Field Emission- Scanning Electron Microscope (FE-SEM) using ULTRA plus instrument. Scanning Electron Microscopic images of the samples are shown in Figure 4.29. From FE-SEM images we observed that the morphology of the boron modified and unmodified HZSM-5 zeolite catalysts were almost the same. However, there was a deposition of boron on the surface of the modified catalysts especially for 5%B-HZSM-5 and 15%B-HZSM-5 which agree with the X-ray diffraction patterns in which the relative crystallinity of both catalysts were greater than the unmodified one. Even though, the SEM between HZSM-5 and 10%-B-HZSM-5 were nearly similar the EDX of 10%-HZSM-5 showed presence of boron.

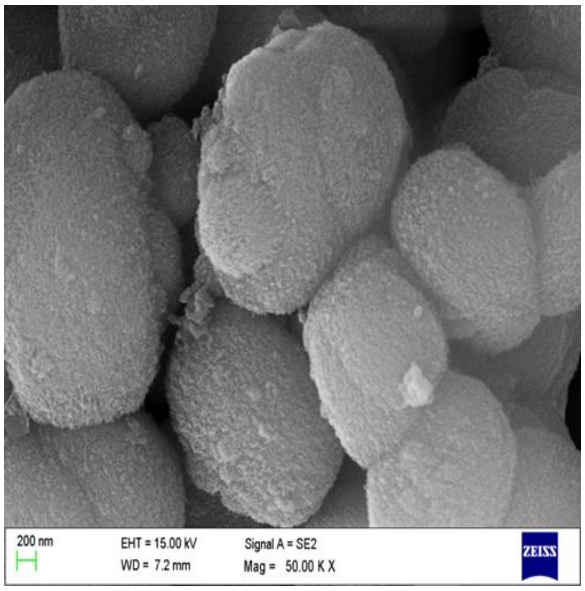

a) HZSM-5

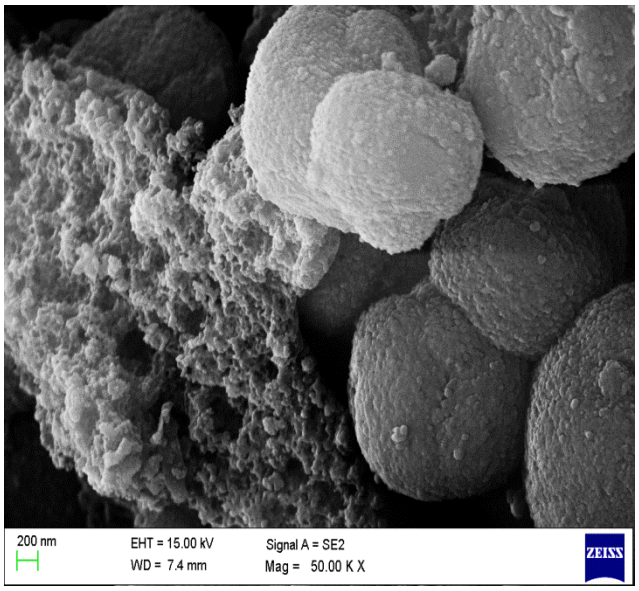

b) B-5%-HZSM-5

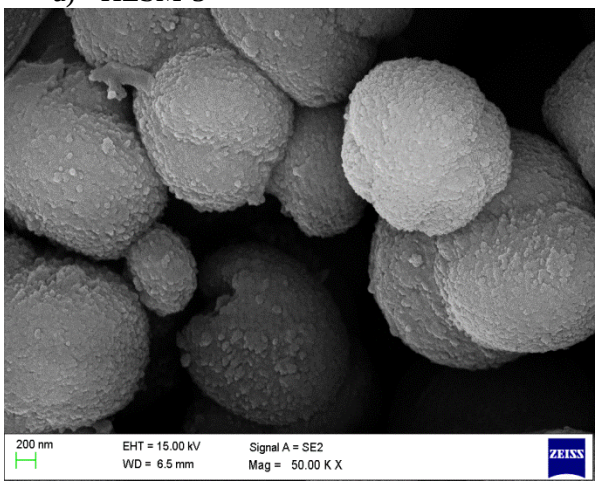

c) B-10%-HZSM-5

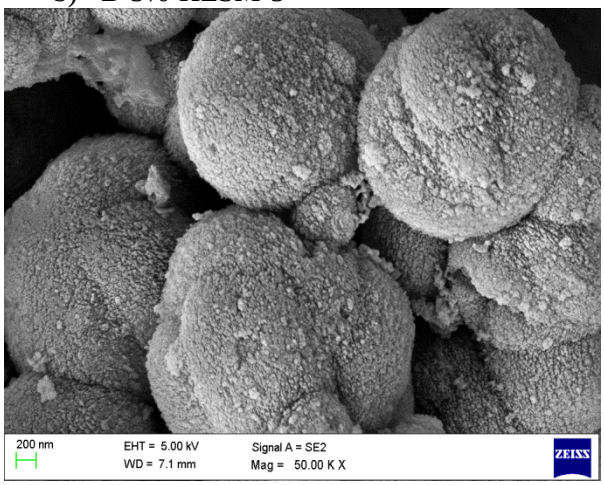

d) B-15%-HZSM-5

Figure 4-29: FE-SEM result of boron modified and unmodified HZSM-5 (SAR= 90)

4.2.2.1.5 Temperature Programmed Desorption of Ammonia (NH_3-TPD)

NH_3-TPD measurements in the temperature range from room temperature to 650 ^oC were performed in Micromeritics ChemiSorb 2720 apparatus. Zeolite samples were put in a quartz cell with U shape and pretreated, insitu, for 1 h at 250 ^oC in a flow of nitrogen (>99%) of 20 ml/min. After cooling to 25 ^oC, adsorption of ammonia was carried out in a flow of ammonia and helium mixture of 40 ml/min. After the catalyst surface became saturated it was kept for some time to remove the excess of ammonia. The temperature-programmed desorption was carried out with a linear heating rate of approximately 10 ^oC/min from 25 ^oC to 650 ^oC in a flow of helium (>99%) of 20 ml/min. The NH_3 that desorbed was measured by a thermal conductivity detector.

From the NH_3-TPD experiments (Figure 4.30), it could be concluded that two types of acid sites were present in H-ZSM-5: (i) weak acid sites corresponding with desorption at low temperature and (ii) strong acid sites corresponding with desorption at high temperature. It was observed that the acidity of HZSM-5 has decreased after modification with boron. This may be due to the deposition of boron on the outer surface of the catalyst which deactivated the active sites.

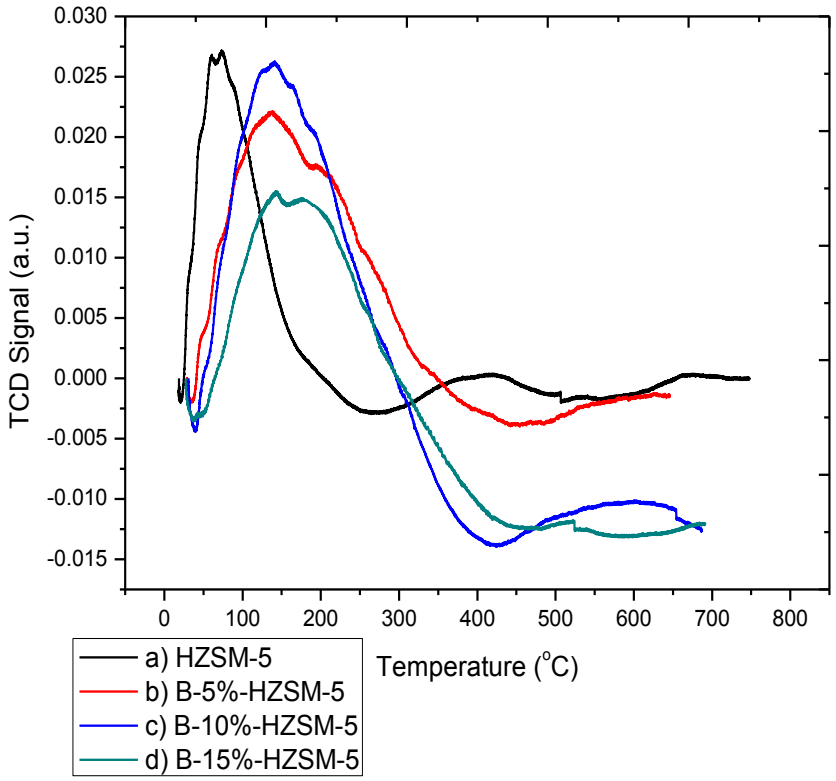

Figure 4-30: Ammonia Temperature Programmed Desorption (NH_3-TPD) of boron modified and unmodified HZSM-5 (SAR=90)

Table 4-20: Ammonia Temperature Programmed Desorption (NH_3-TPD) of boron modified and unmodified HZSM-5 zeolite (SAR=90)

No.	Type of catalyst	Weak acid sites conc. (mmol/g)	Strong acid sites conc. (mmol/g)
1	HZSM-5 (SAR=90)	2.21	6.80
2	B-5%-HZSM-5	1.413	2.377
3	B-10%-HZSM-5	1.385	2.143
4	B-15%-HZSM-5	0.581	2.008

4.2.2.2 Performance of Boron Modified HZSM-5 Catalysts

In this section, the performance of 5, 10 and 15% boron modified HZSM-5 zeolite as catalysts have been compared. The alkylation of benzene with ethanol was carried out over modified HZSM-5 zeolite catalysts with different benzene to ethanol ratio feed. Experiments were carried out in a fixed catalytic bed down flow reactor at a constant feed (benzene and ethanol mixture of 2:1 and 4:1 by volume) rate of 0.4 ml/min and a carrier gas (N_2) flow 0.5 litres per minute (lpm). The WHSV of benzene and ethanol mixture as feed was 32.6 h^{-1}. Nitrogen was used as carrier gas to activate the catalyst. The products of the reaction were analyzed by gas chromatograph.

Tables 4.21 - 4.26 show the effect of reaction temperature on catalytic performance of boron modified HZSM-5. Similar to unmodified HZSM-5, boron modified HZSM-5 catalysts test results showed that ethylbenzene, 1, 2-diethylbenzene and 1, 4-diethylbenzene were the major products, while xylenes, toluene and gaseous hydrocarbons were present in small amounts. Due to the modification of the catalysts using boron, the concentrations of external acid sites on the surface of the catalysts have decreased. As a result of this there has been reduction of further reactions such as isomerization of diethylbenzene, alkylation of diethylbenzene with ethanol to triethylbenzene and disproportionation of diethylbenzene. The gaseous products contained negligible amount of hydrocarbon gases (ethane, methane, ethylene, etc.).

Table 4-21: Effect of reaction temperature on catalytic performance of (B) 5% - HZSM-5 (SAR = 90) catalyst for alkylation of benzene with ethanol in the ratio 2:1

Products (mol %)	**Temperature (^oC)**				
	300	350	400	450	500
Ethanol	0.76	0.60	0.57	0.47	0.41
Benzene	25.82	15.79	13.25	14.35	12.54
Toluene	2.61	3.49	3.45	5.12	5.35
Ethylbenzene	32.34	34.00	36.54	40.79	37.69
p-Xylene	0.51	0.60	0.75	0.40	1.50
m-Xylene	0.00	0.02	0.01	0.63	0.18
o-Xylene	0.10	0.45	0.56	0.09	0.00
1,2-Diethylbenzene	3.45	12.55	16.10	12.02	13.66
1,4-Diethylbenzene	12.75	19.30	18.79	16.62	15.52
Others	21.66	13.20	9.98	9.51	13.15

Figure 4.31 demonstrates the performance of 5%B-HZSM-5 catalyst for benzene to ethanol ratio 2:1 by volume. It is observed that the highest yield of ethylbenzene (40.79%) is seen at 450 ^{o}C while the highest ethylbenzene selectivity (47.89%) is observed at the same temperature 450 ^{o}C. The highest conversion of benzene is found to be (81.15%) at 500 ^{o}C.

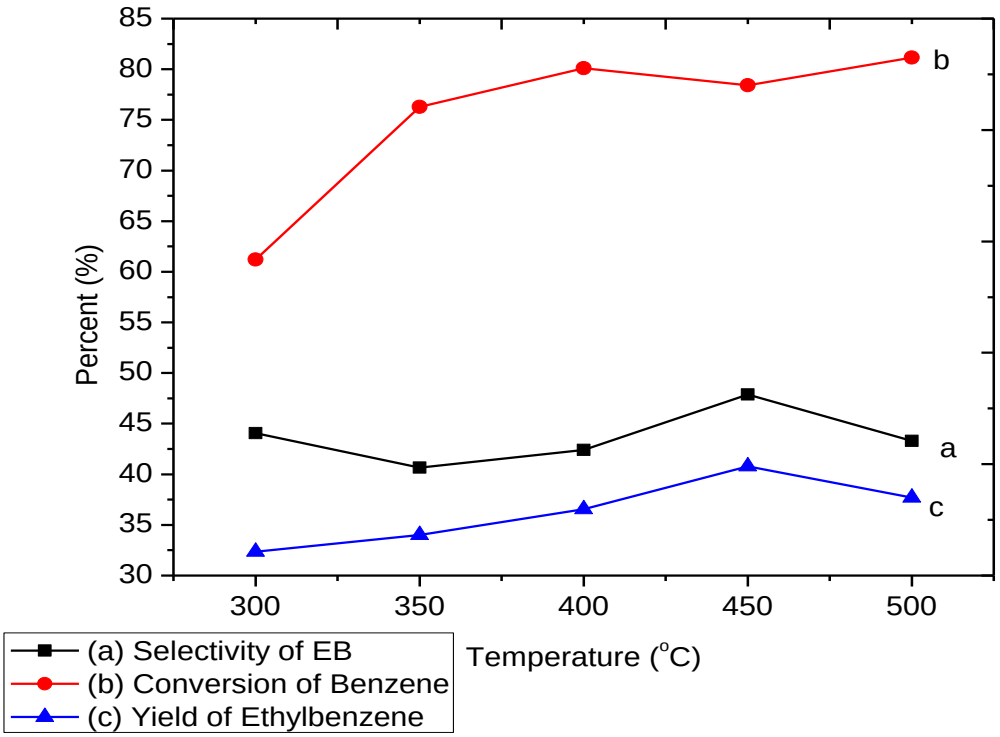

Figure 4-31: Effect of reaction temperature on catalytic performance of (B) 5% - HZSM-5 (SAR = 90) catalyst for alkylation of benzene with ethanol in the ratio 2:1

Table 4-22: Effect of reaction temperature on catalytic performance of (B) 5% - HZSM-5 (SAR = 90) catalyst for alkylation of benzene with ethanol in the ratio 4:1

Products (mol %)	**Temperature (^{o}C)**				
	300	350	400	450	500
Ethanol	0.42	0.32	0.54	0.39	0.31
Benzene	13.67	14.87	17.01	16.38	15.10
Toluene	3.76	5.24	7.01	7.40	6.29
Ethylbenzene	36.24	37.28	38.00	41.30	40.02
p-Xylene	0.94	0.70	0.31	0.65	2.01
m-Xylene	0.01	0.01	1.23	1.80	0.10
o-Xylene	0.67	0.62	0.07	0.11	0.00
1,2-Diethylbenzene	12.20	10.44	10.01	8.83	7.04
1,4-Diethylbenzene	18.50	17.35	16.79	14.39	13.30
Others	13.59	13.17	9.03	8.75	15.83

Figure 4.32 demonstrates the performance of 5%B-HZSM-5 catalyst for benzene to ethanol ratio 4:1 by volume. It is observed that the highest yield of ethylbenzene (41.30%) is obtained at 450 ^{o}C while the highest ethylbenzene selectivity (47.89%) is observed at the same temperature 450 ^{o}C. The highest conversion of benzene is found to be (82.92%) at 300 ^{o}C.

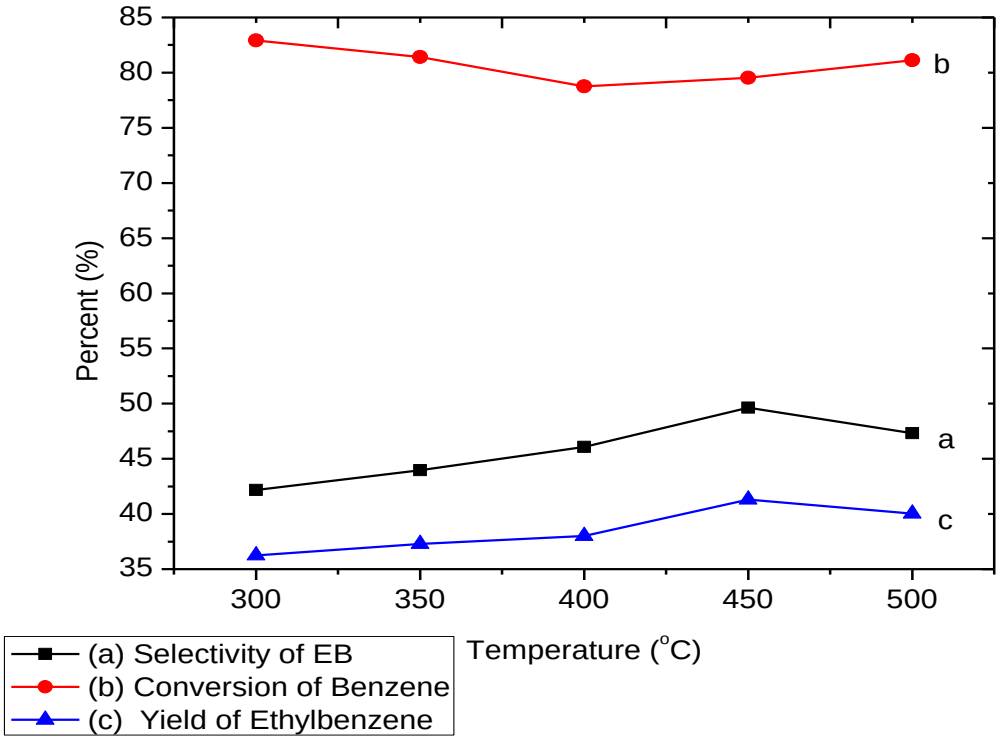

Figure 4-32: Effect of reaction temperature on catalytic performance of (B) 5% - HZSM-5 (SAR = 90) catalyst for alkylation of benzene with ethanol in the ratio 4:1

Table 4-23: Effect of reaction temperature on catalytic performance of (B) 10% - HZSM-5 (SAR = 90) catalyst for alkylation of benzene with ethanol in the ratio 2:1

Products (mol %)	**Temperature (^{o}C)**				
	300	350	400	450	500
Ethanol	0.36	0.49	0.37	0.27	0.31
Benzene	20.82	11.97	10.72	14.93	11.54
Toluene	3.61	2.94	3.45	5.12	5.35
Ethylbenzene	30.34	32.99	37.54	40.79	37.70
p-Xylene	0.61	1.06	0.73	0.41	1.50
m-Xylene	0.00	0.02	0.01	0.63	0.18
o-Xylene	0.96	0.47	0.43	0.09	0.00
1,2-Diethylbenzene	11.45	14.55	14.71	11.02	13.36
1,4-Diethylbenzene	13.57	15.24	15.67	16.26	15.62
Others	18.28	20.27	16.37	10.48	14.44

Figure 4.33 demonstrates the performance of 10%B-HZSM-5 catalyst for benzene to ethanol ratio 2:1 by volume. It is observed that the highest yield of ethylbenzene (40.79%) is obtained at 450 ^{o}C while the highest ethylbenzene selectivity (48.10%) is observed at the same temperature 450^{o}C. The highest conversion of benzene is found to be (83.39%) at 400 ^{o}C.

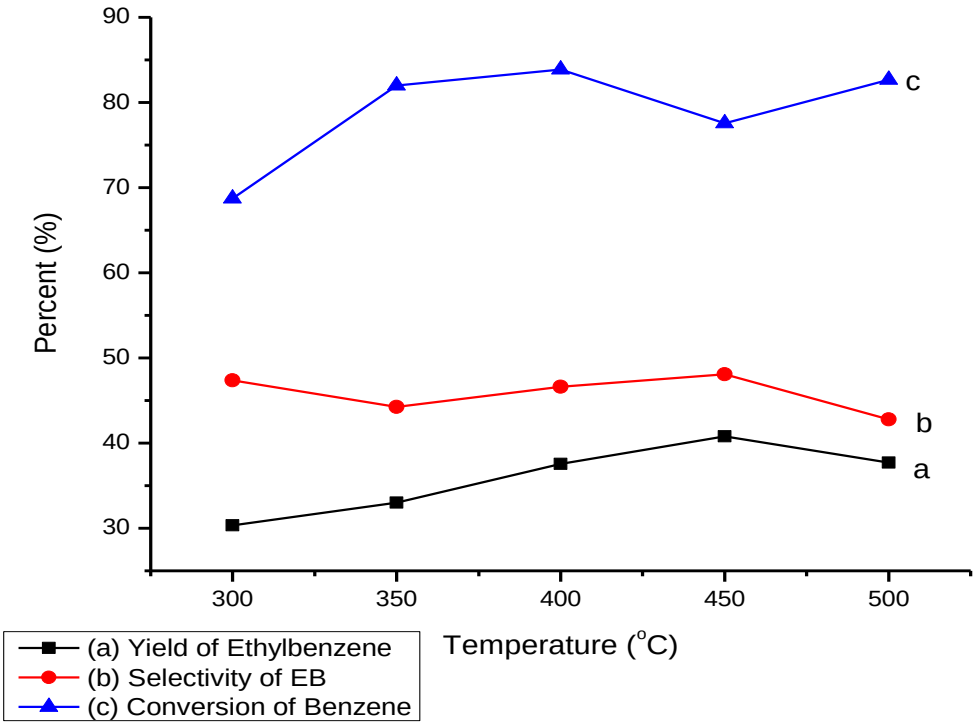

Figure 4-33: Effect of reaction temperature on catalytic performance of 10%(B) - HZSM-5 (SAR = 90) catalyst for alkylation of benzene with ethanol in the ratio 2:1

Table 4-24: Effect of reaction temperature on catalytic performance of 10%(B) - HZSM-5 (SAR = 90) catalyst for alkylation of benzene with ethanol in the ratio 4:1

Products (mol %)	**Temperature (^{o}C)**				
	300	350	400	450	500
Ethanol	0.32	0.22	0.44	0.33	0.41
Benzene	14.76	14.91	15.39	15.48	15.10
Toluene	4.76	4.42	6.28	7.00	7.29
Ethylbenzene	35.84	37.08	39.66	40.38	40.42
p-Xylene	0.84	0.59	0.29	0.65	2.81
m-Xylene	0.01	0.01	0.95	1.80	0.17
o-Xylene	0.78	0.51	0.08	0.11	0.00
1,2-Diethylbenzene	10.27	10.84	9.01	7.83	7.34
1,4-Diethylbenzene	16.70	17.44	15.27	13.39	12.30
Others	15.72	13.98	12.63	13.03	14.16

Figure 4.34 demonstrates the performance of 10%B-HZSM-5 catalyst for benzene to ethanol ratio 4:1 by volume. It is observed that the highest yield of ethylbenzene (40.42%) is obtained at 450 ^{o}C while the highest ethylbenzene selectivity (47.96%) is observed at the same temperature 450 ^{o}C. The highest conversion of benzene is found to be (81.56%) at 300 ^{o}C.

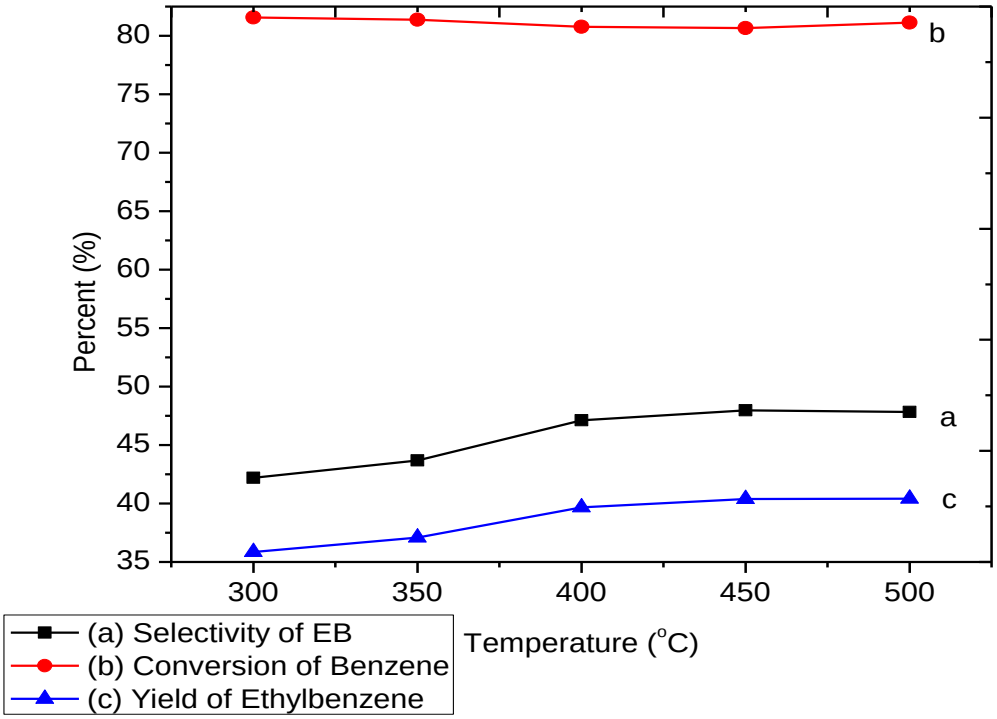

Figure 4-34: Effect of reaction temperature on catalytic performance of 10%(B) - HZSM-5(SAR = 90) catalyst for alkylation of benzene with ethanol in the ratio 4:1

Table 4-25: Effect of reaction temperature on catalytic performance of 15% (B) - HZSM-5 (SAR = 90) catalyst for alkylation of benzene with ethanol in the ratio 2:1

Products (mol %)	**Temperature (^{o}C)**				
	300	350	400	450	500
Ethanol	0.61	0.59	0.41	0.35	0.39
Benzene	22.06	20.38	17.17	16.50	13.96
Toluene	3.78	2.69	3.34	5.67	5.97
Ethylbenzene	38.27	39.12	40.45	40.13	38.10
p-Xylene	0.58	1.24	0.86	0.72	0.68
m-Xylene	0.00	0.02	0.01	0.01	2.11
o-Xylene	0.64	0.01	0.31	0.87	0.09
1,2-Diethylbenzene	3.03	4.66	7.65	6.32	6.69
1,4-Diethylbenzene	12.98	12.84	18.24	18.36	17.65
Others	18.05	18.45	11.56	11.07	14.36

Figure 4.35 demonstrates the performance of 15%B-HZSM-5 catalyst for benzene to ethanol ratio 2:1 by volume. It is observed that the highest yield of ethylbenzene (40.45%) is obtained at 400 ^{o}C while the highest ethylbenzene selectivity (49.49%) is observed at 300 ^{o}C. The highest conversion of benzene is found to be (79.02%) at 500 ^{o}C.

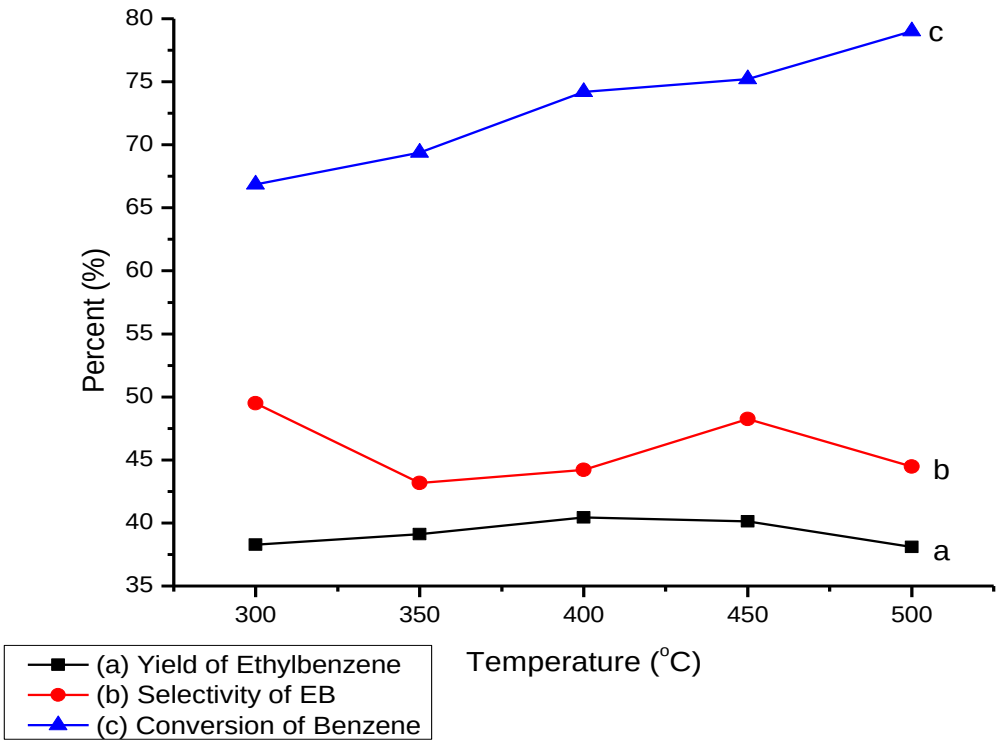

Figure 4-35: Effect of reaction temperature on catalytic performance of 15%(B) - HZSM-5 (SAR = 90) catalyst for alkylation of benzene with ethanol in the ratio 2:1

Table 4-26: Effect of reaction temperature on catalytic performance of 15%(B) - HZSM-5 (SAR = 90) catalyst for alkylation of benzene with ethanol in the ratio 4:1

Products (mol %)	**Temperature (^{o}C)**				
	300	350	400	450	500
Ethanol	0.75	0.41	0.59	0.29	0.11
Benzene	28.75	21.51	15.39	19.71	17.12
Toluene	3.51	3.56	5.57	8.32	8.32
Ethylbenzene	40.52	41.07	42.32	44.18	42.98
p-Xylene	0.57	1.19	0.96	0.59	0.71
m-Xylene	0.00	0.01	0.56	1.85	3.19
o-Xylene	0.74	0.34	0.09	0.06	0.09
1,2-Diethylbenzene	3.01	5.42	7.82	3.69	3.65
1,4-Diethylbenzene	10.47	14.50	16.11	11.19	11.40
Others	11.68	11.99	10.59	10.12	12.43

Figure 4.36 demonstrates the performance of 15%B-HZSM-5 catalyst for benzene to ethanol ratio 4:1 by volume. It is observed that the highest yield of ethylbenzene (44.18%) is obtained at 450 ^{o}C while the highest ethylbenzene selectivity (57.48%) is observed at 300 ^{o}C. The highest conversion of benzene is found to be (80.77%) at 400 ^{o}C.

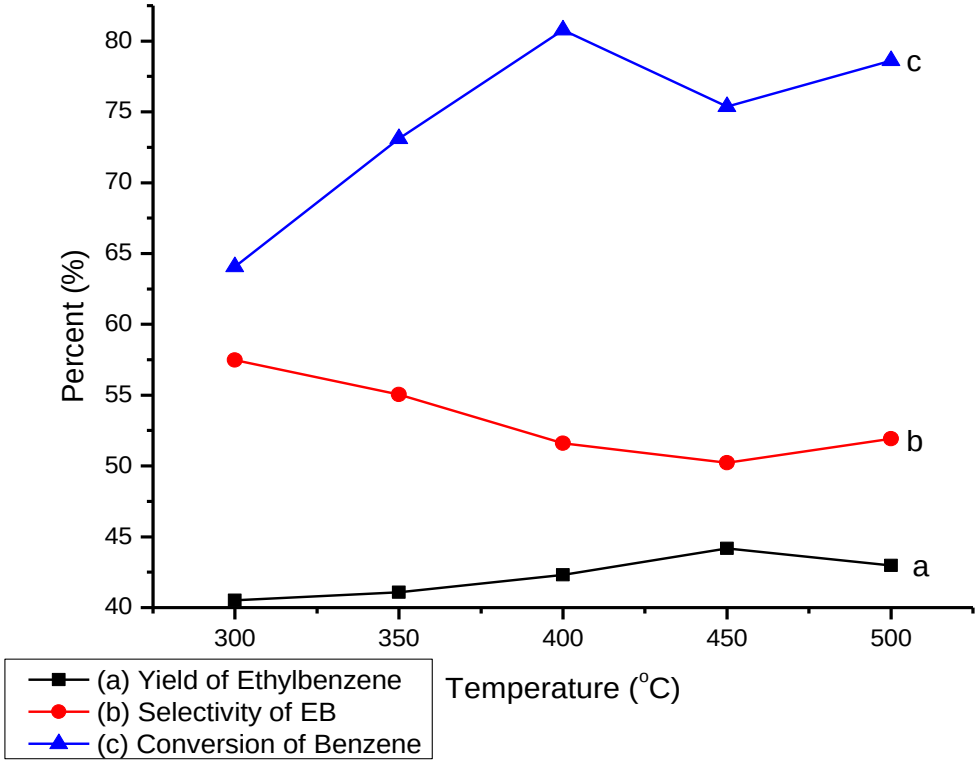

Figure 4-36: Effect of reaction temperature on catalytic performance of 15% (B) - HZSM-5 (SAR = 90) catalyst for alkylation of benzene with ethanol in the ratio 4:1

Summary:

Ethylbenzene was the primary product while diethylbenzene, triethylbenzene, toluene and xylene mixtures also exist in the product. The highest selectivity of ethylbenzene (57.48%) was obtained by 15%B-HZSM-5 while the ethylbenzene selectivity of 48% was obtained by 10%B-HZSM-5 and 5%B-HZSM-5 for 4:1 benzene to ethanol ratio by volume. However, for benzene to ethanol ratio 2:1 all the catalysts showed approximately the same selectivity for ethylbenzene (48%). Except 15%B-HZSM-5, the other two HZSM-5 catalysts modified by boron resulted in approximately 41.00% of ethylbenzene yield. The highest yield of ethylbenzene demonstrated by 15%B-HZSM-5 was 44.18% at 450 ^{o}C for benzene to ethanol ratio 4:1 by volume. The highest conversion of benzene of approximately 83% was obtained by both 5%B-HZSM-5 and 10%Mg-HZSM-5. The existence of excess ethanol may facilitate the

alkylation of benzene to produce ethylbenzene and then further alkylation to diethylbenzene and tri ethylbenzene. Therefore, it would be desirable to use lower ethylating agents.

4.2.3 Selective Alkylation of Benzene with Ethanol over Magnesium-Boron Modified HZSM-5 Zeolite Catalysts (SAR=90)

4.2.3.1 Effect of Physico-chemical Properties

4.2.3.1.1 XRD

XRD patterns of magnesium-boron bimetallic HZSM-5 zeolite catalysts are given in figure 4.37. X-ray powder diffraction was employed to determine the value of relative crystallinity (RC). The commercial zeolite, HZSM-5 was assumed to have 100% crystallinity. The determination of the value was based on the area of the characteristic peaks in the 2Θrange of from 22.5^{o} to 25^{o}. XRD analysis was carried out using powder diffractometer (Bruker D8) at Institute Instrumentation Centre (IIC), Indian Institute of Technology Roorkee. Cu-Kα (λ=1.5417 Å, 40 kv and 30 mA) was used as anode material and the range of scanning angle (2θ) was kept between 5º to 50º with scan speed of 2θ = 1º/min. The powder XRD patterns (Figure 4.37) of all the four samples exhibited well-resolved diffraction peaks, which were characteristic of the MFI framework structure. The high intensity of peaks in the XRD patterns indicated that the zeolite samples were highly crystalline materials and the highest diffraction peaks were seen at 2θ = 23^{o}. There was no mismatch in the pattern of peaks for all the samples in Figure 4.37, so no other phase formations have been found.

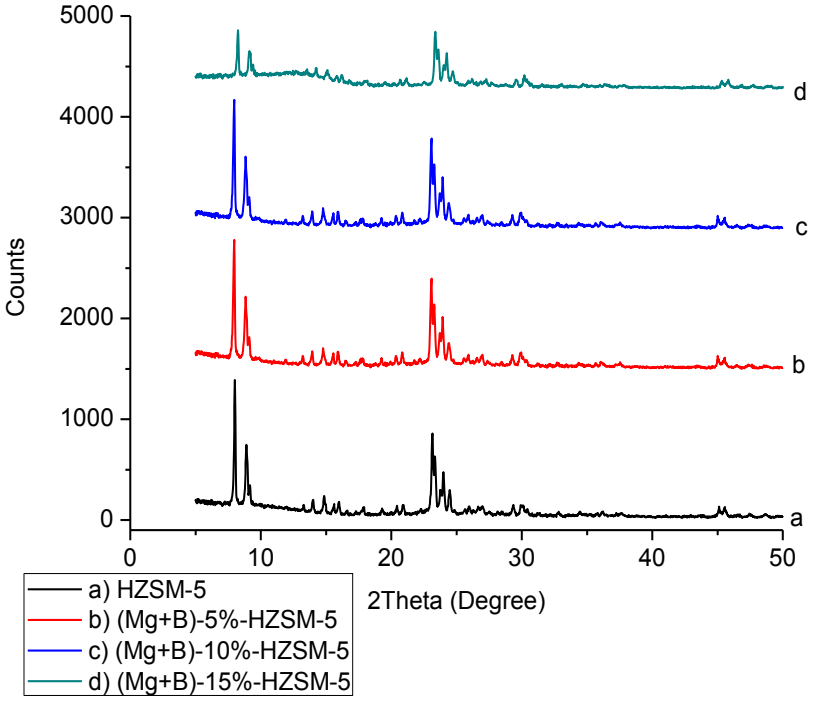

Figure 4-37: X-ray Diffraction patterns of unmodified and magnesium-boron modified HZSM-5 zeolite (SAR = 90)

As we can see from Table 4.27 the crystal size of the modified and unmodified HZSM-5 were the same but the relative crystallinity was higher for (Mg+B)5%-HZSM-5 and (Mg + B)10%-HZSM-5 while the lower relative crystallinity was observed for (Mg+B)15%-HZSM-5.

Table 4-27: Relative crystallinity and crystal size of magnesium- boron modified and unmodified HZSM-5 (SAR=90)

No.	Type of catalyst	Crystal size (Å)	Relative crystallinity (%)
1	HZSM-5	12.9	100
2	(Mg + B)5%-HZSM-5	12.9	106.8
3	(Mg + B)10%-HZSM-5	12.9	100.2
4	(Mg + B) 15% B-HZSM-5	12.9	63.0

4.2.3.1.2 Thermogravimetric Analysis

Thermogravimetric analysis of HZSM-5 modified by bimetallic magnesium-boron is shown on figure 4.38. Thermogravimetric analysis was conducted in order to determine the thermal stability of the zeolite framework and weight loss occurring from zeolite lattice during heating. TGA were conducted on SII 6300 EXSTAR instrument using air as carrier gas at 200 ml/min on a 10 mg of sample. Figure 4.38 presents the TGA of modified and unmodified HZSM-5 heated from ambient temperature to 1000 ^{o}C in temperature progression of 10^{o}C/min. The portion of the curve upto 100 ^{o}C is normally linked with the weight loss due to moisture content of the catalyst, whereas, the portion of the curve from 100 to 1000 ^{o}C is assigned to the weight loss due to the removals of hydrocarbon, moisture contained inside the pores and coke formation. From the experimental investigation, it is seen that high percent weight loss is demonstrated by magnesium-boron modified catalysts. As the amount of percent metal loading is increased the weight lost by the catalysts is also increased as particularly at higher temperatures as shown in the table 4.28.

Table 4-28: Percent weight loss of magnesium-boron bimetallic modified and unmodified HZSM-5 zeolite catalysts from ambient temperature to 1000^{o}C

No.	Name of catalyst	Weight loss (%)
1	HZSM-5 (SAR=90)	5.1
2	(Mg + B)-5%-HZSM-5	6.6
3	(Mg + B)-10%-HZSM-5	7.5
4	(Mg + B)-15%-HZSM-5	7.6

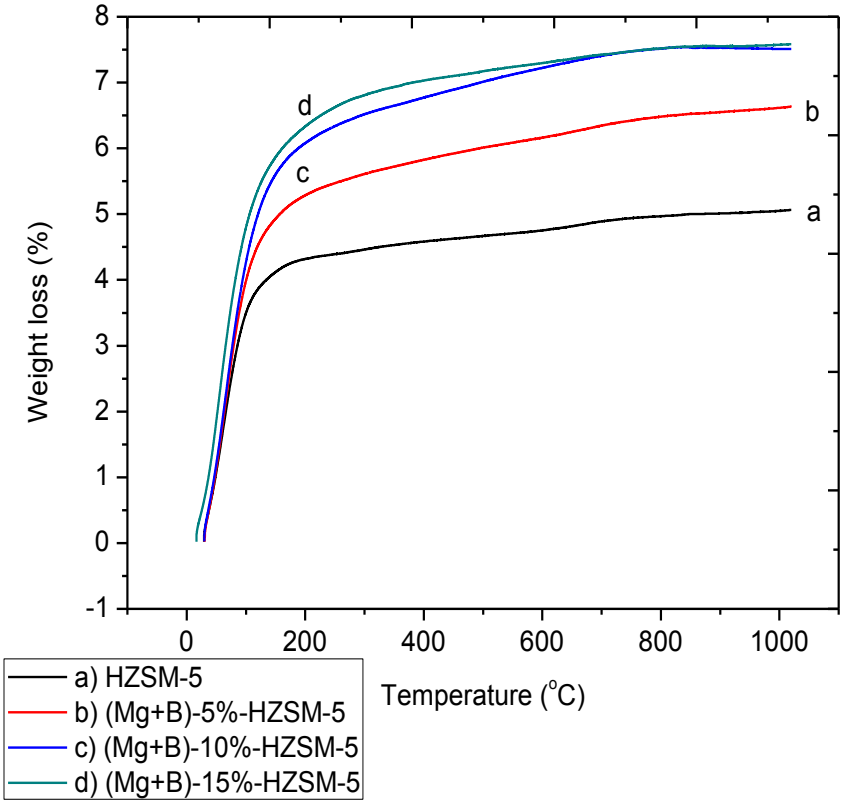

Figure 4-38: TGA graphs of magnesium- boron modified and unmodified HZSM-5 zeolite

4.2.3.1.3 FTIR Analysis

Infrared spectra were obtained at 4 cm^{-1} resolution on Nicolet 6700 series FTIR Spectrometer. The infrared cell used was fitted with KBr windows. A sample of the zeolite powder was accurately weighed and mixed with around 300 mg KBr and then passed into a 10 mm diameter wafer at 15 tonnes/cm^2 pressure. This wafer was placed in the IR cell. The IR cell spectra were recorded at room temperature in air. Background IR correction for air was also made.

The IR structural studies of zeolite have been carried out in the infrared region of wave number 400 to 4000 cm^{-1}, because fundamental vibrations of SiO_4, AlO_4 or TO_4 units are contained in this region. In the KBr pellet technique a small amount of the solid sample was mixed with powdered KBr and pressed into pellet.

The band at (i) 545 cm^{-1} is assigned to the highly distorted double five membered rings present in the ZSM-5 structure, (ii) 3739, 3660 and 3490 cm^{-1} are assigned to weak, medium and strong Brønsted acid sites , respectively, (iii) 1700 cm^{-1} to water bond, (iv) 800 cm^{-1} to Al-O bond and (v) 1350 cm^{-1} to Si-O-Si bond [125].

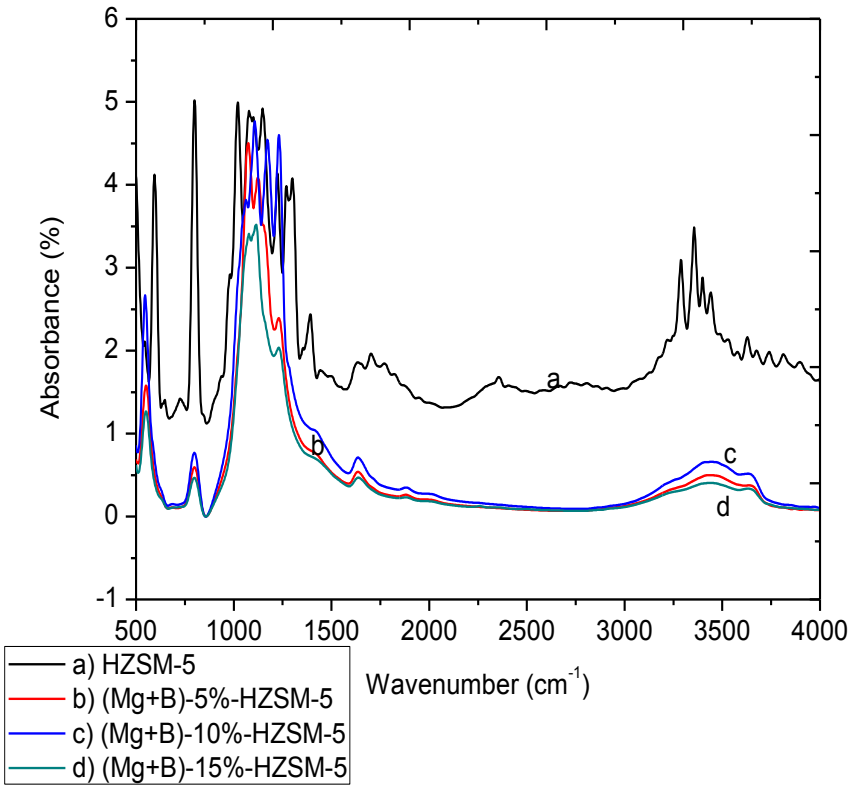

Figure 4-39: FTIR Spectra of bimetallic magnesium-boron modified and unmodified HZSM-5 (SAR = 90) zeolite

4.2.3.1.4 Ammonia Temperature Programmed Desorption (NH_3-TPD)

The ammonia temperature programmed desorption was conducted according to the procedure stated in chapter three. From the NH_3-TPD experiments (Figure 4.40), it could be concluded that two types of acid sites were present in H-ZSM-5: weak acid sites corresponding to desorption at low temperature and strong acid sites corresponding with desorption at high temperature. It was observed that the acidity of HZSM-5 has decreased after modification with bimetallic magnesium-boron. This may be due to the deposition of bimetals on the outer

surface of the catalyst deactivating the active sites. A significant change in acidic sites was observed for (Mg + B)10%-HZSM-5 zeolite catalysts.

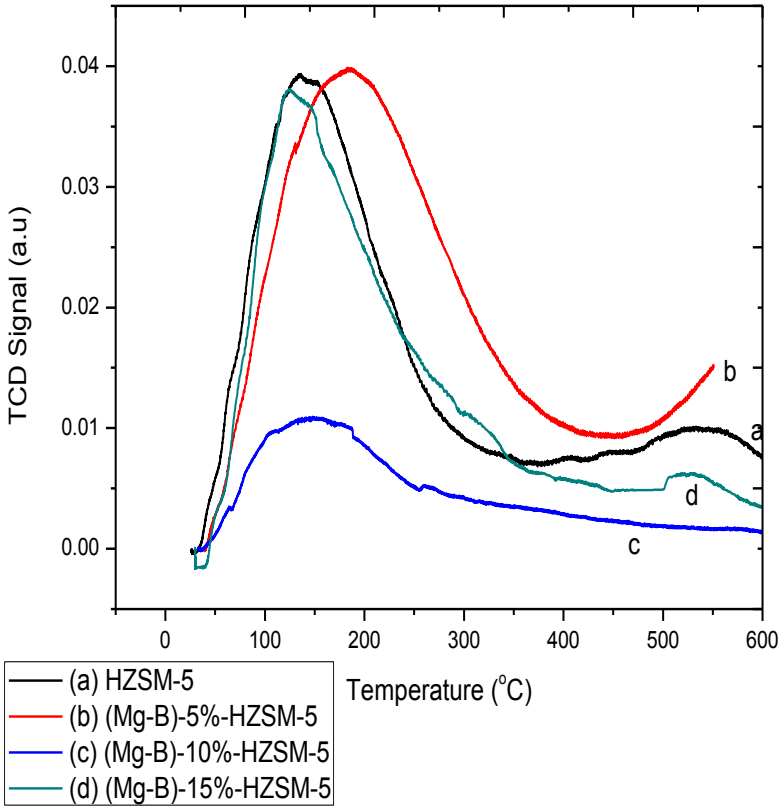

Figure 4-40: Ammonia Temperature Programmed Desorption (NH_3-TPD) of magnesium-boron modified and unmodified HZSM-5 (SAR=90) zeolite

Table 4-29: Ammonia Temperature Programmed Desorption (NH_3-TPD) of magnesium-boron modified and unmodified HZSM-5 (SAR=90) zeolite

No.	Type of catalyst	Weak acid sites conc. (mmol/g)	Strong acid sites conc. (mmol/g)
1	HZSM-5 (SAR=90)	2.21	6.80
2	(Mg + B)-5%-HZSM-5	3.49	5.05
3	(Mg + B) -10%-HZSM-5	0.67	2.03
4	(Mg + B) -15%-HZSM-5	6.99	0.74

4.2.3.2 Performance of Bimetallic Magnesium-Boron Modified HZSM-5 Catalysts

In this section, the performance of 5, 10 and 15% bimetallic magnesium-boron modified HZSM-5 zeolite catalysts have been compared. The alkylation of benzene with ethanol was

carried out over modified and calcined HZSM-5 zeolite catalysts with different benzene to ethanol ratio. Experiments were carried out in a fixed catalytic bed down flow reactor at a constant feed (benzene and ethanol mixture in the ratio 2:1 and 4:1 by volume) rate of 0.4 ml/min and a carrier gas (N_2) flow 0.5 litres per minute (lpm). The WHSV of benzene and ethanol mixture as feed was 32.6 h^{-1}. Nitrogen was used as carrier gas to activate the catalyst. The products of the reaction were analyzed by gas chromatograph.

Tables 4.30 - 4.35 shows the effect of reaction temperature on catalytic performance of bimetallic magnesium-boron modified HZSM-5. Similar to unmodified HZSM-5, magnesium-boron modified HZSM-5 catalysts test results also showed ethylbenzene, 1, 2-diethylbenzene and 1, 4-diethylbenzene as major products while xylenes, toluene and gaseous hydrocarbons were present in small amounts. Due to the modification of the catalysts using magnesium and boron the external acid sites on the surface of the catalysts were decreased. The of decrease in external acid sites on the surface of catalysts caused elimination of subsequent reactions such as isomerization of diethylbenzene, alkylation of diethylbenzene with ethanol to triethylbenzene and disproportionation of diethylbenzene. The gaseous products contained negligible amount of hydrocarbon gases (ethane, methane, ethylene, etc.).

Table 4-30: Effect of reaction temperature on catalytic performance of (Mg+B)5% - HZSM-5 (SAR = 90) catalyst for alkylation of benzene with ethanol in the ratio 2:1

Products (mol %)	**Temperature (^oC)**				
	300	350	400	450	500
Ethanol	5.20	3.21	0.75	0.15	0.08
Benzene	27.19	43.25	32.54	21.62	18.82
Toluene	3.42	1.29	2.49	5.54	6.71
Ethylbenzene	33.23	35.68	38.68	40.53	40.75
p-Xylene	0.45	0.24	0.49	0.54	0.37
m-Xylene	0.33	0.00	0.23	0.61	1.35
o-Xylene	0.04	0.10	0.03	0.04	0.05
1,2-Diethylbenzene	1.06	0.41	1.58	3.09	3.75
1,4-Diethylbenzene	6.50	2.40	9.07	17.99	18.78
Others	22.58	13.42	14.14	9.89	9.34

Figure 4.41 demonstrates the performance of (Mg+B)5%-HZSM-5 catalyst for benzene to ethanol ratio 2:1 by volume. It is observed that the highest yield of ethylbenzene (40.75%) is obtained at 500 ^oC while the highest ethylbenzene selectivity (57.98%) is observed at 400 ^oC. The highest conversion of benzene is found to be 71.72% at 500 ^oC.

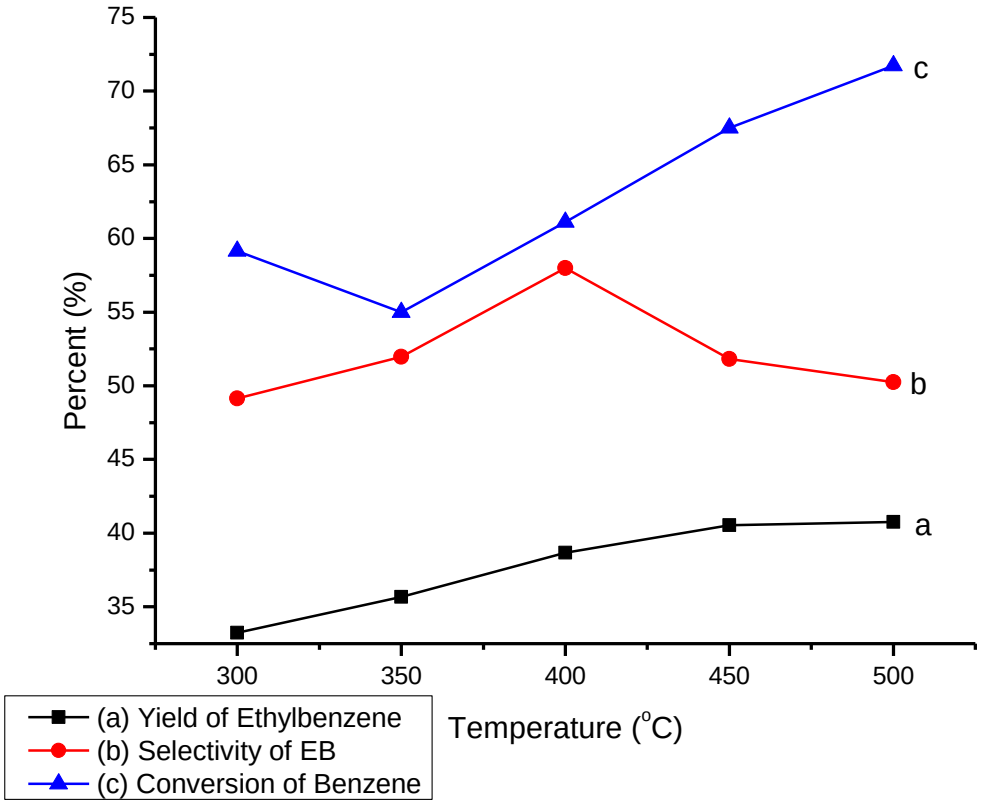

Figure 4-41: Effect of reaction temperature on catalytic performance of (Mg+B)5% - HZSM-5 (SAR = 90) catalyst for alkylation of benzene with ethanol in the ratio 2:1

Table 4-31: Effect of reaction temperature on catalytic performance of (Mg+B)5% - HZSM-5 (SAR = 90) catalyst for alkylation of benzene with ethanol in the ratio 4:1

Products (mol %)	**Temperature (°C)**				
	300	350	400	450	500
Ethanol	0.12	0.52	0.12	0.21	0.22
Benzene	38.90	34.84	24.92	24.73	18.40
Toluene	2.34	3.25	5.93	7.86	8.33
Ethylbenzene	40.92	41.79	42.65	43.64	43.02
p-Xylene	0.35	0.64	0.65	0.48	0.33
m-Xylene	0.00	0.00	0.41	0.63	1.70
o-Xylene	0.33	0.21	0.04	0.03	0.08
1,2-Diethylbenzene	1.34	1.48	2.88	2.61	3.96
1,4-Diethylbenzene	7.52	7.86	12.82	10.96	13.49
Others	8.18	9.41	9.58	8.85	10.47

Figure 4.42 demonstrates the performance of (Mg+B)5%-HZSM-5 catalyst for benzene to ethanol ratio 4:1 by volume. It is observed that the highest yield of ethylbenzene (43.63%) is

obtained at 450 ^{o}C while the highest ethylbenzene selectivity (67.10%) is observed at 300 ^{o}C. The highest conversion of benzene is found to be (77.01%) at 500 ^{o}C.

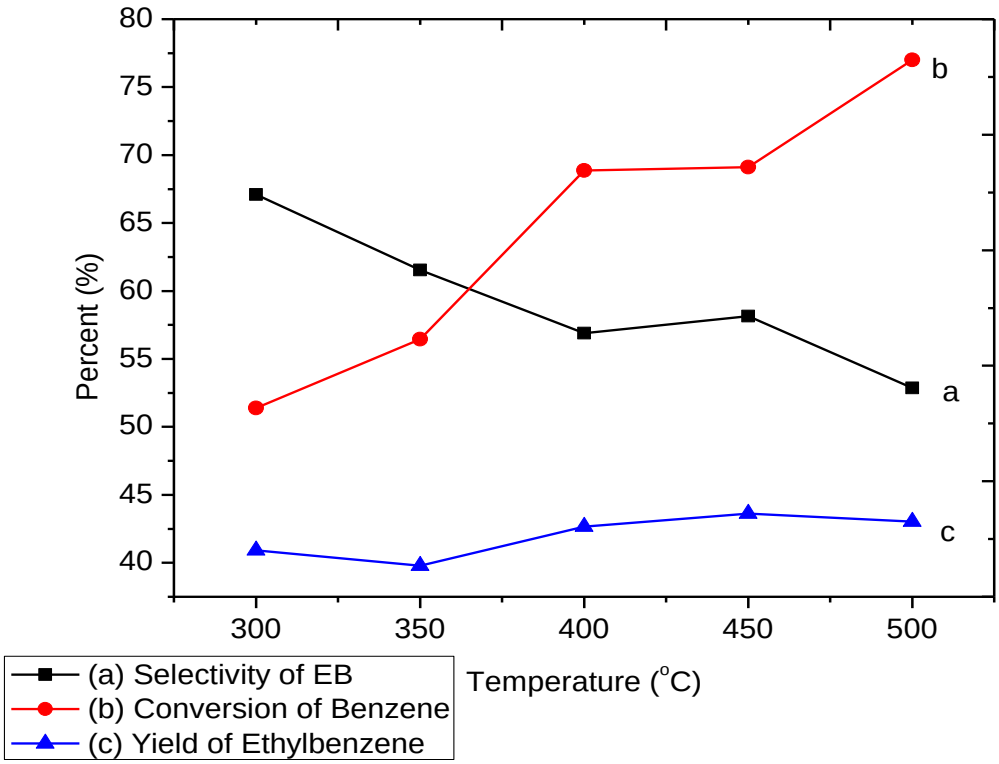

Figure 4-42: Effect of reaction temperature on catalytic performance of (Mg+B)5% - HZSM-5 (SAR = 90) catalyst for alkylation of benzene with ethanol in the ratio 4:1

Table 4-32: Effect of reaction temperature on catalytic performance of (Mg+B)10% - HZSM-5 (SAR = 90) catalyst for alkylation of benzene with ethanol in the ratio 2:1

Products (mol %)	**Temperature (^{o}C)**				
	300	350	400	450	500
Ethanol	19.54	15.87	0.65	2.19	0.42
Benzene	27.01	39.84	18.83	24.80	20.79
Toluene	0.20	1.89	6.16	3.83	7.76
Ethylbenzene	31.70	34.04	40.54	41.50	41.77
p-Xylene	0.01	0.30	0.00	0.69	0.42
m-Xylene	0.00	0.11	0.41	0.28	0.93
o-Xylene	0.01	0.01	0.65	0.04	0.05
1,2-Diethylbenzene	0.01	0.34	2.86	2.02	2.20
1,4-Diethylbenzene	0.21	3.19	20.35	16.21	16.73
Others	21.31	4.41	9.55	8.44	8.93

Figure 4.43 demonstrates the performance of (Mg+B)10%-HZSM-5 catalyst for benzene to ethanol ratio 2:1 by volume. It is observed that the highest yield of ethylbenzene (41.77%) is obtained at 500 ^{o}C while the highest ethylbenzene selectivity (72.34%) is observed at 350 ^{o}C. The highest conversion of benzene is found to be (71.70%) at 350 ^{o}C.

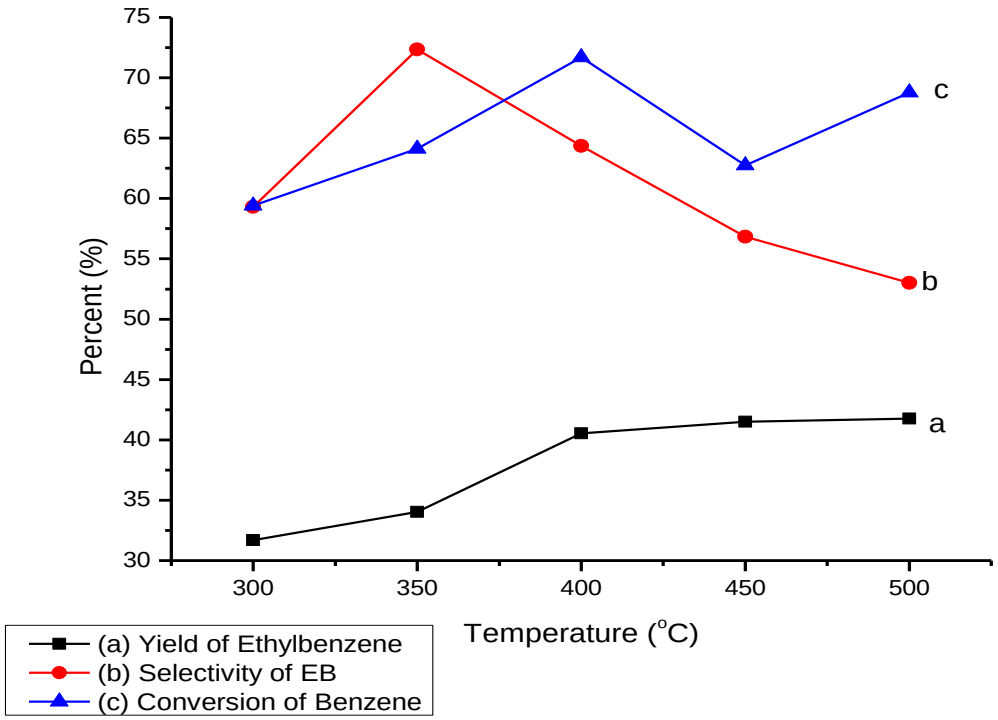

Figure 4-43: Effect of reaction temperature on catalytic performance of (Mg+B)10% - HZSM-5 (SAR = 90) catalyst for alkylation of benzene with ethanol in the ratio 2:1

Table 4-33: Effect of reaction temperature on catalytic performance of (Mg+B)10% - HZSM-5 (SAR = 90) catalyst for alkylation of benzene with ethanol in the ratio 4:1

Products (mol %)	**Temperature (^{o}C)**				
	300	350	400	450	500
Ethanol	0.55	0.59	0.56	0.52	0.58
Benzene	46.84	42.28	29.14	25.48	28.29
Toluene	1.56	2.25	4.74	8.80	11.12
Ethylbenzene	34.85	35.73	39.63	40.77	42.67
p-Xylene	0.19	0.49	0.58	0.56	0.53
m-Xylene	0.07	0.08	0.20	0.55	0.91
o-Xylene	0.02	0.03	0.03	0.03	0.04
1,2-Diethylbenzene	0.57	0.56	1.19	1.41	1.00
1,4-Diethylbenzene	5.02	5.27	10.67	11.33	7.57
Others	10.33	12.72	13.26	10.55	7.29

Figure 4.44 demonstrates the performance of (Mg+B)10%-HZSM-5 catalyst for benzene to ethanol ratio 4:1 by volume. It is observed that the highest yield of ethylbenzene (42.67%) is obtained at 500 ^{o}C while the highest ethylbenzene selectivity (62.06%) is observed at 400 ^{o}C. The highest conversion of benzene is found to be (68.16%) at 450 ^{o}C.

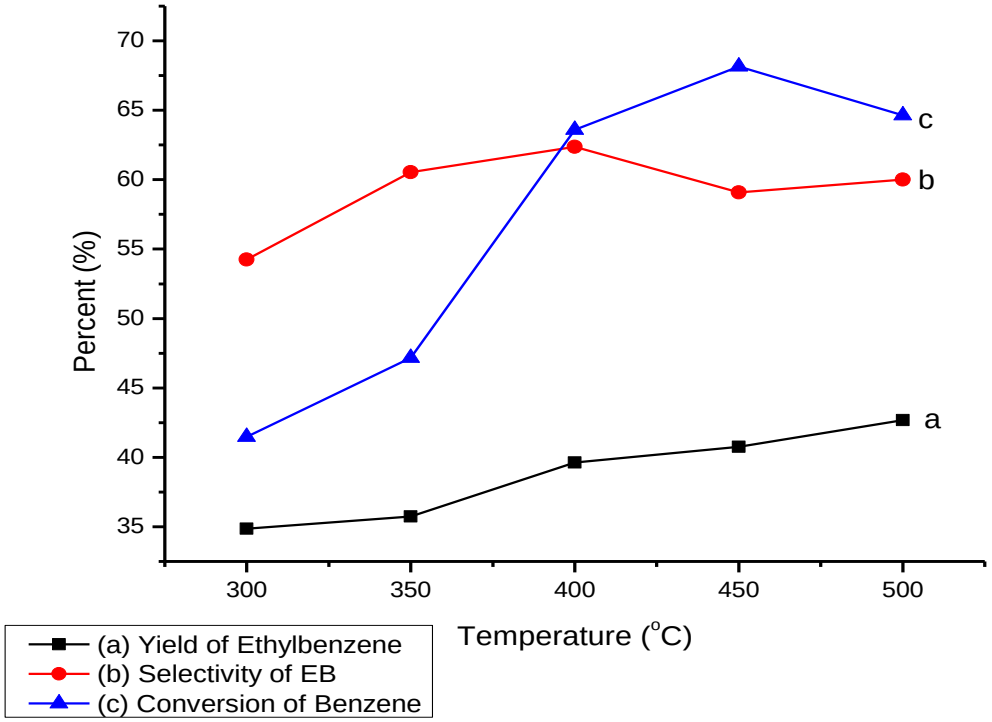

Figure 4-44: Effect of reaction temperature on catalytic performance of (Mg+B)10% - HZSM-5 (SAR = 90) catalyst for alkylation of benzene with ethanol in the ratio 4:1

Table 4-34: Effect of reaction temperature on catalytic performance of (Mg+B)15% - HZSM-5 (SAR = 90) catalyst for alkylation of benzene with ethanol in the ratio 2:1

Products (mol %)	**Temperature (^{o}C)**				
	300	350	400	450	500
Ethanol	5.56	7.77	5.17	4.27	11.52
Benzene	34.37	47.30	34.44	30.00	30.36
Toluene	0.06	0.07	1.50	0.08	0.19
Ethylbenzene	35.21	39.25	41.24	40.15	35.92
p-Xylene	0.01	0.01	0.33	0.04	0.01
m-Xylene	0.00	0.00	0.00	0.00	0.00
o-Xylene	0.00	0.01	0.15	0.12	0.02
1,2-Diethylbenzene	0.01	0.01	0.30	0.02	0.01
1,4-Diethylbenzene	0.02	0.17	9.63	8.96	0.39
Others	24.76	5.41	7.24	16.36	21.58

Figure 4.45 demonstrates the performance of (Mg+B)15%-HZSM-5 catalyst for benzene to ethanol ratio 2:1 by volume. It is observed that the highest yield of ethylbenzene (41.24%) is obtained at 400 ^{o}C while the highest ethylbenzene selectivity (76.22%) is observed at 350 ^{o}C. The highest conversion of benzene is found to be (54.91%) at 450 ^{o}C.

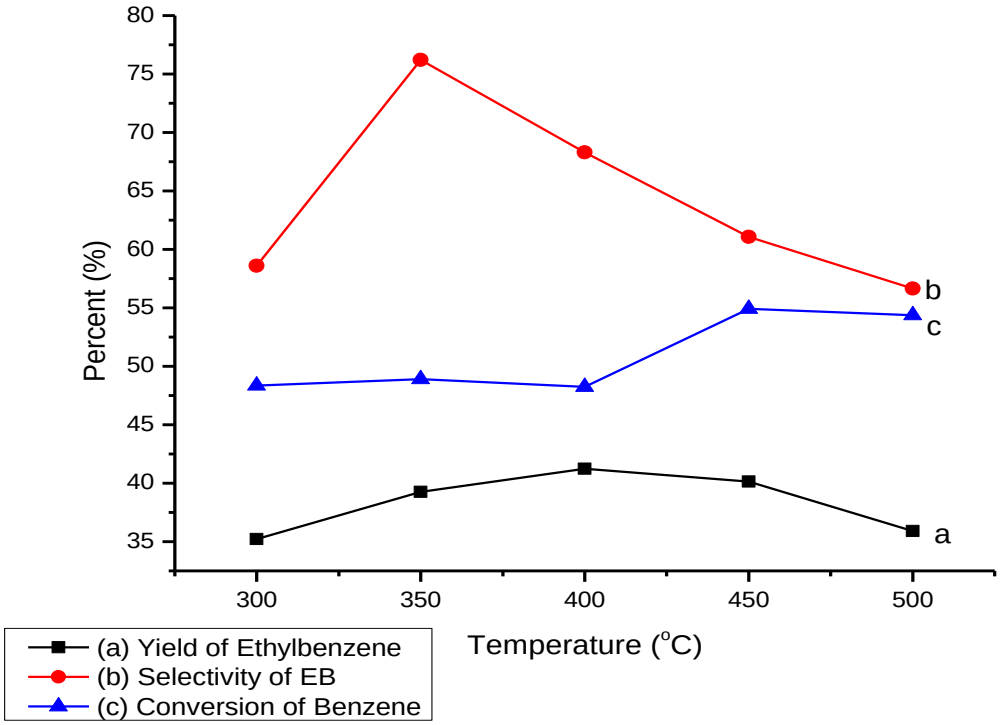

Figure 4-45: Effect of reaction temperature on catalytic performance of (Mg+B)15% - HZSM-5 (SAR = 90) catalyst for alkylation of benzene with ethanol in the ratio 2:1

Table 4-35: Effect of reaction temperature on catalytic performance of (Mg+B)15% - HZSM-5 (SAR = 90) catalyst for alkylation of benzene with ethanol in the ratio 4:1

Products (mol %)	**Temperature (^{o}C)**				
	300	350	400	450	500
Ethanol	0.61	2.10	10.73	5.40	2.57
Benzene	39.06	37.79	34.78	32.36	35.02
Toluene	3.35	2.72	3.87	8.43	11.30
Ethylbenzene	39.27	37.61	36.52	38.28	36.13
p-Xylene	0.24	0.55	0.56	0.52	0.50
m-Xylene	0.00	0.00	0.00	0.00	0.00
o-Xylene	0.31	0.19	0.15	0.33	0.52
1,2-Diethylbenzene	0.24	0.20	0.22	0.25	0.18
1,4-Diethylbenzene	8.43	6.80	7.53	9.48	7.42
Others	8.49	12.04	5.64	4.95	6.36

Figure 4.46 demonstrates the performance of (Mg+B) 15%-HZSM-5 catalyst for benzene to ethanol ratio 4:1 by volume. It is observed that the highest yield of ethylbenzene (39.27%) is obtained at 300 ^{o}C while the highest ethylbenzene selectivity (67.02%) is observed at 400 ^{o}C. The highest conversion of benzene is found to be (59.56%) at 450 ^{o}C.

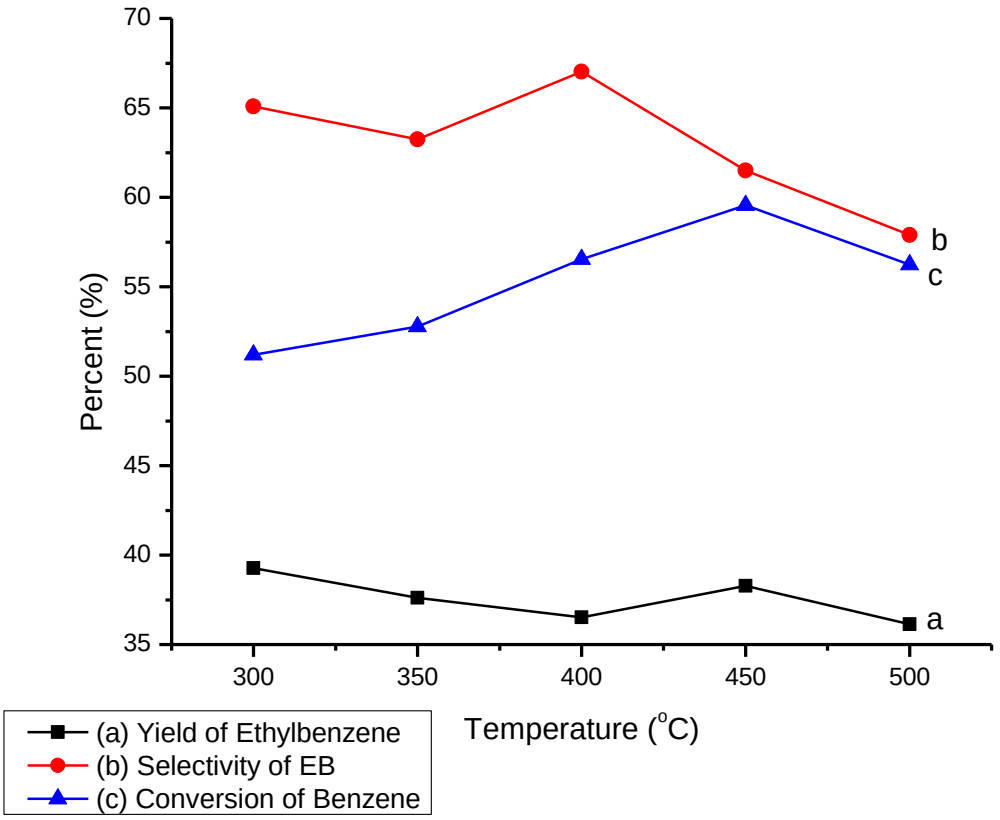

Figure 4-46: Effect of reaction temperature on catalytic performance of (Mg+B)15% - HZSM-5 (SAR = 90) catalyst for alkylation of benzene with ethanol in the ratio 4:1

4.2.3.3 Performance of Unmodified HZSM-5 Catalyst

The results of alkylation of benzene with ethanol using HZSM-5 (silicon to aluminium ratio 90) have been presented in tables 4.36, 4.37 and figures 4.47 and 4.48.

Table 4.36 shows the effect of reaction temperature on catalytic performance of HZSM-5 (SAR=90) catalyst for the alkylation of benzene with ethanol (benzene/ethanol = 2:1 by volume). It can be observed that ethylbenzene, 1, 2-diethylbenzene and 1, 4-diethylbenzene are the major products while xylenes, toluene and gaseous hydrocarbons are also present in small amounts.

Table 4-36: Effect of reaction temperature on catalytic performance of HZSM-5 (SAR = 90) catalyst for alkylation of benzene with ethanol (Benzene/ethanol = 2:1)

Products (mol %)	Temperature (^{o}C)				
	300	350	400	450	500
Ethanol	0.96	1.07	1.32	0.22	1.78
Benzene	21.19	14.87	28.15	17.91	22.55
Toluene	0.34	0.37	0.26	0.33	0.66
Ethylbenzene	35.79	38.42	45.03	41.63	37.63
p-Xylene	0.45	0.30	0.31	0.16	0.19
m-Xylene	0.03	0.02	0.01	0.01	1.07
o-Xylene	0.15	0.39	0.52	1.76	0.73
1, 2-Diethylbenzene	9.14	11.77	4.97	7.82	0.60
1, 4-Diethylbenzene	16.26	18.73	12.57	21.43	30.21
Others	15.69	14.06	6.86	8.73	4.58

Similarly table 4.37 shows the effect of reaction temperature on catalytic performance of HZSM-5 (SAR=90) catalyst for the alkylation of benzene with ethanol (benzene/ethanol = 4:1 by volume). Accordingly we observed that ethylbenzene, 1, 2-diethylbenzene and 1, 4-diethylbenzene are the major products while xylenes, toluene and gaseous hydrocarbons are also present in small amounts. However, the amount of ethylbenzene obtained for benzene to ethanol (benzene/ethanol = 4:1 by volume) ratio is higher than that of 2:1. This must have happened due to suppression of subsequent reactions such as ethylation of ethylbenzene to diethylbenzene and disproportionation of ethylbenzene to benzene and diethylbenzene.

Table 4-37: Effect of reaction temperature on catalytic performance of HZSM-5 (SAR = 90) catalyst for alkylation of benzene with ethanol (Benzene/ethanol = 4:1)

Products (mass %)	Temperature (^{o}C)				
	300	350	400	450	500
Ethanol	1.00	0.65	0.85	0.95	0.75
Benzene	23.45	16.77	26.84	22.94	15.03
Toluene	0.93	1.86	2.85	3.29	3.93
Ethylbenzene	39.65	40.87	45.00	43.95	39.82
p-Xylene	0.41	0.63	0.34	0.40	0.21
m-Xylene	0.00	0.00	0.00	0.00	0.00
o-Xylene	1.05	0.87	1.13	1.33	1.87
1, 2-Diethylbenzene	6.71	10.69	5.57	6.61	10.20
1, 4-Diethylbenzene	14.11	15.19	9.91	11.71	15.80
Others	12.69	12.47	7.51	8.82	12.39

Figure 4.47 demonstrates the effect of reaction temperature on catalytic performance of HZSM-5 (SAR=90) catalyst such as selectivity and yield of ethylbenzene and conversion of benzene for the alkylation of benzene with ethanol (benzene/ethanol = 2:1 by volume). The highest yield (45.03%) and selectivity (63.84%) of ethylbenzene resulted at 400^{o}C. However, the highest conversion (77.65%) of benzene was obtained at 350^{o}C.

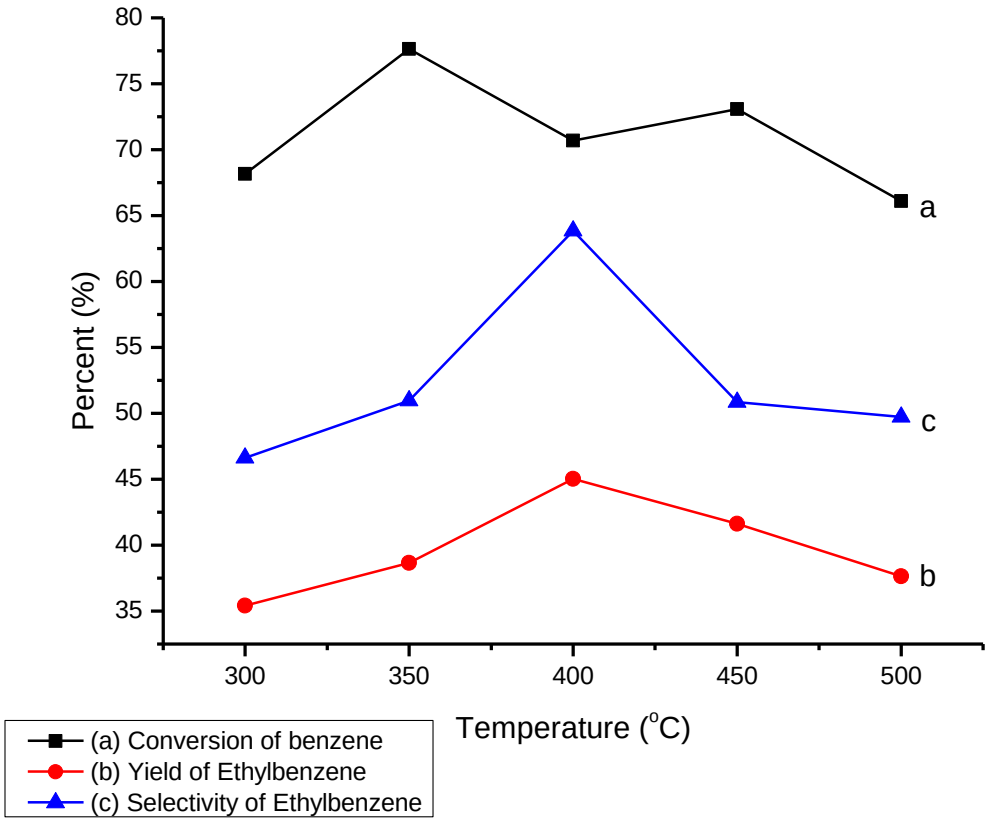

Figure 4-47: Effect of reaction temperature on the performance of HZSM-5 SAR = 90 for benzene to ethanol ratio 2:1

Figure 4.48 shows the effect of reaction temperature on catalytic performance of HZSM-5 (SAR=90) catalyst such as selectivity and yield of ethylbenzene and conversion of benzene for the alkylation of benzene with ethanol (benzene/ethanol = 4:1 by volume). In the case of 4:1 benzene to ethanol ratio similarly the highest yield (45.00%) and selectivity (62.23%) of ethylbenzene were obtained at 400^{o}C. The highest conversion of benzene was 81.23% at 500^{o}C; however, the selectivity of ethylbenzene was poor at this temperature. From our investigations we observed that HZSM-5 zeolite with silicon to aluminium ratio 90 is a promising zeolite to be used as a catalyst.

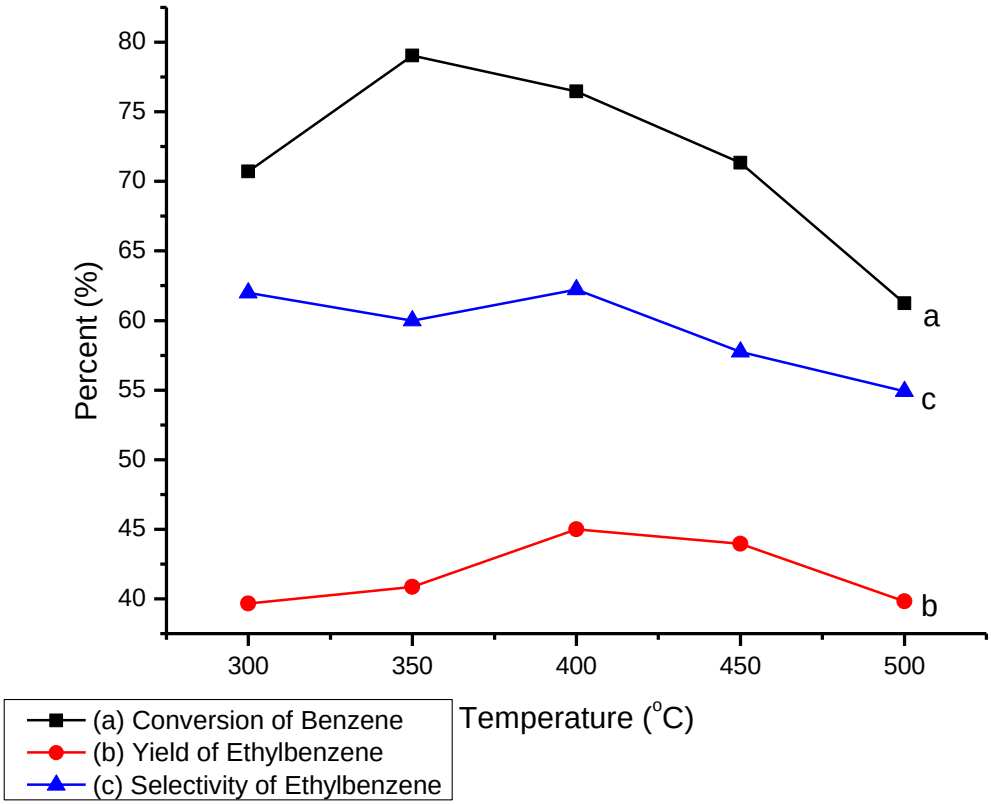

Figure 4-48: Effect of reaction temperature on the performance of HZSM-5 SAR = 90 for benzene to ethanol ratio 4:1

4.3 KINETIC STUDY

This section discusses the kinetic study of alkylation reaction of benzene with ethanol over (B-Mg)-15%-HZSM-5 zeolite catalyst. The kinetic experiments were carried out in presence of (B-Mg)-15%-HZSM-5 catalyst since it was the most active and selective catalyst among all the catalysts examined. The kinetic experiments of the alkylation of benzene with ethanol were carried out in fixed bed tubular reactor in the temperature range from 300 ^{o}C to 500 ^{o}C and atmospheric pressure. The kinetic study was done using different weight hour space velocity from 5 to 32.6 h^{-1}. Nitrogen to feed ratio 4.2 and feed ratio (benzene to ethanol) 4:1 were used. The reaction data was used to calculate the initial reaction rate and activation energy. Many researchers used Langmuir-Hinshelwood- Hougen-Watson (LHHW) model to develop kinetic model of different reactions [126,127]. The kinetic model used to fit the data was Langmuir-Hinshelwood- Hougen-Watson (LHHW) model.

4.3.1 Kinetic Model Development

4.3.1.1 Langmuir-Hinshelwood- Hougen-Watson (LHHW) Model

Reaction mechanism for alkylation of benzene with ethanol can be represented by the following steps which are used to derive the rate equations.

Step 1: Adsorption

Adsorption of ethanol (E) on the surface of vacant sites (S):

$$E + S \underset{k_{-1}}{\overset{k_1}{\rightleftharpoons}} E.S \qquad (4.6)$$

Adsorption of benzene (B) on the surface of the vacant sites (S):

$$B + S \underset{k_{-2}}{\overset{k_2}{\rightleftharpoons}} B.S \qquad (4.7)$$

Step 2: Surface Reaction

Surface reaction between adsorbed ethanol and benzene on the active surface of catalysts is presented by

$$E.S + B.S \underset{k_{-3}}{\overset{k_3}{\rightleftharpoons}} EB.S + W.S \qquad (4.8)$$

$$EB.S + E.S \underset{k_{-4}}{\overset{k_4}{\rightleftharpoons}} DEB.S + W.S \qquad (4.9)$$

$$DEB.S + E.S \underset{k_{-5}}{\overset{k_5}{\rightleftharpoons}} TEB.S + W.S \qquad (4.10)$$

Step 3: Desorption

$$EB.S \underset{k_{-6}}{\overset{k_6}{\rightleftharpoons}} EB + S \qquad (4.11)$$

$$DEB.S \underset{k_{-7}}{\overset{k_7}{\rightleftharpoons}} DEB + S \qquad (4.12)$$

$$TEB.S \underset{k_{-8}}{\overset{k_8}{\rightleftharpoons}} TEB + S \qquad (4.13)$$

From equation (4.6) to (4.13), the rate equations can be represented as

$$(-r_1) = k_1\left(C_E C_S - \frac{C_{E.S}}{K_1}\right), \quad K_1 = \frac{k_1}{k_{-1}} \tag{4.14}$$

$$(-r_2) = k_2\left(C_B C_S - \frac{C_{B.S}}{K_2}\right), \quad K_2 = \frac{k_2}{k_{-2}} \tag{4.15}$$

$$(-r_3) = k_3\left(C_{B.S} C_{E.S} - \frac{C_{EB.S}\, C_{W.S}}{K_3}\right), \quad K_3 = \frac{k_3}{k_{-3}} \tag{4.16}$$

$$(-r_4) = k_4\left(C_{EB.S} C_{E.S} - \frac{C_{DEB.S}\, C_{W.S}}{K_4}\right), \quad K_4 = \frac{k_4}{k_{-4}} \tag{4.17}$$

$$(-r_5) = k_5\left(C_{DEB.S} C_{E.S} - \frac{C_{TEB.S}\, C_{W.S}}{K_5}\right), \quad K_5 = \frac{k_5}{k_{-5}} \tag{4.18}$$

$$(-r_6) = k_6\left(C_{EB.S} - \frac{C_{EB}\, C_S}{K_6}\right), \quad K_6 = \frac{k_6}{k_{-6}} \tag{4.19}$$

$$(-r_7) = k_7\left(C_{DEB.S} - \frac{C_{DEB}\, C_S}{K_7}\right), \quad K_7 = \frac{k_7}{k_{-7}} \tag{4.20}$$

$$(-r_8) = k_8\left(C_{TEB.S} - \frac{C_{TEB}\, C_S}{K_8}\right), \quad K_8 = \frac{k_8}{k_{-8}} \tag{4.21}$$

Where K_1, K_2, K_3, K_4, K_5, K_6, K_7 and K_8 are the equilibrium constants for respective reactions

It is assumed that the surface reaction is the rate controlling step, and then the rate of surface reactions are given as follows,

From Eq. (4.16),

$$(-r_3) = k_3 C_{E.S}\ C_{B.S} \tag{4.22}$$

From Eq. (4.17),

$$(-r_4) = k_4 C_{EB.S}\ C_{E.S} \tag{4.23}$$

From Eq. (4.18),

$$(-r_5) = k_5 C_{DEB.S} C_{E.S} \quad (4.24)$$

If the adsorption and desorption steps are very fast, then the concentrations of adsorbed species can be calculated by assuming adsorption and desorption steps are at equilibrium. The concentration of adsorbed species can be obtained as follows:

From Eq. (4.14),

$$\frac{r_1}{k_1} = 0$$
$$C_{E.S} = K_1 C_E C_S \quad (4.25)$$

From Eq. (4.15),

$$\frac{r_2}{k_2} = 0$$
$$C_{B.S} = K_2 C_B C_S \quad (4.26)$$

From Eq. (4.19),

$$\frac{r_6}{k_6} = 0$$
$$C_{EB.S} = \frac{C_{EB} C_S}{K_6} \quad (4.27)$$

From Eq. (4.20),

$$\frac{r_7}{k_7} = 0$$
$$C_{DEB.S} = \frac{C_{DEB} C_S}{K_7} \quad (4.28)$$

From Eq. (4.21),

$$\frac{r_8}{k_8} = 0$$
$$C_{TEB.S} = \frac{C_{TEB} C_S}{K_8} \quad (4.29)$$

On substituting these values in surface reaction rates

$$(-r_3) = k_3 K_1 K_2 C_E C_B C_S^2 \quad (4.30)$$

$$(-r_4) = \frac{k_4 K_1 C_{EB} C_E C_S^2}{K_6} \quad (4.31)$$

$$(-r_5) = \frac{k_5 K_1 C_{DEB} C_E C_S^2}{K_7} \quad (4.32)$$

Now, the total concentration of active sites on the surface, C_T, can be expressed as the sum of concentration of all sites on which reactants and products are adsorbed and the concentration of vacant sites which yields,

$$C_T = C_S + C_{E.S} + C_{B.S} + C_{EB.S} + C_{DEB.S} + C_{TEB.S} \quad (4.33)$$

$$C_S = \frac{C_T}{1 + K_1 C_E + K_2 C_B + \frac{C_{EB}}{K_6} + \frac{C_{DEB}}{K_7} + \frac{C_{TEB}}{K_8}} \quad (4.34)$$

Substituting Eq. (4.34) into Eq. (4.30 - 4.32), then

$$(-r_3) = \frac{k_3' C_E C_B}{\left(1 + K_1 C_E + K_2 C_B + \frac{C_{EB}}{K_6} + \frac{C_{DEB}}{K_7} + \frac{C_{TEB}}{K_8}\right)^2} \quad (4.35)$$

$$k_3' = k_3 K_1 K_2 C_T^2$$

$$(-r_4) = \frac{k_4' C_E C_{EB}}{\left(1 + K_1 C_E + K_2 C_B + \frac{C_{EB}}{K_6} + \frac{C_{DEB}}{K_7} + \frac{C_{TEB}}{K_8}\right)^2} \quad (4.36)$$

$$k_4' = \frac{k_4 K_1 C_T^2}{K_6}$$

$$(-r_5) = \frac{k_5' C_E C_{DEB}}{(1 + K_1C_E + K_2C_B + \frac{C_{EB}}{K_6} + \frac{C_{DEB}}{K_7} + \frac{C_{TEB}}{K_8})^2} \quad (4.37)$$

$$k_5' = \frac{k_5 K_1 C_T^2}{K_7}$$

It is important to note that the adsorption of water is negligible. Hence, K_W equals to zero in the above surface coverage expressions.

For each temperature, the space-time-conversion data have been analyzed and the rates of reaction were obtained by differential analysis of the plug flow reactor equation:

$$r_{obs} = \frac{dX_B}{d(W / F_{BO})} \quad (4.38)$$

$$\frac{dX_B}{dz} = \frac{(r_i A)(\text{bulk density})}{F_{Bo}} \quad (4.39)$$

Where r_{obs} = experimentally observed rate of reaction of B, W = mass of the catalyst, B = benzene, X_B = fractional benzene conversion, F_{BO} = feed rate of benzene, z= bed length and A= bed cross sectional area

The intrinsic rate constant can be expressed according to the Arrhenius equation:

$$k = k_o \exp(-E/RT) \quad (4.40)$$

Conventionally, the temperature dependence relations of the adsorption equilibrium constants can be expressed according to the following thermodynamic relations:

$$K_i = \exp\left(-\frac{\Delta G^o_{ads,i}}{RT}\right) \quad (4.41)$$

Where, $\Delta G^o_{ads,i}$ is the Gibbs free energy for adsorption of species i at standard conditions (298 K and 1 atm) which is further related to the change of enthalpy $\Delta H^o_{ads,i}$ and change of entropy $\Delta S^o_{ads,i}$ of adsorption as follows:

$$\Delta G^o_{ads,i} = \Delta H^o_{ads,i} - T\Delta S^o_{ads,i} \quad (4.42)$$

From Eq. (4.41) and Eq. (4.42),

$$K_i = \exp\left(\frac{\Delta S^o_{ads,i}}{R} - \frac{\Delta H^o_{ads,i}}{RT} \right) \qquad (4.43)$$

Alternatively, the above Eq. (4.43) can be represented with the centred temperature form as:

$$K_i = \exp(D_i - F_i(1/T - 1/T_o)) \qquad (4.44)$$

Where $D = \frac{\Delta S_{ads}}{R}$ and $F = \frac{\Delta H_{ads}}{R}$

If we assume that the adsorption of water and nitrogen does not compete with the adsorption of hydrocarbons, the influence of water and nitrogen adsorption could be neglected. With these assumption, the rate equations, Eq. (4.35) and Eq. (4.36) becomes

$$(-r_3) = \frac{k_3' \, p_E \, p_B}{\left(1 + K_1 p_E + K_2 p_B + \frac{p_{EB}}{K_6} + \frac{p_{DEB}}{K_7}\right)^2} \qquad (4.45)$$

$$k_3' = k_3 \, K_1 \, K_2 \, C_T^2$$

$$(-r_4) = \frac{k_4' \, p_E \, p_{EB}}{\left(1 + K_1 p_E + K_2 p_B + \frac{p_{EB}}{K_6} + \frac{p_{DEB}}{K_7}\right)^2} \qquad (4.46)$$

$$k_4' = \frac{k_4 \, K_1 C_T^2}{K_6}$$

Eq. (4.37) was ignored due to low amount of TEB.

The partial pressures in the above equations are related to the conversion and total pressure P by the following relationship:

$$p_B = \frac{(1 - x_B) \, P}{(6.5 + x_B)} \qquad (4.47)$$

$$p_E = \frac{(0.25 - x_B) \, P}{(6.5 + x_B)} \qquad (4.48)$$

$$p_{EB} = \frac{(x_B)\,P}{(6.5 + x_B)} \qquad (4.49)$$

$$p_{DEB} = \frac{(x_B)\,P}{(6.5 + x_B)} \qquad (4.50)$$

$$(-r_3) = \frac{k_3'\,(0.25 - x_B)\,(1 - x_B)\,P^2/(6.5+x_B)^2}{\left(1 + \left(K_1(0.25 - x_B) + K_2(1 - x_B) + \frac{x_B}{K_6} + \frac{x_B}{K_7}\right)(P/(6.5+x_B))\right)^2} \qquad (4.51)$$

$$k_3' = k_3\,K_1\,K_2\,C_T^2$$

$$(-r_4) = \frac{k_4'\,(0.25 - 0.5x_B)\,(1 - x_B)\,P^2/(6.5+x_B)^2}{\left(1 + \left(K_1(0.25 - x_B) + K_2(1 - x_B) + \frac{x_B}{K_6} + \frac{x_B}{K_7}\right)(P/(6.5+x_B))\right)^2} \qquad (4.52)$$

$$k_4' = \frac{k_4\,K_1\,C_T^2}{K_6}$$

In order to estimate the unknown parameters in Eq. (4.51) and (4.52), the differential equations were solved by Runge-Kutta method (MATLAB ODE 45 subroutine). These parameters were estimated by treating each temperature data separately. As the rate equation is non-linear with respect to unknown parameters, a non-linear regression program based on Marquardt's algorithm was used to obtain a mathematical fit for the above rate equation by minimizing the objective function for the residual sum of squares.

$$\emptyset = \sum_{i=0}^{n} (yi - yi')^2 \qquad (4.53)$$

Where n is the number of responses, y_i the experimental conversion and y_i' is the predicted conversion.

Table 4-38: Estimated parameter values

Constants	Kinetic parameter	
	Activation Energy, E_a (kJ/mol)	Pre-exponential factor, k_o (kgmol/kgcat.h)
k_3'	14.3	169.85
k_4'	15.4	479.19
		(L/mol)
K_1	22.68	$5.36*10^{-3}$
K_2	165.6	$2.36*10^{-2}$
K_6	4.49	28.02
K_7	21.44	$1.12*10^{3}$

The kinetic constants evaluated and tabulated at various temperatures were used to determine the activation energy and frequency factor using Arrhenius relationship, Eq. (4.40).

Summary:

Ethylbenzene was the primary product while diethylbenzene, triethylbenzene, toluene and xylene mixtures also exist in the product. The highest selectivity of ethylbenzene (76.22%) was obtained by (Mg+B)15%-HZSM-5 and the lowest ethylbenzene selectivity (57.98%) was obtained by (Mg+B)5%-HZSM-5 using 2:1 benzene to ethanol ratio by volume. However, for benzene to ethanol ratio 4:1 (Mg+B)5%-HZSM-5 and (Mg+B)15%-HZSM-5 catalysts have shown approximately the same selectivity for ethylbenzene (67.01%). The highest yield of ethylbenzene demonstrated by (Mg+B)5%-HZSM-5 was 43.63% at 450 ^{o}C for benzene to ethanol ratio 4:1 by volume. The highest conversion of benzene, approximately 77.01%, was obtained by (Mg+B)5%-HZSM-5 for 4:1 benzene to ethanol ratio by volume. The existence of excess ethanol may facilitate the alkylation of benzene to produce ethylbenzene and then further alkylation to diethylbenzene and tri ethylbenzene. Therefore, it would be desirable to use lower amount of ethylating agents.

CHAPTER FIVE
CONCLUSION AND RECOMMENDATION

5.1 CONCLUSIONS

In the present work, the alkylation of benzene with ethanol was investigated over boron, magnesium monometallic and boron-magnesium bimetallic modified HZSM-5 (SAR=31 and 90) catalysts. From the present study, the following conclusions can be made:

1. The variation of Si/Al ratio in HZSM-5 catalysts significantly affected the catalytic performance of the catalysts.
2. The benzene to ethanol ratio during alkylation reaction of benzene with ethanol significantly affected the selectivity of ethylbenzene.
3. During alkylation of benzene with ethanol using either modified or unmodified HZSM-5 catalysts, ethylbenzene was the primary product while diethylbenzene, triethylbenzene, toluene and xylene mixtures were also observed in the product.
4. From the experimental results we observed that for HZSM-5 silicon to aluminium ratio 31 (SAR=31) with benzene to ethanol ratio 2:1 by volume the highest selectivity of ethylbenzene (72.79%) and higher conversion of benzene (75.17%) was obtained by bimetallic catalyst (Mg(5%)-B(4%)-HZSM-5) at 500^{o}C and 400^{o}C respectively. Boron modified showed lower benzene conversion (62.2%) while magnesium modified showed approximately the same benzene conversion (71.7%) when compared to unmodified HZSM-5 (71.3%). The existence of abundant ethanol may facilitate the alkylation of benzene to produce ethylbenzene and then further alkylation to diethylbenzene and tri ethylbenzene.
5. For magnesium monometallic modified HZSM-5 (SAR=90), the highest selectivity of ethylbenzene (71.14%) was obtained by 15%Mg-HZSM-5 while the lowest ethylbenzene selectivity (49.74%) was obtained by10%Mg-HZSM-5 for 2:1 benzene to ethanol ratio by volume. For benzene to ethanol ratio 4:1 also the highest selectivity for ethylbenzene (67.59%) was observed by 15%Mg-HZSM-5 while the lowest selectivity of ethylbenzene (57.43%) was obtained by 5%Mg-HZSM-5. In terms of ethylbenzene yield all HZSM-5 catalysts modified by magnesium resulted approximately in the range of 34-42%. The highest conversion of benzene (71.82%) was obtained by 15%Mg-HZSM-5.

6. For boron modified HZSM-5, the highest selectivity of ethylbenzene (57.48%) was obtained by 15%B-HZSM-5 while the lowest ethylbenzene selectivity (42%) was obtained by10%B-HZSM-5and 5%B-HZSM-5 for 4:1 benzene to ethanol ratio by volume. However, for benzene to ethanol ratio 2:1 all the catalysts showed approximately the same selectivity for ethylbenzene (48%). Except 15%B-HZSM-5, in terms of ethylbenzene yield both HZSM-5 catalysts modified by boron resulted on approximately 40.00%. The highest yield of ethylbenzene demonstrated by 15%B-HZSM-5 was 44.18% at 450^{o}C for benzene to ethanol ratio 4:1 by volume. The highest conversion of benzene approximately (83%) was obtained by both 5%B-HZSM-5 and 10%Mg-HZSM-5.
7. For boron-magnesium bimetallic modified HZSM-5, the highest selectivity of ethylbenzene (76.22%) was obtained by (Mg + B)-15%-HZSM-5 and the lowest ethylbenzene selectivity (49.15%) was obtained by (Mg + B)-5%-HZSM-5 using 2:1 benzene to ethanol ratio by volume. However, for benzene to ethanol ratio 4:1 (Mg + B)-5%-HZSM-5 and (Mg + B)-15%-HZSM-5 catalysts were showed approximately the same selectivity for ethylbenzene (67.01%). The highest yield of ethylbenzene demonstrated by (Mg + B)-5%-HZSM-5 was 43.63% at 450^{o}C for benzene to ethanol ratio 4:1 by volume. The highest conversion of benzene approximately (77.01%) was obtained by (Mg + B)-5%-HZSM-5 for 4:1 benzene to ethanol ratio by volume.
8. Modifications of HZSM-5 using boron, magnesium monometallic and bimetallic are promising for the alkylation of benzene with ethanol.
9. The highest selectivity of ethylbenzene was obtained by bimetallic modified HZSM-5 due to synergetic effect.
10. A reaction scheme with three parallel routes leading to the formations of ethylbenzene, diethylbenzene and triethylbenzene, was considered for the kinetic study. The kinetic parameters were determined by using LHHW type kinetic models. LHHW model could satisfactorily correlate the rate data and this model give good fit between the experimental and calculated data.

5.2 RECOMMENDATIONS

Based on the experiments conducted in this study, some of the improvements could be done in order to know the insights of catalysts and to enhance the overall alkylation reaction of benzene with ethanol activity.

1. Catalysts may be characterized by other techniques such as XPS, HRTEM and in-situ FTIR to elucidate the insights of catalysts such as composition, atomic morphology and functional groups before and after reactions. Pyridine-FTIR may be used for the detail characterization of Lewis and Brønsted acid sites of catalysts.
2. Different bimetallic catalysts including combination of noble transition metals and /or transition-transition metals can be developed for alkylation of benzene with ethanol to enhance the catalytic activity and stability.
3. Till date, numerous catalyst systems have been reported in literature for the alkylation of benzene with different ethylating agents to produce ethylbenzene, while direct synthesis of diethylbenzene from alkylation of benzene with ethylating agents rather limited. Catalysts can be developed for selective conversion of either alkylation of benzene or ethylbenzene disproportionation to diethylbenzene due to its wide spread industrial applications.

REFERENCES

1. T. C. Tsai, S. B. Liu and I. Wang, Disproportionation and Transalkylation of Alkylbenzenes over Zeolite Catalysts, Applied Catalysis A: General, 181, 355-398, (1999).
2. R. Alibeyli, A. Karaduman, H. Yeniova, A. Ates and A. Y. Bilgesü, Development of a Polyfunctional Catalyst for Benzene Production from Pyrolysis Gasoline, Applied Catalysis A: General, 238, 279-287, (2003).
3. C. Perego and P. Ingallina, Recent Advances in the Industrial Alkylation of Aromatics: New Catalysts and New Processes, Catalysis Today, 73, 3-22, (2002).
4. H. Chandawar, B. Kulkarni and P. Ratnasamy, Alkylation of Benzene with Ethanol over ZSM-5 zeolites, Applied Catalysis, 4, 287-295, (1982).
5. https://www.ihs.com/products/ethylbenzene-chemical-economics-handbook.html, accessed on 2/9/2015.
6. https://en.wikipedia.org/wiki/Ethylene, accessed on 5/11/2015.
7. https://en.wikipedia.org/wiki/Ethanol_fuel, accessed on 12/11/2015.
8. V. R. Vijayaraghavan and J. A. Raj, Ethylation of Benzene with Ethanol over Substituted Large Pore Aluminophosphate-based Molecular Sieves, Journal of Molecular Catalysis A: Chemical, 207, 41-50, (2004).
9. Y. Li, B. Xue and X. He, Catalytic Synthesis of Ethylbenzene by Alkylation of Benzene with Diethyl Carbonate over HZSM-5, Catalysis Communications, 10, 702-707, (2009).
10. W. S. Chang, Y. Z. Chen and B. L. Yang, Oxidative Dehydrogenation of Ethylbenzene over V^{iv} And V^{v} Magnesium Vanadate's, Appl. Catal. A: General, 124, 221-243, (1995).
11. https://en.wikipedia.org/wiki/Ethylbenzene, accessed on 1/1/2015.
12. C. Perego, S. Amarilli, A. Carati, C. Flego, G. Pazzuconi, C. Rizzo and G. Bellussi, Mesoporous Silica-Alumina as Catalysts for the Alkylation of Aromatic Hydrocarbons with Olefins, Microporous and Mesoporous Materials, 27, 345-354, (1999).
13. World Health Organization International Agency for Research on Cancer, IARC Monographs on the Evaluation of Carcinogenic Risks to Humans, Some Industrial Chemicals, 77, 15-22, (2000).
14. L. Sun, X. Guo, M. Liu and X. Wang, Ethylation of coking benzene over nanoscale HZSM-5 zeolites: Effects of hydrothermal treatment, calcination and La_2O_3 modification, Applied Catalysis A: General, 355, 184-191, (2009).

15. B. Wang, W. Huang, Y. Wen, Z. Zuo, Z. Gao and L. Yin, Styrene from toluene by side chain alkylation over a novel solid acid-base catalyst, Catalysis Today, 173, 38-43, (2011).
16. B. G. Johnson and S. E. Arshad, Hydrothermally synthesized zeolites based on kaolinite: A review, Applied Clay Science, 97-98, 215-221, (2014).
17. G. Feng, A first principle study on Fe incorporated MTW-type zeolite, Microporous and Mesoporous Materials, 199, 83-92, (2014).
18. S. Mintova, Progress in zeolite synthesis promotes advanced applications, Microporous and Mesoporous Materials, 189, 11-21, (2014).
19. B. Yilmaz, N. Trukhan, U. Müller, Industrial Outlook on Zeolites and Metal Organic Frameworks, Chinese Journal of Catalysis, 0253-9837, 01-08, (2012).
20. S. Kulprathipanja (Editor), Zeolites in Industrial Separation and Catalysis, Wiley-VCH: Weinheim, ISBN: 978-3-527-32505-4, (2010).
21. H. V. Bekkum, E.M. Flanigen and J. C. Jansen (Editors), Introduction to Zeolite Science and Practice, Studies in Surface Science and Catalysis Vol. 58, Elsevier: Amsterdam - Oxford - New York – Tokyo, (1991).
22. S. M. Auerbach, K. A. Carrado and P. K. Dutta (Editors), Hand Book of Zeolite Science and Technology, Marcel Dekker, Inc., New York: Basel, (2003).
23. R. Xu, W. Pang, J. Yu, Q. Huo and J. Chen, Chemistry of Zeolites and Related Porous Materials: Synthesis and Structure, John Wiley & Sons (Asia) Pte Ltd, (2007).
24. D. Georgiev, B. Bogdanov, K. Angelova, I. Markovska and Y. Hristov, Review on synthetic zeolites - structure, classification, current trends in zeolite synthesis, International Science conference 4^{th}-5^{th}, Stara Zagora, Bulgaria, (2009).
25. http://www.ch.ic.ac.uk/vchemlib/course/zeolite/ structure.html, accessed on 23/2/2015.
26. http://en.wikipedia.org/wiki/Zeolite, accessed on 10/11/2015.
27. J. Čejka, H. V. Bekkum, A. Corma, F. Schüth (Eds.), Introduction to Zeolite Science and Practise, Studies Surface Science Catalysis, 3rd ed. 168 Elsevier: Amsterdam, (2007).
28. S. C. Cundy and A. P. Cox, The hydrothermal synthesis of zeolites: history and development from the earliest days to the present time, Chemical Review, 103, 663-702, (2003).
29. International Zeolite Association, S.C., Atlas of Zeolite Framework types URL: http://topaz.ethz.ch/IZA-SC/StdAtlas.htm, accessed on 14/12/2015.

30. M. E. Davis and R. J. Davis, Fundamentals of chemical reaction engineering. McGraw-Hill Higher Education, New York, NY. ISBN 0-07-245007-X, (2003).
31. http://www.iza-structure.org/, accessed on 5/12/2015.
32. D. J. Earl and M. W. Deem, Toward a Database of Hypothetical Zeolite Structures, Eduardo Glandt special issue, Industrial & Engineering Chemical Research, 45, 5449-5454, (2006).
33. http://izasc-mirror.la.asu.edu/fmi/xsl/IZA-SC/ft.xsl, accessed on 14/12/2015.
34. J. R. Anderson, K. Foger, T. Mole, R. A. Rajadhyakska, and J. V. Sanders, Journal of Catalysis, 58, 114, (1979).
35. A. Boreave, A. Auroux and C. Guimon, Nature and strength of acid sites in HY zeolites: a multi technical approach, Microporous Materials, 11, 275-291, (1997).
36. D. W. Breck, Zeolite molecular sieves: structure, chemistry and use, London, Wiley (1974).
37. R. Szostak, Handbook of Molecular Sieves, New York: Van Nostrand Reinhold, (1992).
38. N. Y. Chen and W. E. Garwood, Some Catalytic Properties of ZSM-5, a New Shape Selective Zeolite, Journal of Catalysis, 52, 453-458, (1978).
39. S. M. Csicsery, ACS Monograph 171, Shape Selective Catalysis, Zeolite Chemistry and Catalysis, J. A. Rabo, ed., (American Chemical Society, Washington); pp. 680, (1976).
40. E. G. Derouane, Zeolite : Science and Technology, Molecular Shape-Selective Catalysis by Zeolites, Edited by F. Ramoa Ribeiro, Alirio E. Rodrigues, L. Deane Rollmann, Claude Naccache (Martinus Nijhoff Publishers, The Hague / Boston /Lancaster); p. 347, (1984).
41. M. W. Anderson and J. Klinowski, Solid-State NMR Studies of Shape Selectivity in Zeolites, Studies in Surface Science and Catalysis, 52, 91-112, (1989).
42. P. B. Weisz, V. J. Frilette, R. W. Maatman and F. B. Mower, Catalysis by Crystalline Aluminosilicates II: Molecular-Shape Reactions, Journal of Catalysis, 1, 307-312, (1962).
43. D. Chen, H. P Rebo, K. Moljord and A. Holmen, Effect of coke deposition on transport and adsorption in zeolites studied by a new microbalance reactor, Chemical Engineering & Science, 51, 2687-2692, (1996).
44. G. Coudurier, A. Auroux, J. C. Vedrine, R. D. Farlee, L. Abrams and R. D. Shannon, Properties of Boron-Substituted ZSM-5 and ZSM-11 Zeolites, Journal of Catalysis, 108, 1-14, (1987).

45. V. Valtchev, G. Majano, S. Mintova and J. P. Ramirez, Tailored crystalline microporous materials by post-synthesis modification, Chemical Society Review, 42, 263, (2013).
46. J. P. Ramírez, J. C. Groenb, A. Brückner, M.S. Kumar, U. Bentrup, M. N. Debbagh, and L. A. Villaescusa, Evolution of isomorphously substituted iron zeolites during activation: comparison of Fe-beta and Fe-ZSM-5, Journal of Catalysis 232, 318-334, (2005).
47. G. J. Kim, B. R. Cho and J. H. Kim, Structure modification of mordenite through isomorphous Ti substitution: characterization and catalytic properties, Catalysis Letters 22, 259-270, (1993).
48. J. A. Rossin, C. Saldarriaga and M. E. Davis, Synthesis of cobalt containing ZSM-5, Zeolites, 7, 295, (1987).
49. K. G. Ione, L. A. Vostrikova and V. M. Mastikhin, Synthesis of Crystalline Metal Silicates Having Zeolite Structure and Study of their Catalytic Properties, Journal of Molecular Catalysis, 31, 355-370, (1985).
50. K. G. Ione and L. A. Vostrikova, Isomorphism and Catalytic Properties of Silicates with the Zeolite Structure, Russian Chemical Review, 56, 231, (1987).
51. G. T. Kokotailo, S. L. Lawton, D. H. Olson and W. M. Meier, Structure of synthetic zeolite ZSM-5, Nature, 272, 437-438, (1978).
52. D. H. Olson, G.T. Kokotailo, S. L. Lawton and W. M. Meier, Crystal Structure and Structure-Related Properties of ZSM-5, Journal of Physical Chemistry, 85, 2238-2243, (1981).
53. http://izasc.ethz.ch/fmi/xsl/IZA-SC/ftc_tm.xsl?-db=Atlas_main&-lay=tm&STC=MFI&-find, accessed on 19/09/2015.
54. S. M. Csicssery, Chemistry in Britain, 5, 473, (1985).
55. K. J. Chao, T. S. Tasi, M. S. Chen and L. Wang, kinetic studies on formation of zeolites ZSM-5, J. Chemical Society Faraday trans. I. 77, 547, (1981).
56. P. A Jacobs, H. K. Beyer and J. Valyon, Properties of the end members in the pentasil family of zeolites, zeolite, 1, 161, (1981).
57. C. Baerlocher, Proceeding 6th International Zeolite Conference, Reno, (Ed. D. Olson, A. Bisio), p. 823. Butterworth, UK, (1984).
58. H. G. Karge, K. Hatada, Y. Zheng and R. Fiedorow, Conversion of alkylbenzenes over zeolite catalysts II. Disproportionation of ethylbenzene over Faujasite-type zeolites, Zeolites, 3, 13, (1983).

59. N.Y Chen, W. E. Garwood and F. G. Dwyer, Shape selective catalysis in industrial application, 2nd Edition, ISBN 0-8247-9737-X, Marcel Dekker, Inc. New York, (1996).
60. A. A. O'Kelly, J. Kellett, and J. Plucker, Monoalkylbenzenes by Vapour Phase Alkylation with Silica - Alumina Catalyst, Industrial Engineering Chemical, 39, 154, (1947).
61. P. B. Venuto, L. A. Hamilton, P. S. Landis and J. J. Wise, Organic Reactions Catalyzed by Crystalline Aluminosilicates I. Alkylation Reactions, Journal of Catalysis 5, 81, (1966).
62. C. G. Wight, US Patent 4169111, Manufacture of Ethylbenzene, Union Oil Company of California, (1979).
63. F. Cavani, V. Arrigoni and G. Bellussi, European Patent 0432814 A1, Process for Alkylating Benzene, to Eniricerche, Environmental Chemistry, Snamprogetti, (1991).
64. G. Bellussi, G. Pazzuconi, C. Perego, G. Girotti, G. Terzoni, Liquid Phase Alkylation of Benzene with Light Olefins catalysed by β Zeolite, Journal of Catalysis, 157, 227, (1995).
65. L. Forni, G. Cremona, F. Missineo, G. Bellussi, C. Perego and G. Pazzuconi, Transalkylation of m-diethylbenzene over large-pore zeolites, Applied Catalysis A: General, 121, 261-272, (1995).
66. J. C. Cheng, T. F. Degnan, J. S. Beck, Y. Y. Huang, M. Kalyanaraman, J. A. Kowalasky, C. A. Loehr, D. N. Mazzone, Science and Technology in Catalysis, 1998, Kodansha Ltd., Tokyo, 53, (1999).
67. T. F. Degnan, C. M. Smith, C. R. Venkat, Alkylation of aromatics with ethylene and propylene: recent developments in commercial processes. Applied Catalysis A: General, 221, 283-294, (2001).
68. T. Ren, M. Patel and K. Blok, Olefins from conventional and heavy feed stocks: energy use in steam cracking and alternative processes. Energy, 31, 425-451, (2006).
69. T. Odedairo, and S. Al-Khattaf, Kinetic Investigation of Benzene Ethylation with Ethanol over USY Zeolite in Riser Simulator, Industrial Engineering Chemical Research, 49, 1642-1651 (2010).
70. Levesque and Dao, Benzene or toluene alkylation in presence of aqueous ethanol, Energy Conversion Engineering Conference, IECEC-89., Proceedings of the 24th Intersociety, (1989).

71. J. Gao, L. Zhang, J. Hu, W. Li and J. Wang, Effect of zinc salt on the synthesis of ZSM-5 for alkylation of benzene with ethanol, Catalysis communication, 10, 1615-1619, (2009).
72. S. Barman, N. C. Pradhan and J. K. Basu, Kinetics of alkylation of benzene with ethyl alcohol catalyzed by Ce-exchanged NaX zeolite, Indian Chemical Engineering, 48, (2006).
73. A. Corma, V. M. Soria and E. Schnoeveld, Alkylation of Benzene with Short-Chain Olefins over MCM-22 Zeolite: Catalytic Behaviour and Kinetic Mechanism, Journal of Catalysis, 192, 163-173, (2000).
74. D. B. Lukyanov and T. Vazhnova, Highly selective and stable alkylation of benzene with ethane into ethylbenzene over bifunctional PtH-MFI catalysts, Journal of Molecular Catalysis A: Chemical, 279, 128-132, (2008).
75. K. S. Wong, T. Vazhnova, S. P. Rigby and D. B. Lukyanov, Temperature effects in benzene alkylation with ethane into ethylbenzene over a PtH-MFI bifunctional catalyst, Applied Catalysis A: General, 454, 137-144, (2013).
76. Y. Li, B. Xue and X. He, Synthesis of ethylbenzene by alkylation of benzene with diethyl carbonate over parent MCM-22 and hydrothermally treated MCM-22, Journal of Molecular Catalysis A: Chemical, 301, 106-113, (2009).
77. H. Hu, Q. Zhang, J. Cen and X. Li, High suppression of the formation of ethylbenzene in benzene alkylation with methanol over ZSM-5 catalyst modified by platinum, Catalysis Communications, 57, 129-133, (2014).
78. D. B. Lukyanov and T. Vazhnova, A kinetic study of benzene alkylation with ethane into ethylbenzene over bifunctional PtH-MFI catalyst, Journal of Catalysis, 257, 382-389, (2008).
79. F. F. Madeira, N. S. Gnep, P. Magnoux, S. Maury and N. Cadran, Ethanol transformation over HFAU, HBEA and HMFI zeolites presenting similar Brønsted acidity, Applied Catalysis A: General, 367, 39-46, (2009).
80. J. Cejka, B. Wichterlova and S. Bednarova, Alkylation of toluene with ethene over H-ZSM-5 zeolites, Applied Catalysis A: General, 79, 215-226, (1991).
81. F. F. Madeira, K. B. Tayeb, L. Pinard, H. Vezin, S. Maury and N. Cadran, Ethanol transformation into hydrocarbons on ZSM-5 zeolites: Influence of Si/Al ratio on catalytic performances and deactivation rate. Study of the radical species role, Applied Catalysis A: General, 443-444, 171-180, (2012).

82. N. Sharanappa, S. Pai and V.V. Bokade, Selective alkylation and disproportionation of ethylbenzene in the presence of other aromatics, Journal of Molecular Catalysis A: Chemical, 217, 185-191, (2004).
83. Y. Sugi, Y. Kubota, K. Komura, N. Sugiyama, M. Hayashi, J.H. Kim and G. Seo, Shape-selective alkylation and related reactions of mononuclear aromatic hydrocarbons over H-ZSM-5 zeolites modified with lanthanum and cerium oxides, Applied Catalysis A: General, 299, 157-166, (2006).
84. T. Odedairo and S. Al-Khattaf, Ethylation of benzene: Effect of zeolite acidity and structure, Applied Catalysis A: General, 385, 31-45, (2010).
85. C. Ding, X. Wang, X. Guo and S. Zhang, Characterization and catalytic alkylation of hydrothermally dealuminated nanoscale ZSM-5 zeolite catalyst, Catalysis Communications, 9, 487-493, (2007).
86. J. Kim, S. Namba and T. Yasbima, Preparation of highly para-selective metallosilicate catalysts for alkylation of ethylbenzene with ethanol, Applied Catalysis A: General, 100, 27-36, (1993).
87. B. Xue, G. Zhang, N. Liu, J. Xu, Q. Shen and Y. Li, Highly selective synthesis of para-diethylbenzene by alkylation of ethylbenzene with diethyl carbonate over boron oxide modified HZSM-5, Journal of Molecular Catalysis A: Chemical, 395, 384-391, (2014).
88. T. Odedairo and S. Al-Khattaf, Kinetic analysis of benzene ethylation over ZSM-5 based catalyst in a fluidized-bed reactor, Chemical Engineering Journal, 157, 204-215, (2010).
89. B. Zhang, Z. Wang, P. Ji, Y. Liu, H. Sun, W. Yang and P. Wu, Efficient liquid-phase ethylation of benzene with ethylene over mesoporous MCM-22 catalyst, Microporous and Mesoporous Materials, 179, 63-68, (2013).
90. V. Bhandarkar and S. Bhatia, Selective formation of ethyltoluene by alkylation of toluene with ethanol over modified HZSM-5 zeolites, Zeolites, 14, (1994).
91. P. Levesque and L. H. Dao, Alkylation of Benzene Using an Aqueous Solution of Ethanol, Applied Catalysis, 53, 157-167, (1989).
92. A. Corma, F. J. Liopis, C. Martínez, G. Sastre and S. Valencia, The benefit of multipore zeolites: Catalytic behaviour of zeolites with intersecting channels of different sizes for alkylation reactions, Journal of Catalysis, 268, 9-17, (2009).
93. N. E. Villarreal, B. I. Kharisov, I. I. Ivanova and B. V. Romanovskii, Optimal conditions of toluene alkylation by ethanol using pentasil zeolite as catalyst, Applied Catalysis A: General, 224, 161-166, (2002).

94. M. Raimondo, G. Perez, A. D. Stefanis, A. G. Tomlinson and O. Ursini, PLS vs. zeolites as sorbents and catalysts: Effects of acidity and porosity on alkylation of benzene by primary alcohols, Applied Catalysis A: General, 164, 119-126, (1997).
95. J. A. Raj, J. P. Malar and V. R. Vijayaraghavan, Shape-selective reactions with AEL and AFI type molecular sieves alkylation of benzene, toluene and ethylbenzene with ethanol, 2-propanol, methanol and t-butanol, Journal of Molecular Catalysis A: Chemical, 243, 99-105, (2006).
96. U. Sridevi, K. B. Rao and N. C. Pradhan, Kinetics of alkylation of benzene with ethanol on $AlCl_3$-impregnated 13X zeolites, Chemical Engineering Journal 83, 185-189, (2001).
97. B. Zhang, Y. Ji, Z. Wang, Y. Liu, H. Sun, W. Yang and P. Wu, Liquid-phase alkylation of benzene with ethylene over postsynthesized MCM-56 analogues, Applied Catalysis A: General, 443-444, 103-110, (2012).
98. B. A. Ogunbadejo, M. S. Osman, P. Arudra, A. M. Aitani and S. S. Al-Khattaf, Alkylation of toluene with ethanol to para-ethyltoluene over MFI zeolites: Comparative study and kinetic modelling, Catalysis Today, 243, 109-117, (2015).
99. T. Odedairo and S. Al-Khattaf, Comparative study of zeolite catalyzed alkylation of benzene with alcohols of different chain length: H-ZSM-5 versus mordenite, Catalysis Today, 204, 73-84, (2013).
100. A. Galadima and O. Muraza, Role of zeolite catalysts for benzene removal from gasoline via alkylation: A review, Microporous and Mesoporous Materials, 213, 169-180, (2015).
101. Y. S. Bhat and A. B. Halgeri, Desired and undesired ethylbenzene dealkylation over MFI zeolite catalyst, Applied Catalysis A: General, 101, 95-104, (1993).
102. Y. Li, B. Xue and Y. Yang, Synthesis of ethylbenzene by alkylation of benzene with diethyl oxalate over HZSM-5, Fuel Processing Technology, 90, 1220-1225, (2009).
103. T. Vazhnova, S. P. Rigby and D. B. Lukyanov, Benzene alkylation with ethane in ethylbenzene over a PtH-MFI catalyst: Kinetic and IR investigation of the catalyst deactivation, Journal of Catalysis, 301, 125-133, (2013).
104. A. N. Ebrahimi, A. Z. Sharak, S. A. Mousavia, F. Aghazadeh and A. Soltani, Modification and optimization of benzene alkylation process for production of ethylbenzene, Chemical Engineering and Processing, 50, 31-36, (2011).
105. Y. Li, B. Xue and X. He, Catalytic synthesis of ethylbenzene by alkylation of benzene with diethyl carbonate over HZSM-5, Catalysis Communications, 10, 702-707, (2009).

106. B. Xue, Y. Li, S. Wang, H. Liu and C. Xu, Selective synthesis of ethylbenzene by alkylation of benzene with diethyl carbonate over MCM-22 modified by MgO, Reaction Kinetics, Mechanisms and Catalysis, 100, 417-425, (2010).
107. H. A. Zaidi and K. K. Pant, Catalytic activity of copper oxide impregnated HZSM-5 in methanol conversion to liquid hydrocarbons, The Canadian Journal of Chemical Engineering, 83, 970-977, (2005).
108. H. A. Zaidi and K. K. Pant, Transformation of Methanol to Gasoline Range Hydrocarbons Using HZSM-5 Catalysts Impregnated with Copper Oxide, Korean Journal of Chemical Engineering, 22, 353-357, (2005).
109. I. Eswaramoorthi and A. K. Dalai, Synthesis, characterisation and catalytic performance of boron substituted SBA-15 molecular sieves, Microporous and Mesoporous Materials, 93, 1-11, (2006).
110. K. M. Nigam, V. K. Srivastava and K. D. P. Nigam, Homogeneous-Heterogeneous Reactions in a Tubular Reactor: An Analytical Solution, The Chemical Engineering Journal, 25, 147-150, (1982).
111. L. R. Gonzalez, F. Hermes, M. Bertmer, E. R. Castellon, A. J. Lopez and U. Simon, The acid properties of H-ZSM-5 as studied by NH_3-TPD and Al-MAS-NMR spectroscopy, Applied Catalysis A: General, 328, 174-182, (2007).
112. J. G. Post and J. H. C. van Hooff, Acidity and activity of H-ZSM-5 measured with NH_3-t.p.d. and n-hexane cracking, Zeolites, 4, 9-14, (1984).
113. S. Siffert, L. Gaillard, L. Su, Alkylation of benzene by propylene on a series of beta zeolites, Journal of Molecular Catalysis A: Chemical, 153, 267-279, (2000).
114. M. Osman, L. Atanda, M. Hossain, S. Al-Khattaf, Kinetics modelling of disproportionation and ethylation of ethylbenzene over HZSM-5: effects of SiO_2/Al_2O_3 ratio, Chemical Engineering Journal, 222, 498-511, (2013).
115. X. Hongchuan, L. Xiangping, F. Yuan, Y. Xianfeng, H. Wenhui, C. Yueying, Z. Feng, Z. Anmin, Z. Hongpeng and L. Xuebing, Catalytic dehydration of ethanol over post-treated ZSM-5 zeolites, Journal of Catalysis, 312, 204-215, (2014).
116. N. R. Meshram, S. G. Hegde, S. B. Kulkarni and P. Ratnasamy, Disproportionation of toluene over HZSM-5 zeolites. Applied Catalysis, 3, 359-367, (1983).
117. L.E. Aneke, L.A. Gerritsen, P. J. Vandenberg and W. A Dejong, The disproportionation of toluene over a HY/b-AlF_3/Cu catalyst, Journal of Catalysis, 59, 26-36, (1979).

118. S. Narayanan, A. Sultana, Q. C. Le and A. Auroux, A Comparative and Multi technical Approach to the Acid Character of Templated and Non-Templated ZSM-5 Zeolites, Applied Catalysis A: General, 168, 373-384, (1998).
119. R. Szostak, Molecular Sieves: Principle of Synthesis and Identification. New York. Van Nostrand Reinhold, (1989).
120. K. Segawa, M. Sakaguchi and Y. Kurusu, Investigation of Acidic Properties of H-Zeolites as a Function of Si/ Al Ratio, Amsterdam: Elsevier, (1998).
121. A. V. Ivanov, G. W. Graham and M. Shelef, Adsorption of Hydrocarbons by ZSM-5 Zeolites with Different SiO_2/ Al_2O_3 Ratios; a Combined FTIR and Gravimetric Study, Applied Catalysis. B: Environment, 21, 243-258, (1999).
122. C. Costa, I. P. Dzikh, J. M. Lopes, F. Lemos and F. R. Ribeiro, Activity-Acidity Relationship in Zeolite ZSM-5, Application of Brønsted-Type Equations, Journal of Molecular Catalysis A: Chemical, 154, 193-201, (2000).
123. T. W. Chu and C. D. Chang, Isomorphous Substitution in Zeolites Frameworks, 1. Acidity of Surface Hydroxyls in [B]-, [Ga]- and [Al]- ZSM-5, The Journal of Physical Chemistry, 89, 1569-1571, (1985).
124. N. Y. Topsoe, K. Pedersen and E. G. Deroune, Infrared and Temperature Programmed Desorption Study of the Acidic Properties of HZSM-5 Type Zeolite, Journal of Catalysis, 70, 41-52, (1981).
125. M. Kapur and M. K. Mondal, Mass transfer and related phenomena for Cr(VI) adsorption from aqueous solutions onto Mangifera indica sawdust, Chemical Engineering Journal, 218, 138-146, 2013.
126. M. Osman, M. M. Hossain, and S. Al-Khattaf, Kinetics, Study of Ethylbenzene Alkylation with Ethanol over Medium and Large Pore Zeolites, Industrial Engineering Chemical Research, 52, 13613-13621, (2013)
127. M. Kamil, S. S. Alam and S. K. Saraf, Kinetics of hydrodesulphurization of thiophene in benzene over a cobalt molybdenum catalyst, Industrial Journal of Chemical Technology, 1, 319-324, (1994)

APPENDIXES

Appendix A

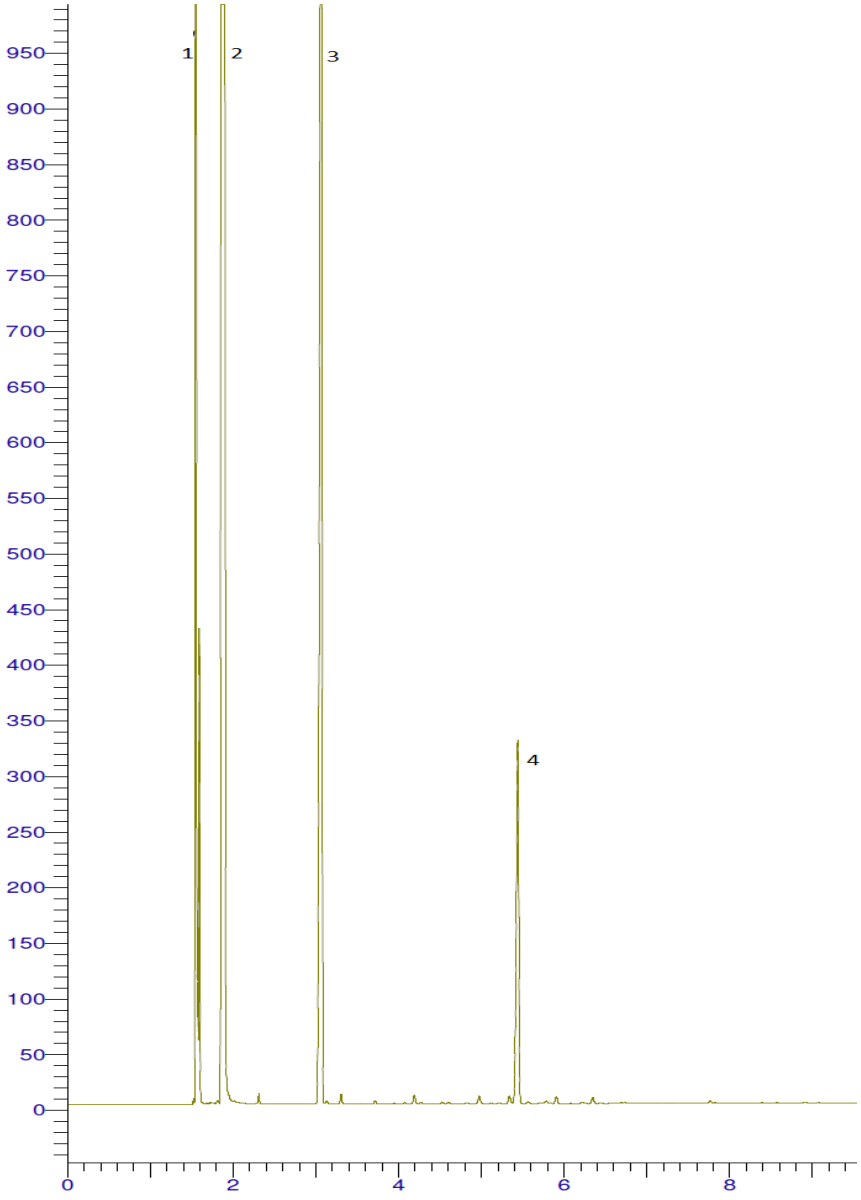

Figure A1-1: GC-MS peak for calibration of retention time of ethanol, benzene, ethylbenzene and diethylbenzene

Table A1-1: Retention time of ethanol, benzene, ethylbenzene and diethylbenzene

Peak No.	Name	Retention Time (min)
1	Ethanol	1.5
2	Benzene	1.8
3	Ethylbenzene	3.1
4	Diethylbenzene	5.4

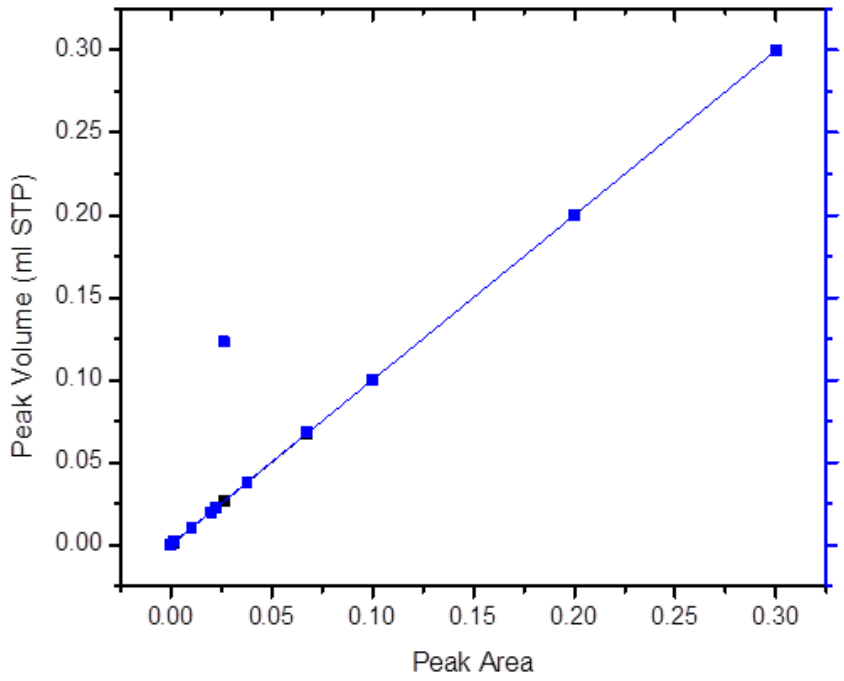

Figure A2-2: TCD calibration for NH_3-TPD with r^2= 97.9